Impact of Rossby waves on ozone distribution and dynamics of the stratosphere and troposphere

Grigory Nikulin

IRF Scientific Report 285
September 2005

ISSN 0284-1703
ISBN 91-7305-946-3

INSTITUTET FÖR RYMDFYSIK
Swedish Institute of Space Physics

Kiruna, Sweden

Impact of Rossby waves on ozone distribution and dynamics of the stratosphere and troposphere

av

Grigory Nikulin

Akademisk avhandlingen

Som med vederbörligt tillstånd av Rektorsämbetet vid Umeå universitet för avläggande av doktorsexamen i Atmosfärfysik II kommer att offentligen försvaras i aulan på Rymdcampus, fredagen den 4 november 2005, kl. 10.00. Avhandlingen kommer att försvaras på engelska.

Examinator: Prof. Sheila Kirkwood, Institutet för rymdfysik, Kiruna, Sweden

Opponent: Docent Ulrike Langematz, Institut für Meteorologie, Freie Universität Berlin, Berlin, Germany

Swedish Institute of Space Physics

Kiruna

DOCTORAL DISSERTATION

Impact of Rossby waves on ozone distribution and dynamics of the stratosphere and troposphere

Grigory Nikulin

Swedish Institute of Space Physics, Kiruna

Abstract

Waves are an integrated part of the atmospheric circulation on different spatial and time scales. The atmospheric circulation is strongly affected by wave-induced momentum transport at the same time as the circulation itself defines conditions for wave generation, propagation and dissipation. An important aspect of wave processes is their influence on transport and distribution of atmospheric chemical compounds. Several physical mechanisms concerning the impact of Rossby waves on ozone distribution and circulation in the stratosphere and troposphere are studied in the thesis.

Summertime total ozone variability over Middle Asia and Northern Scandinavia shows similar wave-like behaviour with typical periods of 10-20 days and amplitudes of 20-50 Dobson units. These variations are caused by eastward travelling Rossby waves in the upper troposphere/lower stratosphere region. The passage of a wave crest results in convergence of ozone-poor air below the tropopause and divergence of ozone-rich air above leading to a decrease in total ozone column. Wave-trough passage has the opposite effect. The same mechanism plays the primary role in the formation of so called ozone miniholes which are related to the tropospheric blocking phenomenon. An intense low ozone episode was observed over Scandinavia and the North Sea during the European heat wave of August 2003. A strong anticyclone was formed in the troposphere over Europe as a part of a Rossby wave train and its influence was apparent up to 50 hPa. At the same time the anticyclone coincides with a displaced Artic pool of low-ozone air in the stratosphere at 30 hPa, aloft of the anticyclone. It is most likely that low-ozone air at 30 hPa is associated with free Rossby waves (normal modes) propagating westward. A combination of the two above-mentioned processes results in the total ozone minimum over Northern Europe for summer 2003.

Interannual variability of the atmospheric circulation and total ozone during winter is strongly controlled by the diabatic (Brewer-Dobson) circulation which in turn is driven by upward propagating waves from the troposphere. In the Northern Hemisphere (NH) midlatitudes, wintertime total ozone shows antiphase behaviour with the Arctic Oscillation (AO) index on interannual and decadal time-scales. Weaker wave activity leads to less northward ozone transport from the tropics and to a stronger AO (a colder and more isolated polar vortex). As a consequence of low temperatures inside the polar vortex, more heterogeneous chemical ozone loss occurs that also influences midlatitude total ozone through export of ozone depleted air from the vortex. The picture is the opposite for stronger wave activity. In all months from October to March, the NH midlatitude ozone buildup has a stable statistical relation ($|r|=0.7$) with different parameters approximating the strength of the mean meridional circulation, namely: eddy heat flux, temperature tendency and the vertical residual velocity.

Rossby wave activity occurs as episodic wave events with duration 1-2 weeks and this wave forcing of the mean meridional circulation is not uniform during winter. The November-December averaged stratospheric eddy heat flux is strongly anticorrelated with the January-February averaged eddy heat flux in the midlatitude stratosphere and troposphere. These intraseasonal variations are actually related to the stratospheric vacillations observed in models. Weaker upward wave fluxes in early winter lead to stronger upward wave fluxes from the troposphere as well as to a stronger polar night jet during midwinter and vice versa. Hence anomalous strong or weak upward wave activity fluxes in early winter define, to a considerable extent, the subsequent evolution of the midwinter circulation in the stratosphere and troposphere.

Keywords: ozone, wave activity, trends, Brewer-Dobson circulation, Rossby waves, Arctic Oscillation, low ozone events.

IRF Scientific Report 285
Language: English
ISSN 0284-1703 September 2005
ISBN 91-7305-946-3 pp. 32+5 papers

Impact of Rossby waves on ozone distribution and dynamics of the stratosphere and troposphere

Grigory Nikulin

Swedish Institute of Space Physics

Kiruna

September 2005

Swedish Institute of Space Physics
Box 812, E-98128 Kiruna, Sweden

IRF Scientific Report 285
ISSN 0284-1703
ISBN 91-7305-946-3

Printed in Sweden
Swedish Institute of Space Physics
Kiruna
September 2005

Abstract

Waves are an integrated part of the atmospheric circulation on different spatial and time scales. The atmospheric circulation is strongly affected by wave-induced momentum transport at the same time as the circulation itself defines conditions for wave generation, propagation and dissipation. An important aspect of wave processes is their influence on transport and distribution of atmospheric chemical compounds. Several physical mechanisms concerning the impact of Rossby waves on ozone distribution and circulation in the stratosphere and troposphere are studied in the thesis.

Summertime total ozone variability over Middle Asia and Northern Scandinavia shows similar wave-like behaviour with typical periods of 10-20 days and amplitudes of 20-50 Dobson units. These variations are caused by eastward travelling Rossby waves in the upper troposphere/lower stratosphere region. The passage of a wave crest results in convergence of ozone-poor air below the tropopause and divergence of ozone-rich air above leading to a decrease in total ozone column. Wave-trough passage has the opposite effect. The same mechanism plays the primary role in the formation of so called ozone miniholes which are related to the tropospheric blocking phenomenon. An intense low ozone episode was observed over Scandinavia and the North Sea during the European heat wave of August 2003. A strong anticyclone was formed in the troposphere over Europe as a part of a Rossby wave train and its influence was apparent up to 50 hPa. At the same time the anticyclone coincides with a displaced Artic pool of low-ozone air in the stratosphere at 30 hPa, aloft of the anticyclone. It is most likely that low-ozone air at 30 hPa is associated with free Rossby waves (normal modes) propagating westward. A combination of the two above-mentioned processes results in the total ozone minimum over Northern Europe for summer 2003.

Interannual variability of the atmospheric circulation and total ozone during winter is strongly controlled by the diabatic (Brewer-Dobson) circulation which in turn is driven by upward propagating waves from the troposphere. In the Northern Hemisphere (NH) midlatitudes, wintertime total ozone shows antiphase behaviour with the Arctic Oscillation (AO) index on interannual and decadal time-scales. Weaker wave activity leads to less northward ozone transport from the tropics and to a stronger AO (a colder and more isolated polar vortex). As a consequence of low temperatures inside the polar vortex, more heterogeneous chemical ozone loss occurs that also influences midlatitude total ozone through export of ozone depleted air from the vortex. The picture is the opposite for stronger wave activity. In all months from October to March, the NH midlatitude ozone buildup has a stable statistical relation ($|r|=0.7$) with different parameters approximating the strength of the mean meridional circulation, namely: eddy heat flux, temperature tendency and the vertical residual velocity.

Rossby wave activity occurs as episodic wave events with duration 1-2 weeks and this wave forcing of the mean meridional circulation is not uniform during winter. The November-December averaged stratospheric eddy heat flux is strongly anticorrelated with the January-February averaged eddy heat flux in the midlatitude stratosphere and troposphere. These intraseasonal variations are actually related to the stratospheric vacillations observed in models. Weaker upward wave fluxes in early winter lead to stronger upward wave fluxes from the troposphere as well as to a stronger polar night jet during midwinter and vice versa. Hence anomalous strong or weak upward wave activity fluxes in early winter define, to a considerable extent, the subsequent evolution of the midwinter circulation in the stratosphere and troposphere.

Keywords: ozone, wave activity, trends, Brewer-Dobson circulation, Rossby waves, Arctic Oscillation, low ozone events.

Sammanfattning

Vågor är en integrerad del av den atmosfäriska cirkulationen på de olika rumsliga och tidsmässiga skalor. Den atmosfäriska cirkulationen påverkas starkt av det moment som överförs av vågor samt cirkulationen själv definierar konditioner för vågornas generering, spridning och absorption. En viktig aspekt av vågornas processer är deras påverkan på transporten och distribution av kemiska atmosfäriska substanser. Denna avhandling utforskas flera fysiska mekanismer av Rossby vågornas påverkan på ozon distributionen och cirkulationen i stratosfären och troposfären..

Under sommaren visar variationer i ozonet över Mellanöstern och norra Skandinavien den våglika mönster som har en typisk period av 10-20 dagar och amplituden på 20-50 DU. Dessa variationer beror på Rossby vågor som förflyttas ostvart i den övre troposfären och den undre stratosfären. Vågryggspassage resulterar i konvergens av ozonfattig luft under tropopausen och divergens av ozonrik luft över tropopausen och leder till minskningen av den totala ozonmängden. Passage av vågdalen har en motsatt effekt. Samma mekanism är den främsta orsaken till formationen av den så kallade mini-hålen i ozonet som är relaterade till det troposfäriska blockeringsfenomenet. En väldigt låg ozonnivå observerades över Skandinavien och det norra havet under den europeiska värmevågen under augusti 2003. Ett starkt högtryck formades i troposfären över Europa som en del av Rossby vågor som kom i en följd och dess påverkan kunde observeras upp till 50 hPa. Den sammanföll med ett område med låg ozonmängd som förflyttades från stratosfären i den arktiska regionen på 30 hPa. Det är mest troligt att luftmassan med låg ozonmängd beror på de fria Rossby vågor som förflyttas västerut. Kombinationen av de två ovannämnda processerna resulterar i den totala ozonminimum över norra Europa för sommaren 2003.

Variationen från år till år av den atmosfäriska cirkulationen och den totala ozonmängden under vintern är under stark kontroll av den diabatiska (Brewer-Dobson) cirkulationen som i sin tur drivs av uppgående vågor från troposfären. I den norra hemisfärens mellanlatituder under vintern visar den totala ozonmängden osynkronisk beteende med den Arktiska Oscillation (AO) index på tidsskalor om år till årtionden. En svagare vågintensitet leder till minskning av mängden ozon som transporteras från tropikerna norrut och till starkare AO (kallare och mer isolerad polarvirveln). Som följd av de låga temperaturerna i den polarvirveln, förstörs ozonet i större skala i heterogena kemiska reaktioner och det samtidigt påverkar ozonmängden i mellanlatituderna genom att luftmassan med låg ozonmängd förflyttas till mellanlatituderna från polarvirveln. Under perioden från oktober till mars ökningen av ozonmängden i den norra hemisfären har starka statistiska relationer ($|r|=0.7$) med olika parametrar som är bundna till styrkan av den meredionala cirkulationen. Dessa parametrar är: vågflöden, lufttemperaturens tendenser och den vertikala överbliven lufthastigheten.

Aktiviteten av Rossby vågor kan observeras episodiskt och har en livslängd på 1-2 veckor. Samtidigt är vågornas påverkan på den Brewer-Dobson cirkulationen inte konstant under vintern. Variationer i början och slutet på vinterperioden i själva verket är bundna till de stratosfäriska oscillationer som man kan observera i modeller. De svagare vågflöden riktade uppåt i början av vinter leder till starkare vågflöden från troposfären samt till starkare polarvind under mitten av vinterperioden. Man kan dra slutsatsen att onormalt starka eller svaga uppåtgående vågflöden i början av vinterperioden definierar senare utveckling av cirkulationen under mitten av vinterperioden i stratosfären och troposfären.

Nyckelord: ozon, vågaktivitet, trender, Brewer-Dobson cirkulation, Rossby vågor, Arktisk Oscillation, lokal ozonförtunning.

Contents

Included paper

Paper I. Roldugin, V. C., Nikulin, G. N., and Henriksen, K., Wave-like ozone movements, Phys. Chem. Earth (B), 25, 511-514, 2000

Paper II. Nikulin, G. N. and Repinskya, R. P., Modulation of total ozone anomalies in the midlatitude Northern Hemisphere by the Arctic oscillation, Izvestia - Atmospheric and Oceanic Physics, 37, 633-643, 2001

Paper III. Karpetchko, A. and Nikulin, G., Influence of early winter upward wave activity flux on midwinter circulation in the stratosphere and troposphere, J. Climate, 17, 4443-4452, 2004

Paper IV. Orsolini, Y. J. and Nikulin, G., A low-ozone episode during the European heat wave of August 2003, Q. J. Roy. Meteorol. Soc., in press, 2005

Paper V. Nikulin, G. and Karpechko, A., The mean meridional circulation and midlatitude ozone buildup, Atmos. Chem. Phys. Discuss., 5, 4223-4256, 2005

1. Introduction

The work presented in this thesis concerns variability in the ozone layer and the atmospheric circulation over the Northern Hemisphere related to the impact of Rossby waves from synoptical to decadal time-scales. Rossby waves owe their origin to the rotation and sphericity of the Earth (Rossby, 1939; Blinova, 1943) representing, for example, large-scale meanders of the jet stream in the extratropics. Interaction of Rossby waves with the atmospheric circulation influences the atmospheric circulation itself and the ozone distribution on both local and hemispheric scales.

During winter, wave forcing associated to Rossby waves plays a primary role in driving the Brewer-Dobson (BD) circulation, which is responsible for poleward ozone transport and adiabatical warming of the polar stratosphere (Newman et al., 2001; Salby and Callaghan, 2002). The latter factor is critical for formation of polar stratospheric clouds (PSC) and consequently for triggering chemical ozone loss (Solomon, 1990). Wave forcing has attracted a special interest in the context of the observed negative trends in stratospheric temperatures and extratropical ozone (Ramaswamy et. al., 2001; Staehelin et al., 2001). Now it is recognized that interannual and decadal variability in both temperature and ozone result from a combination of dynamical, radiative and chemical processes, one of these being wave forcing (WMO, 2003). However, inasmuch as many processes are interrelated a clear separation between chemistry, radiation and dynamics is still questionable.

Recent studies (e. g. Christiansen, 2001; Polvani and Waugh, 2004) show that upward propagating wave activity from the troposphere into the stratosphere can influence the subsequent circulation in both the troposphere and stratosphere through downward propagation of wave-induced stratospheric anomalies. Taking into account wave-induced stratospheric anomalies can improve statistical forecast of surface weather (Baldwin et al., 2003; Christiansen, 2005).

Despite global-scale influence, Rossby waves are also involved in dynamical processes and redistribution of ozone on synoptical scales. In particular an anomalous, strong, quasi-stationary anticyclone or “blocking” can cause an abnormal weather situation, the European heat wave of August 2003 for example (Black et al., 2004), as well as a strong dynamically-induced local decrease in total ozone, so called ozone miniholes (Newman et al., 1988). Blockings over the Atlantic/European region dominantly develop as a part of a Rossby wave train through convergence of wave activity into an amplifying blocking ridge (Nakamura et al., 1997).

Section 2 introduces fundamental basics of the atmospheric circulation touched in the thesis: the zonal mean circulation, Rossby waves, the Brewer-Dobson circulation and ozone distribution. In Section 3 the focus is on local synoptic variability in total ozone caused by baroclinic Rossby waves during summer (Paper I and IV). Winter midlatitude total ozone variability in relation to the Brewer-Dobson circulation (Paper V) and large-scale modes of atmospheric variability - the Arctic and North Atlantic oscillations (Paper II) is presented in Section 4. Finally, Section 5 describes the influence of early winter wave activity on the subsequent evolution of the stratospheric and tropospheric circulation during midwinter (Paper III).

2. Background

2.1 The governing equations

The atmosphere is in perpetual motion and this motion can be described by the laws of thermodynamics and fluid dynamics. The governing equations, in a general form, consist of the

momentum (Navier-Stokes) equation

$$\frac{d\mathbf{U}}{dt} + 2\Omega \times \mathbf{U} = -\frac{1}{\rho}\nabla p - g + \frac{\mu}{\rho}\nabla^2 \mathbf{U}\,, \tag{2.1}$$

the mass continuity equation

$$\frac{1}{\rho}\frac{d\rho}{dt} + \nabla \bullet \mathbf{U} = 0\,, \tag{2.2}$$

the thermodynamics energy equation

$$\frac{dT}{dt} - \frac{1}{c_p \rho}\frac{dp}{dt} = Q\,, \tag{2.3}$$

and the equation of state

$$p = \rho RT\,. \tag{2.4}$$

Here, $\mathbf{U}$ is the velocity vector (u, v, w); p is the pressure; ρ is the density; T is the temperature; and Ω , g , R , Q , c_p and μ are the angular speed of rotation of the earth, the gravity acceleration, the gas constant, the net diabatic heating rate, the isobaric specific heat capacity and the coefficient of viscosity of air, respectively. For large-scale processes in the free atmosphere (above the boundary layer) some approximations simplifying the governing equations of atmospheric motions can be introduced. Scale analysis (see e. g. Holton, 1992; Salby, 1995) shows that the horizontal pressure gradient and Coriolis forces dominate in the horizontal momentum equations. Hence horizontal large-scale motions can be approximated by the geostrophic relation

$$u_g = -\frac{1}{\rho f}\frac{\partial p}{\partial y}, \qquad v_g = \frac{1}{\rho f}\frac{\partial p}{\partial x}, \tag{2.5}$$

where u_g and v_g are the zonal and meridional geostrophic velocities, and $f = 2\Omega \sin\varphi$ is the Coriolis parameter (φ is the latitude). The geostrophic wind is the result of balance between the horizontal pressure gradient and Coriolis forces and blows along isobars with low pressure to the left in the NH. A similar scale analysis indicates that the vertical momentum equation is balanced by the vertical pressure gradient and gravity forces and satisfies the hydrostatic equilibrium written as

$$\frac{1}{\rho}\frac{dp}{dz^*} = -g\,, \tag{2.6}$$

where z^* is the geometric altitude. A combination of the hydrostatic (2.6) and geostrophic (2.5) approximations together with the equation of state (2.4) determines the vertical structure of the geostrophic wind through the thermal wind relation

$$\frac{\partial u}{\partial z} = -\frac{R}{Hf}\frac{\partial T}{\partial y}, \quad \frac{\partial v}{\partial z} = \frac{R}{Hf}\frac{\partial T}{\partial x}, \tag{2.7}$$

where the log-pressure vertical coordinate is $z = -H \ln(p/1000\,hPa)$ and H is the mean scale height. The thermal wind balance (2.7) relates the vertical shear of the geostrophic wind with the horizontal temperature gradient.

One useful and important quantity used in the atmospheric science is potential temperature Θ defined as

$$\Theta = T\left(\frac{1000\,hPa}{p}\right)^{\frac{R}{C_p}}. \qquad (2.8)$$

Under dry-adiabatic motion Θ is conserved and an air parcel moves along isentropes (constant Θ surfaces) which gives the opportunity to use Θ as a tracer for dry-adiabatic motion. The dry-adiabatic approximation is reasonably valid for atmospheric processes when the timescale of heat transfer is long compared to the timescales of air motion.

2.2 Vertical temperature distribution

The Earth's atmosphere is a complex system with many interactions and feedbacks between dynamics, chemistry and radiation. The absorption and distribution of short-wave solar radiation are the main contributors driving the global scale circulation of the atmosphere. The initially solar forced circulation is modified by other agents such as the Earth's rotation and waves. Three vertical regions of the first 100 km of the atmosphere are usually distinguished, namely: the troposphere, stratosphere and mesosphere, which are defined according to the temperature distribution with height (Fig. 2.1). The lowest part is the troposphere where weather occurs and temperature decreases with height up to the tropopause. Above the tropopause, in the stratosphere, the bulk of ozone is contained and temperature increases, reaching a maximum at the stratopause that is due to absorption of ultra-violet (UV) radiation by ozone. In the uppermost region, the mesosphere, temperature decreases with height and the summer polar

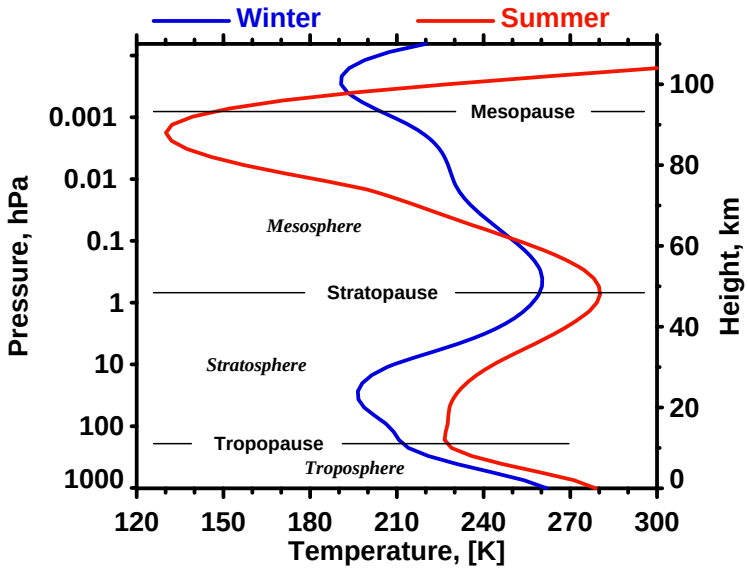

Figure 2.1. Schematical vertical structure of the atmosphere based on temperature profiles at Kiruna (20°E, 68°N) for January 15 (blue) and July 15 (red). Data are from the MSISE-90 model.

mesopause represents the coldest place in the atmosphere because of the gravity wave induced upwelling. This thesis focuses on the troposphere and stratosphere and thus examines processes in the altitude region between the ground and approximately 50 km (1 hPa).

2.3 Zonal mean thermal and dynamical structure of the atmosphere

The simplest approach to presenting the thermal and dynamical structure of the atmosphere is a zonal mean when we assume that the circulation is zonally symmetric. Figure 2.2 shows the zonal mean temperature and potential temperature in January. In the lower and middle

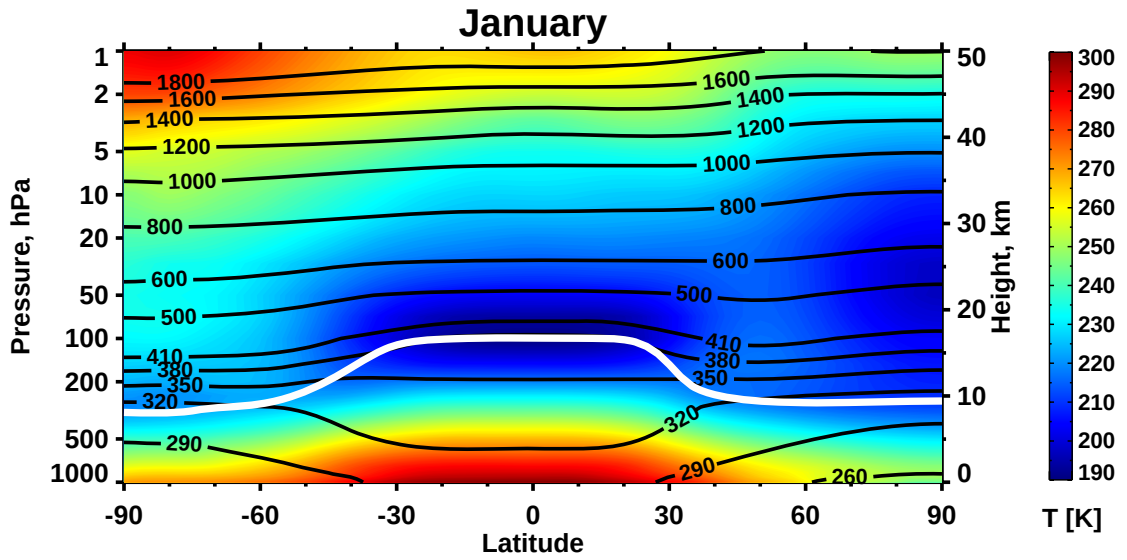

Figure 2.2. Latitude-altitude cross section of zonal mean temperature (colors) and potential temperature (contours, [K]) for January. The white line denotes the zonal mean tropopause. Data are based on the 1979-2002 climatology from the ERA-40 Reanalysis (temperature and potential temperature) and the NCEP/NCAR Reanalysis (tropopause).

troposphere temperature has a maximum in the tropics and decreases toward both Poles. The meridional temperature distribution reverses in the upper troposphere/lower stratosphere (UTLS) where the high tropical tropopause is colder than the winter polar stratosphere as a result of the wave driven BD circulation. Above approximately 25 km, temperature has almost a uniform increase from the winter pole to the summer pole that is consistent with distribution of the solar radiation. Potential temperature rises with height in contrast to usual temperature and together with the tropopause bring one important separation of the stratosphere. Beginning from approximately the 380 K surface, all isentropes lie entirely in the stratosphere and 380 K can be treated as the lower boundary of the so called “overworld” (Hoskins, 1991). Below 380 K the tropopause crosses several isentropes and a region between 380 K and the extratropical tropopause is defined as the lowermost stratosphere (Holton et al., 1995). There is a crucial distinction between the lowermost stratosphere and the overworld: transport in the overworld is controlled by the large-scale BD circulation while transport in the lowermost stratosphere is strongly affected by synoptic-scale processes (blocking anticyclones, cut-off lows and tropopause folds).

Zonal mean zonal wind and the meridional temperature gradient are shown in Fig. 2.3. In the lower part of the atmosphere the main features are two subtropical westerly jet streams reaching their maximum at the tropopause. Above the tropopause, winds decrease with altitude and then increase again with opposite direction in the two hemispheres. Observed zonal winds are in

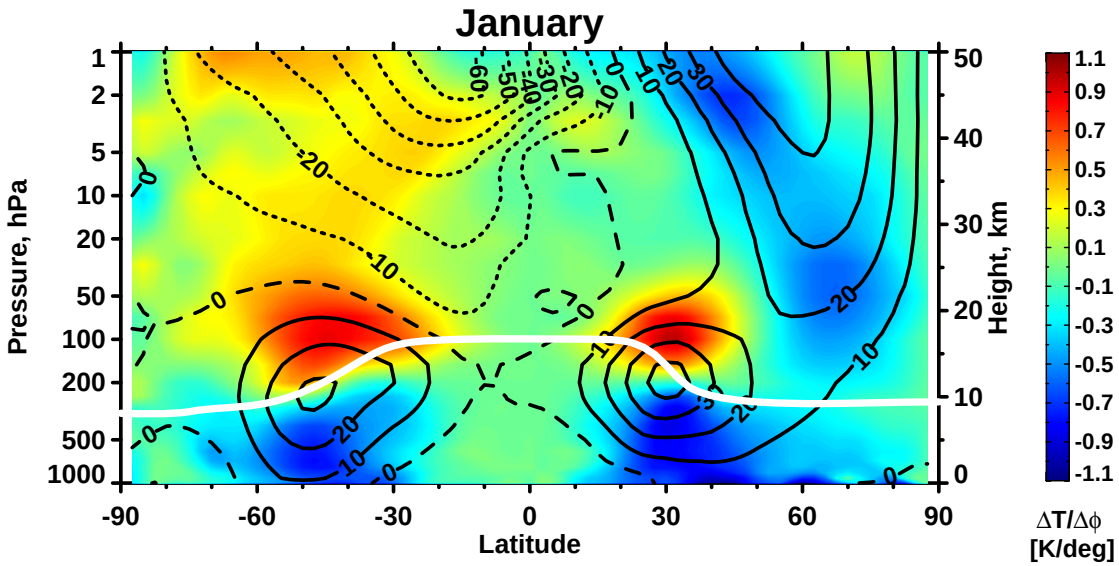

Figure 2.3. Latitude-altitude cross section of zonal mean meridional temperature gradient (colors) and zonal wind (contours: negative-eastward, positive-westward, [m/s]) for January. The negative (positive) gradient is directed poleward (equatorward). The white line denotes the zonal mean tropopause. Data are based on the 1979-2002 climatology from the ERA-40 Reanalysis (temperature gradient and zonal wind) and the NCEP/NCAR Reanalysis (tropopause).

good agreement with the thermal wind relation (2.7) so the vertical wind shear is proportional to the meridional temperature gradient as is clearly seen from Fig. 2.3. In the NH stratosphere the meridional temperature gradient is northward, hence westerly winds are conserved and intensify with altitude forming the polar night jet. In the SH, westerly winds weaken and turn into easterly winds above 50 hPa because of the equatorward temperature gradient. It should be noted that the thermal wind balance as well as the geostrophic approximation do not work near the equator where the Coriolis force is negligible small.

2.4 Rossby waves

The atmosphere is capable to support many different types of wave motions. The rotation and sphericity of the Earth cause a certain kind of wave motion called Rossby waves which extend on synoptical to planetary scales. The theory of Rossby waves was originally developed by Rossby (1939) and Blinova (1943) who showed that the restoring force for Rossby waves originates from the meridional gradient of the Coriolis parameter ($\beta = 2\Omega\cos\varphi / a$) also known as the Rossby parameter.

The basic properties of Rossby waves can be derived from a barotropic nondivergent model on a midlatitude beta-plane. For barotropic Rossby waves, taking a normal mode solution, the zonal phase speed is

$$C_x = \bar{u} - \frac{\beta}{k^2 + l^2} \tag{2.9}$$

and the group velocity is defined as

$$C_g = \left(C_{gx}; C_{gy}\right) = \left(\bar{u} + \frac{\beta\left(k^2 - l^2\right)}{\left(k^2 + l^2\right)^2}; \frac{\beta k l}{\left(k^2 + l^2\right)^2} \right), \tag{2.10}$$

where k and l are the zonal and meridional wavenumbers, $\bar{u}$ is the mean zonal flow. From (2.9) it is clearly seen that, relative to the mean zonal flow, the intrinsic phase speed $\beta/(k^2 + l^2)$ is always westward. Since the intrinsic phase speed depends on k and l, Rossby waves are dispersive waves whose intrinsic phase speed increases rapidly with wavelength. Relative to the earth, waves with the longest wavelength propagate westward while slow smaller-scale waves are advected eastward by the westerly zonal flow that is typical for synoptical disturbances. In contrast to the intrinsic phase speed which is always westward relative to the zonal flow, the intrinsic zonal group velocity can be either eastward or westward relative to the zonal flow depending on ratio of k and l. If the intrinsic westward phase speed of Rossby waves is equal to the westerly zonal wind these waves are stationary relative to the earth $C_x = 0$ and the zonal group velocity is always eastward in this case.

Rossby waves can be separated into forced waves which are continually maintained by an excitation mechanism and free waves (e. g. global normal modes) which are not so maintained. Forced stationary Rossby waves are of primary importance for the understanding the atmospheric circulation in the troposphere and the stratosphere. These waves are generated in the troposphere by longitudinally dependent heat sources or by flow over topography. The vertical propagation of stationary Rossby waves from the troposphere into the stratosphere depends on zonal wind and the horizontal wavenumber (Charney and Drazin, 1961). The Charney-Drazin criterion for vertical propagation of stationary Rossby waves is written as

$$0 < \bar{u} < \bar{u}_c \approx \frac{\beta}{k^2 + l^2} \tag{2.11}$$

where $\bar{u}_c$ is the critical velocity. Stationary waves propagate upward only in westerly zonal wind ($\bar{u} > 0$) that does not exceed the critical velocity ($\bar{u} < \bar{u}_c$). Since $\bar{u}_c$ increases with horizontal wavelength (2.11), longer waves have a wider range of westerly flow for upward propagation into the stratosphere. During winter westerly winds dominate in the extratropical stratosphere (Fig. 2.3) creating favourable conditions for vertical propagation of ultra-long Rossby waves (mainly zonal Fourier harmonics 1, 2, 3) which are observed in the winter stratosphere (Pawson and Kubitz, 1996). Easterly winds in the summer extratropical stratosphere impede upward propagation of tropospheric Rossby waves. However, in the summer stratosphere with easterly winds, free Rossby waves are often evident (Hoppel et al., 1999; Akiyoshi et al., 2004). In the winter stratosphere Rossby waves are principally responsible for driving the Brewer-Dobson circulation (Holton et al., 1995), for formation of the "surf zone" through irreversible isentropic mixing related to Rossby wave breaking (McIntyre and Palmer, 1984) and for sudden stratospheric warmings (Matsuno, 1971; McIntyre, 1982). Also an increased number of studies show that stratospheric response to upward propagating Rossby waves has a tendency to propagate downward, influencing the subsequent tropospheric circulation (e. g. Baldwin et al., 2003; Karpetchko and Nikulin, 2004 (Paper III); Polvani and Waugh, 2004).

2.5 The Brewer-Dobson circulation

Several studies of tracer distribution in the atmosphere (Dobson et al., 1929; Brewer, 1949; Dobson, 1959) have led to a general qualitative suggestion about the existence of a meridional stratospheric cell in each hemisphere with rising motions in the tropics, subsequent poleward drift and descending motions in middle and polar latitudes. Murgatroyd and Singelton (1961) estimated the zonal mean meridional circulation in the stratosphere and the mesosphere from the thermodynamic and continuity equations neglecting eddy transport terms in the thermodynamic equation. They found the poleward stratospheric cell in agreement with the previous suggestions based on tracer distribution. However, neglecting eddy transport was questionable and studies of the Eulerian zonal mean circulation (e.g. Vincent, 1968) have shown the existence of two cells per hemisphere. The second cell consists of rising motions over the polar region and descending motions over midlatitudes which is opposite to the single, poleward directed, cell. These contradictions were solved at the end of 1970s with the development of the Lagrangian mean (LM) and transformed Eulerian mean (TEM) formulations (Andrews and McIntyre, 1976, 1978) as well as with understanding that the tracer transport is governed by drift of air parcels, or the Lagrangian circulation. In the presence of waves, the zonal mean Eulerian and Lagrangian circulations can differ not only in magnitude but also in direction because of the Stokes drift associated with waves (Dunkerton, 1978; Wallace, 1978). Practical estimations of the Lagrangian circulation from observations which are mainly fixed in space (i.e. an Eulerian representation) are not well defined. As an approximation of Lagrangian motions projected on the meridional plane the TEM formulation introduced by Andrews and McIntyre (1976) can be used. In the TEM meridional and vertical velocities ($\overline{v}^*$, $\overline{w}^*$) the part of circulation resulting from eddy transport (the Stokes drift) is removed from the Eulerian velocities ($\overline{v}$, $\overline{w}$):

$$\overline{v}^* = \overline{v} - \frac{R}{\rho_0 H}\frac{\partial\left(\rho_0 \overline{v'T'}/N^2\right)}{\partial z}, \tag{2.12}$$

$$\overline{w}^* = \overline{w} + \frac{R}{H}\frac{\partial\left(\overline{v'T'}/N^2\right)}{\partial y}, \tag{2.13}$$

where variables with overbars denote zonal means, primed variables denote eddy components, ρ_0 is the background density and N^2 is the square of the buoyancy frequency. Known as residual velocities $\overline{v}^*$ and $\overline{w}^*$ are qualitatively related to the Lagrangian mean motions and represent an approximation of the average net drift of the air parcel. Figure 2.4 shows the Eulerian zonal mean (a) and residual (b) streamfunctions for January. The Eulerian circulation (Fig. 2.4 top) includes an equatorward wave-induced cell north of 45°N but this cell has no net effect on mass transport and exists only in order to cancel the Stokes drift. In turn, the residual circulation (Fig. 2.4 bottom), being an Eulerian quantity, approximates mass transport and is consistent with the one-cell circulation suggested by Brewer (1949), Dobson (1956) and obtained by Murgatroyd and Singelton (1961). In fact Murgatroyd and Singelton (1961) calculated a simplified version of the residual circulation but the theoretical background for neglecting eddy transport appeared nearly 20 years later. Now the circulation shown in Fig. 2.4 (bottom) is well known with a general name “the Brewer-Dobson circulation” describing a meridional stratospheric cell with tropical upwelling and extratropical downwelling.

The governing equation (2.1)-(2.3) can be rewritten in the quasi-geostrophic TEM formulation as follows:

$$\frac{\partial \overline{u}}{\partial t} - f\,\overline{v}^{*} = \frac{1}{\rho_0}\nabla \bullet \boldsymbol{F} + \overline{\boldsymbol{X}}\,, \tag{2.14}$$

$$\frac{\partial \overline{T}}{\partial t} + \overline{v}^{*}\frac{\partial \overline{T}}{\partial y} + \overline{w}^{*}\frac{N^2 H}{R} = Q\,, \tag{2.15}$$

$$\frac{\partial \overline{v}^{*}}{\partial y} + \frac{1}{\rho_0}\frac{\partial\left(\rho_0 \overline{w}^{*}\right)}{\partial z} = 0\,. \tag{2.16}$$

On the right-hand side of the momentum equation (2.14) $\overline{X}$ is the zonal force due to small-scale processes and the vector $\boldsymbol{F}$ is the Eliassen-Palm (EP) flux defined as

$$\boldsymbol{F} = \left(F_y, F_z\right) = \left(-\rho_0 \overline{u'v'},\ \ \frac{\rho_0 f R}{N^2 H}\overline{v'T'}\right). \tag{2.17}$$

The TEM momentum equation shows that the eddy heat ($\overline{v'T'}$) and momentum ($\overline{u'v'}$) fluxes act in combination through the divergence of the EP flux to induce changes in the zonal mean circulation. It is recognized that the BD circulation is driven by upward propagating waves, while divergence of the EP flux represents a net wave forcing (Andrews et al., 1987; Haynes et al., 1991). The vertical component of the EP flux (F_z) which is proportional to the zonal mean

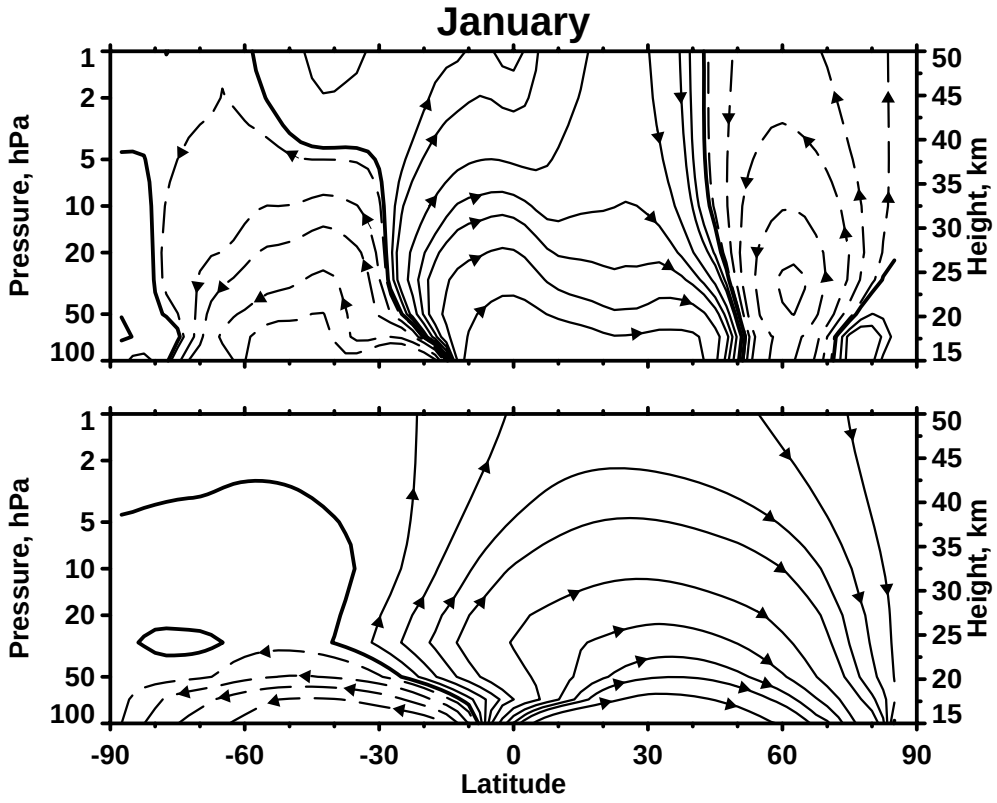

Figure 2.4. Latitude-altitude cross sections of the Eulerian zonal mean (top) and residual (bottom) streamfunctions for January based on the 1979-2002 climatology from the ERA-40 Reanalysis.

eddy heat flux (HF) is widely used as a proxy of wave forcing of the residual circulation (Fusco and Salby, 1999; Newman et al., 2001; Randel et al., 2002). Large-scale waves can propagate from the troposphere into the stratosphere only during wintertime when zonal winds are westerly (Charney and Drazin, 1961). Hence the maximum of planetary wave activity propagation into the stratosphere, as well the strongest residual circulation, occur in the winter hemisphere. Planetary waves, transporting westward momentum, break in the winter stratosphere and produce a westward zonal force which in combination with the Coriolis force results in the net poleward drift. This mechanism driving the BD circulation is also called "gyroscopic pumping" (McIntyre, 2000).

The BD circulation is responsible, in particular, for driving the atmosphere away from radiative equilibrium and for poleward tracer transport. Rising motions in the tropics lead to adiabatic cooling so temperatures are lower than radiatively determined values which results in diabatic heating to relax back to the radiatively determined state. The picture is the opposite in middle and high latitudes where descending motions cause adiabatic warming and correspondingly diabatic cooling. The residual circulation estimated from the TEM thermodynamic and continuity equations (2.15)-(2.16) is usually referred to as the diabatic circulation to emphasize that the circulation is derived from the thermodynamic budget. However the name "adiabatic" also is used in a more comprehensive sense meaning the circulation across isentropic surfaces (e. g. Holton et al., 1995). Both the BD circulation as a general concept and the residual circulation as a certain numerical approximation of the BD circulation are diabatic.

2.6 Ozone distribution

Triatomic oxygen (O_3), also named ozone, plays a key role in the atmosphere. Ozone is mainly formed in the stratosphere through recombination of molecular oxygen (O_2) with atomic oxygen (O) resulting from photodissociation of O_2 by UV radiation (Brasseur and Solomon, 1986). Harmful UV radiation in the interval 220-290 nm is fully absorbed by O_3 in the middle atmosphere before reaching the ground thus the ozone layer protects biological life on the Earth. Also heating related with absorption by O_3 defines the vertical structure of the atmosphere (Fig. 2.1) providing the existence of the stratosphere.

The amount of ozone can be expressed in relative (mass or volume mixing ratios) or absolute (density, pressure, number density) units. Relative units are preferable for dynamical studies because they are conserved following the motion in the absence of sources and sinks (no influence of compressibility of the atmosphere). Figure 2.5 shows the zonal mean mass mixing ratio ($\overline{\chi}_{O_3}$) and partial pressure ($\overline{p}_{O_3}$) of ozone for January. A maximum of $\overline{\chi}_{O_3}$ is observed near 35 km in the tropics where the flux of solar UV and photodissociation of O_2 are large. Changes of $\overline{\chi}_{O_3}$ locally can be described by the TEM continuity equation

$$\frac{\partial \overline{\chi}_{O_3}}{\partial t} = -\overline{v}^* \frac{\partial \overline{\chi}_{O_3}}{\partial y} - \overline{w}^* \frac{\partial \overline{\chi}_{O_3}}{\partial z} + \frac{1}{\rho_0} \nabla \bullet \mathbf{M} + \overline{S}\,, \tag{2.18}$$

where $\nabla \bullet \mathbf{M}$ is eddy transport and $\overline{S}$ is the sum of all chemical sources and sinks. Outside of the ozone-generating region, ozone is delivered by mean ($\overline{v}^*$, $\overline{w}^*$) and eddy ($\nabla \bullet \mathbf{M}$) transport. High $\overline{\chi}_{O_3}$ in the sunless winter stratosphere is a direct result of the BD circulation which is strongest in the winter hemisphere. Though the maximum of relative concentration of ozone ($\overline{\chi}_{O_3}$) is located in the middle stratosphere, the absolute concentration of ozone ($\overline{p}_{O_3}$ in Fig. 2.5) maximizes in the lower stratosphere because air density decreases exponentially with altitude. Ozone lifetime is of order 1 day at 30 km and several weeks in the lower stratosphere

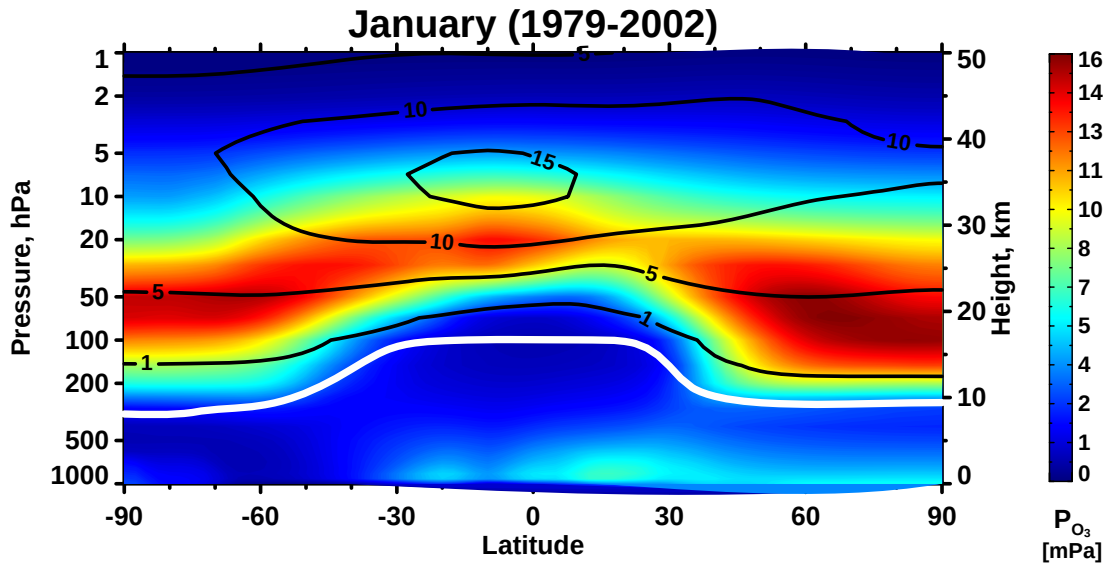

Figure 2.5. Latitude-altitude cross section of zonal mean partial pressure (colors) and mass mixing ratio (contours, [ppm]) of ozone for January. The white line denotes the zonal mean tropopause. Data are based on the 1979-2002 climatology from the ERA-40 Reanalysis (ozone) and the NCEP/NCAR Reanalysis (tropopause).

(Brasseur and Solomon, 1986) thus the lower stratosphere represents the transport-controlled region for ozone.

Total ozone content in a vertical column of the atmosphere is expressed in Dobson units (DU) which correspond to 0.01 mm thickness of ozone layer brought to standard pressure and temperature. Since the maximum of $\overline{p}_{O_3}$ in the extratropics is observed in the lower stratosphere, almost all variability in extratropical total ozone comes also from the lower stratosphere. Figure 2.6 presents the zonal-mean total ozone as a function of latitude and month. Maxima of total ozone, resulting from wintertime poleward transport and accumulation in the lower stratosphere, are found during the respective spring in each hemisphere: March-April near the North Pole and September-October over the 40°-60°S region. The essential difference

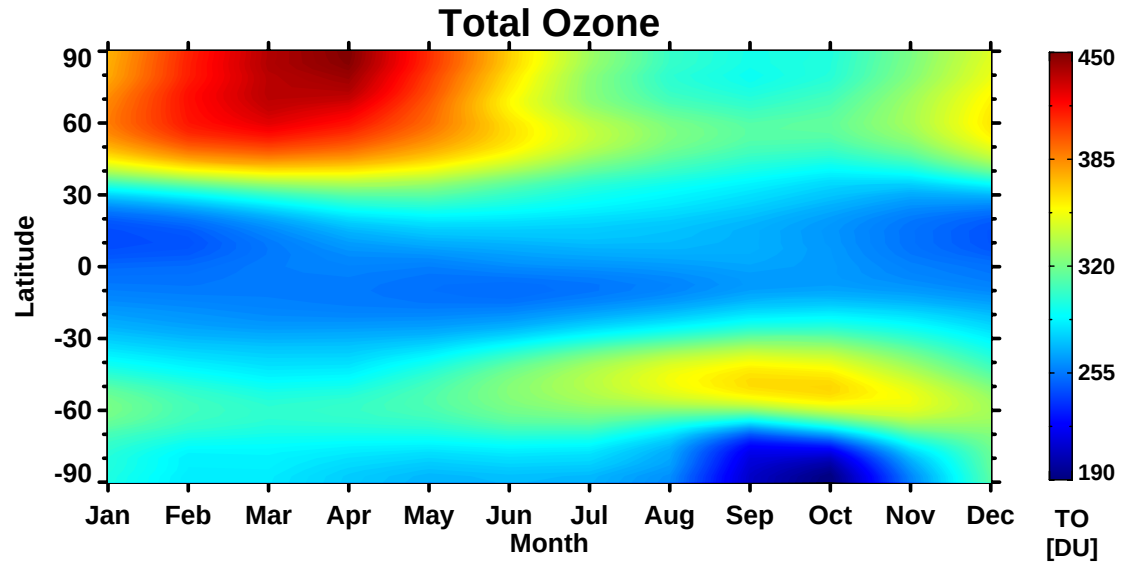

Figure 2.6. Annual cycle in zonal mean total ozone based on the 1979-2002 climatology from the ERA-40 Reanalysis.

between the hemispheres is the existence of the Antarctic ozone minimum in spring. This minimum, referred to as the Antarctic ozone hole, is due to heterogeneous ozone destruction on surfaces of PSC particles involving chlorine from man-made chlorofluorocarbons (CFCs). The Arctic stratosphere has strong interannual variability and analogous ozone destruction occurs here only during "cold" winters when temperature falls below the necessary threshold for PSC formation. The tropical minimum of total ozone (approximately 30°S-30°N) is observed at all seasons because of the high tropical tropopause and poleward ozone transport.

3. Ozone variability on synoptical scale

3.1 Ozone-weather relationship

Besides of the annual cycle presented in Fig. 2.6, total ozone undergoes strong day-to-day variations associated with synoptical processes and these variations can be comparable with the annual cycle magnitude. Dobson et al. (1929), based on total ozone observations from several European sites, found that on average high total ozone values coincide with cyclones and low values with anticyclones. The weather-ozone relationship results from redistribution of ozone in the lower stratosphere by horizontal and vertical advection (e. g. Reed, 1950; Salby and Callaghan, 1993; Wirth, 1993). The passage of a wave crest (anticyclone) causes ascending motions in the upper troposphere and lifting of the tropopause as well as adiabatical cooling (Fig. 3.1a). Since the concentration of ozone is low below the tropopause and rapidly increasing above (Fig 3.1c), such ascending motion results in convergence of ozone-poor air below the tropopause and divergence of ozone-rich air above, leading to net decrease in total ozone column. The passage of a wave trough (cyclone) has the opposite effect and total ozone increases (Fig 3.1b). The same mechanism explains the fact that total ozone correlates well with temperature and geopotential in the UTLS region. Meridional advection also plays an important role in the ozone-weather relationship. Ozone amount increases northward in the NH

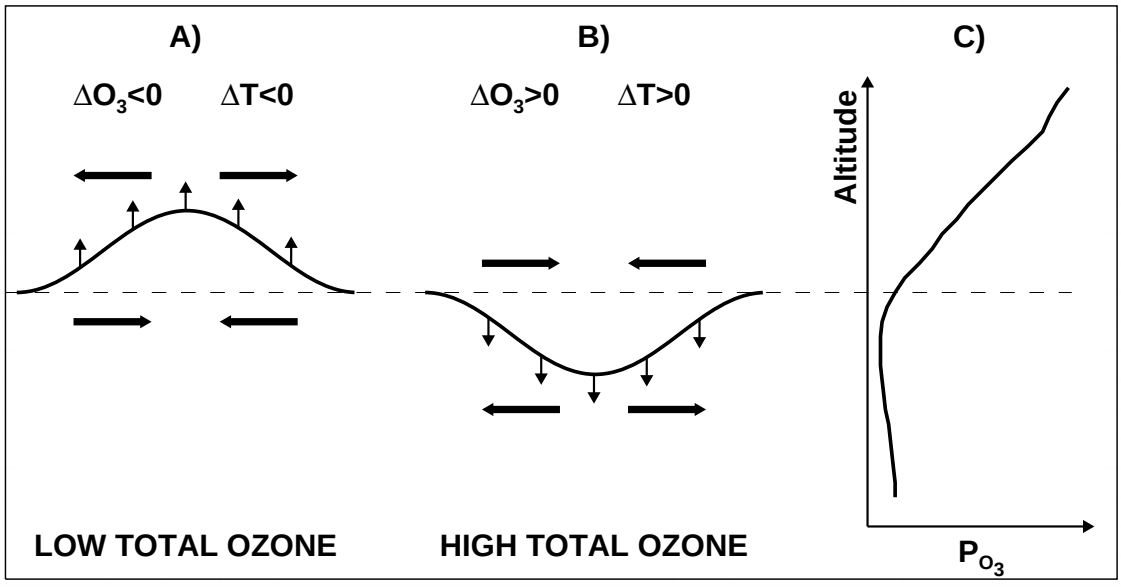

Figure 3.1. Schematic picture, showing changes in ozone and temperature associated with passage of a ridge (a) and a trough (b) near the tropopause. Dashed line represents an average position of the tropopause while thick line is deviations of the tropopause from the average. A profile of p_{O_3} based on the 1989-2001 climatology for January at Sodankylä (67.4°N, 26.6°E) is shown in (c).

extratropics (with the exception of the summer polar region) thus southward advection associated with troughs brings air with higher ozone concentration while northward advection in ridges brings air with lower ozone concentration. The maximum negative correlation between total ozone and geopotential are found in the region which coincides with the strongest northward ozone gradient (Stanford et al., 1995). Hence both vertical and meridional advection works in the same direction producing growth of total ozone in troughs and reduction in ridges.

3.2 Baroclinic waves in summer total ozone

During summertime, medium-scale baroclinic waves (zonal wavenumbers 4-7) frequently dominate in the SH midlatitude troposphere (Randel and Standford, 1985). These waves have eastward phase velocity with a period 5-15 days and a high degree of zonal symmetry. In contrast, in the NH troposphere, medium-scale waves do not show such zonal symmetry and phase continuity (Yu et al., 1984) probably due to orographical heterogeneity (Hayashi and Golder, 1983). Yu et al. (1984) suggested that in the NH several uncorrelated medium-scale wave packets can be emitted from active baroclinic regions. Numerical modelling (Simmons and Hoskins, 1979) showed that baroclinic waves develop downstream of an initial disturbance in a baroclinically unstable atmosphere. The main regions of baroclinic instabilities are the midlatitude jet streams (storm tracks) and baroclinic waves in the storm tracks tend to be organised in localised wave packets with downstream development (Chang, 1993).

In SH summer, medium-scale baroclinic waves prevail in dynamical variability of the UTLS region and influence the global distribution of chemical compounds such ozone (Schoeberl and Krueger, 1983) and water vapour (Stone et al., 1996). During summertime wave-like ozone oscillations are observed more locally in NH middle and high latitudes. Hitchman et al. (1999) have described oscillations in total ozone related to synoptic baroclinic waves with a period about 2 weeks and amplitude of 40 DU at Fairbanks (65°N, 155°W) during Arctic summer 1997. Roldugin et al. (2000) (Paper I) have found waves in total ozone at Aral Sea (46.8°N, 61.7°E) and Karaganda (50°N, 73°E) in Middle Asia and at Tromsø (69.6°N, 19.0°E) and Murmansk (69.0°N, 33.0°E) in Northern Scandinavia during several summers in 80s-90s. The waves have periods of 10-20 days and amplitudes of about 20-50 DU that is similar to the results reported by Hitchman et al. (1999) for Fairbanks. Mainly the period of the waves is the same in Middle Asia and Northern Scandinavia when the waves are well pronounced over both regions, for example 1986 (15 days), 1987 (16 days) and 1989 (12 days) but can also be different as in 1990 (14 days in Middle Asia and 21 days in Northern Scandinavia). Analogous waves are observed in geopotential (at the 500-70 hPa levels) and tropopause pressure, in agreement with the ozone-weather relationship described in paragraph 3.1. By cross-correlation analysis, the wave disturbances over Middle Asia were determined as moving eastward with a zonal phase speed of about 15 deg/day or 13 m/s, thus the ozone waves are caused by eastward travelling waves.

These eastward travelling waves in the NH summer troposphere are usually defined as medium-scale baroclinic waves. Figure 3.2 shows the zonal wind at 250 hPa for July 1987 when the 16-day wave was observed over Middle Asia and Northern Scandinavia. Both regions are located eastward (downstream) and slightly poleward of the jet stream maxima. A similar position of the jet stream maxima exists for other years with pronounced waves over both regions (for example 1986, 1989, 1990). A westward position of the baroclinically active regions relative to Middle Asia and Northern Scandinavia is in agreement with downstream development of baroclinic waves from models (Simmons and Hoskins, 1979) and observations (Chang, 1993). Wave packets emitted from the North Atlantic storm track have a tendency to refract equatorward to the subtropical jet (Hakim, 2003), consistent with the existence of a waveguide between two jet streams (Fig. 3.2). Hence wave motions with equal periods for both regions may be caused by the same wave packet propagating from the North Atlantic. The

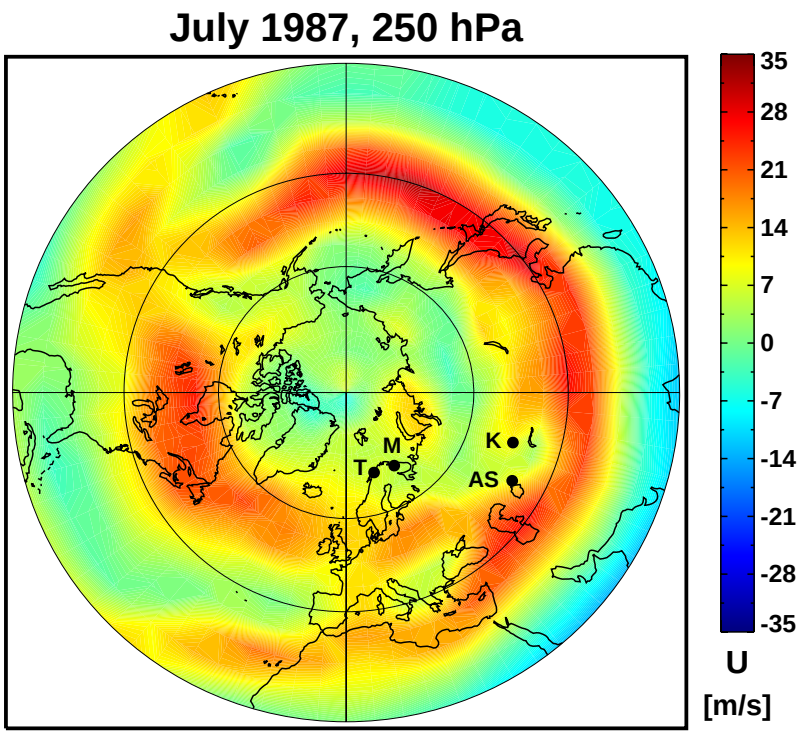

Figure 3.2. Zonal wind at 250 hPa for July 1987. Tromsø (T), Murmansk (M), Aral Sea (AS), and Karaganda (K) are marked by dots.

suggestion made by Roldugin et al. (2000) (Paper I), that the waves may be generated by Scandinavian mountains and convective motions over the hot Kara Kum desert in Middle Asia, is most likely not correct however. The sources of the observed waves are likely to be baroclinically unstable regions associated with the jet streams.

3.3 A low ozone episode over Scandinavia in August 2003

Another phenomenon related with ozone redistribution in the lower stratosphere is low ozone episodes (LOEs) or so called “ozone miniholes”, though a particular definition depends on the threshold chosen. In contrast to the Antarctic ozone hole, which is due to chemical ozone loss, ozone miniholes are dynamical in origin and presenting substantial transient decreases in total ozone during several days (1000-3000 km horizontal scale) over middle and high latitudes of both hemispheres. Two main mechanisms are responsible for the formation of LOEs, namely: meridional transport from regions with lower ozone concentration and adiabatic lifting (Fig. 3.1a) associated with anticyclonic conditions in the troposphere. LOEs tend to occur during the October-January period in the NH and the distribution of LOEs is strongly biased toward the North Atlantic/European region (Hood et al., 2001). Such bias is a consequence of the climatological minimum in total ozone during fall and winter over the North Atlantic/European region that is related to the structure of quasi-stationary Rossby waves (Hood and Zaff, 1995).

There have been many studies of intense LOEs occurring in the fall and winter-spring seasons (Newman et. al., 1988; McKenna et al., 1989; Rabbe and Larsen, 1995; Allen and Nakamura, 2002; Koch et al., 2005) while only a few studies have investigated LOEs during the summer season (Lloyd at al., 1999; Orsolini et al., 2003; Orsolini and Nikulin, 2005 (Paper IV)). Orsolini et al. (2003) showed that two LOEs over Northern Europe in summer 2000 resulted from the conjunction of two factors: a) the occurrence of an anticyclonic centre in the

troposphere, b) the displacement aloft of the anticyclone, of the mid-stratospheric pool of low-ozone air which develops over the Arctic in summer, due to the ozone gas phase destruction acting during long sunlight hours. An intense LOE was observed over Scandinavia and the North Sea during the European heat wave of August 2003 (Orsolini and Nikulin, 2005) (Paper IV). The mechanism of LOE formation is similar to that described Orsolini et al. (2003): the conjunction of an anomalous strong anticyclone over Europe, and a displaced Arctic pool of low-ozone air in the stratosphere at 30 hPa, aloft of the anticyclone. The anomalous anticyclonic conditions are related to the blocking phenomenon when a high amplitude anticyclone develops, remains nearly stationary and breaks down the eastward movement of migratory weather systems. Nakamura et al. (1997) have found that the incoming wave activity flux associated with a quasi-stationary Rossby wave train plays a dominant role in blocking development over Europe, whereas synoptic-scale transients are very important over the North Pacific. In fact the anomalous strong anticyclone over Europe in August 2003 developed as a part of a Rossby

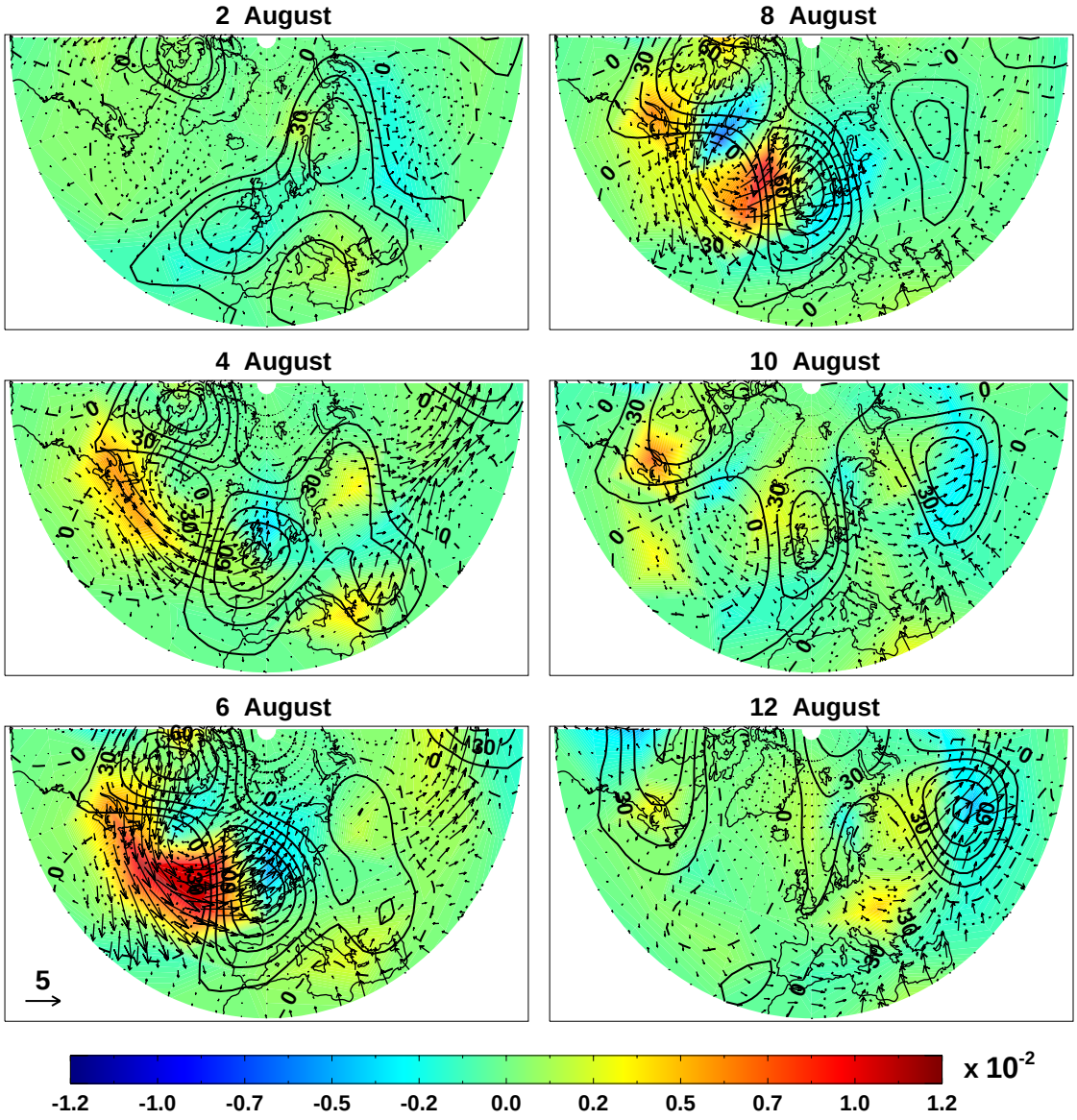

Figure 3.3. The 100 hPa WAF, units of m^2 s^{-2}, and band-passed geopotential (gpm) on six days in August 2003 (August 2, 4, 6, 8, 10, 12). The horizontal WAF component si shown as arrows and the vertical component is colour shaded. Geopotential contours are 15 gpm.

wave train originated from the Western Atlantic (Fig. 3.3). In order to investigate the blocking life cycle, wave activity flux (WAF) associated with quasi-geostrophic, quasi-stationary disturbances, embedded on a non-zonal basic state, is calculated following the method of Takaya and Nakamura (2001). The WAF is parallel to the local three-dimensional group velocity in the WKB limit. The basic state is defined as the 31-day running mean and disturbances are departures of low-pass-filtered data (cut-off period 8 days) from the basic state. The wave train began to form on August 2 over the Atlantic with the developing blocking over Europe at the leading edge of the wave train. In the following days, August 4-8, increasing horizontal WAF across the Atlantic converged into the amplifying European blocking and no wave activity propagation was evident farther downstream. On August 6-8, the upward WAF increased noticeably, upstream of the blocking. After the peak, a release of wave activity (August 10-12) was observed downstream of the dissipating blocking. Schematically, the blocking evolution leading to the LOE in August 2003 was similar to the composite evolution of the strongest blocking episodes that involve wave trains over the Atlantic (Nakamura et al., 1997).

The observed wave train is a rather deep event in vertical extent. Only waves with the longest wavelength can propagate through westerlies into the stratosphere (Charney and Drazin, 1961). Although synoptic-scale waves forming wave trains are strongly evanescent they can also propagate upward in zonally confined waveguides (Canzizni et al., 2003). A longitude-altitude cross-section at on August 10 at 60°N (Fig. 9, Paper IV) shows that wave train anomalies extend well into the middle stratosphere. The disturbances are still strong at 50 hPa, but have weak influence at 30 hPa where low ozone concentration is found. The wavenumber-frequency analysis of the geopotential at 60°N and 30 hPa, over the period July 6 to August 22, reveals westward propagating wave 1 and 2, with respective periods of 15 and 20 days. These waves are not related to the wave train since they exist during the whole summer and may be identified as free Rossby waves (normal modes) which are also observed in mid-stratospheric ozone (Hoppel et al., 1999; Akiyoshi et al., 2004). Intense LOEs occur several times during summer depending on the formation and intensity of tropospheric anticyclones, and their position with respect to westward travelling mid-stratospheric ozone waves.

4. Decadal and interannual variability in midlatitude total ozone

4.1 Processes affecting ozone in the extratropics

Since the discovery of the Antarctic ozone hole (Farman et al., 1985) and the ozone decrease in mid and high latitudes of both hemispheres (e. g. Stolarski et. al., 1991) a lot of efforts has been directing to explain the observed ozone changes. Now it is well documented that winter-spring ozone variations in the polar regions are a result of ozone loss involving activation of stratospheric chlorine from man-made CFCs under low temperatures (Solomon, 1999) and planetary wave activity which strongly defines poleward ozone transport and the evolution of the polar vortices (Newman et al., 2001; Salby and Callaghan, 2002; Weber et al., 2003). Bromine compounds also make an important contribution to polar ozone loss (Chipperfield and Pyle, 1998). Interhemispheric differences in topography and consequently in wave activity determine the asymmetry of polar ozone loss in two hemispheres. Wave activity is weaker in the SH and the well developed and stable Antarctic vortex creates the necessary dynamical preconditions (low temperatures) for triggering of ozone loss during August-November almost every year. As an exception, an unusual strong wave event in September 2002 led to the first observed major warming in the SH and the smallest ozone hole since 1988 (Newman and Nash,

2005). Wave activity is stronger in the NH which results in the warmer and more disturbed Arctic vortex as well as more intense poleward ozone transport compared to the SH. Ozone loss in the Arctic stratosphere occurs only in some years, during limited periods, when the low temperatures necessary for PSC formation are reached.

While ozone variability in the polar regions has been adequately explained a detailed understanding of the midlatitude ozone trends and interannual variations is still required (WMO, 2003). Several mechanisms affecting ozone at the NH midlatitudes have been proposed. Chemical processes (direct or indirect) include ozone loss through chlorine activation on the surface of sulphate aerosols and ice particles (Solomon et al., 1996, 1998), transport of ozone-depleted or chlorine-activated air from the polar vortex (Knudsen and Andersen, 2001; Chipperfield, 2003; Handjinicolaou and Pyle, 2004). Purely dynamical processes contributing to midlatitude ozone variability can be separated into two general groups: the tropospheric circulation which is responsible for ozone redistribution in the UTLS region and poleward ozone transport by the Brewer-Dobson circulation in the stratosphere. The tropospheric influence is related to several factors: intrusions of ozone-poor air from the tropical upper troposphere (Hood et al., 1999); the amplitude and phases of quasi-stationary planetary scale waves (Kurzeja, 1984; Hood and Zaff, 1995); large-scale modes such as the Arctic Oscillation and the North Atlantic Oscillation (Appenzeller et al., 2000; Nikulin and Repinskya, 2001 (Paper II)). The poleward ozone transport in the stratosphere strongly depends on wave forcing and includes mean meridional advection and eddy transport (e. g. Randel et al., 2002; Nikulin and Karpechko, 2005 (Paper V)). However, most of the mentioned processes are interrelated thus clear separation of contributions from different processes to ozone variability is still not well defined.

4.2 Antiphase behaviour of midlatitude total ozone and the AO and NAO indexes

The NAO (Bliss and Walker, 1932) and its global extension AO or Northern Annular Mode (NAM) (Thompson and Wallace, 1998; Hartmann et al., 2000) are large-scale modes of atmospheric variability in the NH extratropics related to decadal and interannual variability in circulation of the troposphere and the stratosphere (Hurrel, 1995; Thompson and Wallace, 2000; Thompson et al., 2000). The statistical relationship between total ozone anomalies over Western Europe and the characteristics of the Azores high - the surface pressure (p_{AH}) at its center and the latitude (φ_{AH}) of the center were studied by Bekoryukov et al. (1995). They have found that during winter (1957-1993), total ozone anomalies anticorrelate with both parameters and a negative trend in total ozone is associated with a positive trend of the quantities p_{AH} and φ_{AH}. The Azores high is an integral part of the NAO and the following studies have shown consistent antiphase behaviour between total ozone over Western Europe and the NAO index (Zvyagintsev and Kruchenitskii, 1995; Appenzeller et al., 2000; Brönnimann et al., 2000). Since the AO can be expressed as a hemispheric extension of the NAO, and indexes of the NAO and AO are coherent (Thompson and Wallace, 1998), it is not surprising that a negative correlation between total ozone and the AO index was also found in the NH extratropics (Thompson and Wallace, 2000; Brönnimann et al., 2000; Nikulin and Repinskya, 2001 (Paper II)). About 40% of variance in March total ozone north of 40°N (1979-1993) can be linked to the AO (Thompson and Wallace, 2000).

Nikulin and Repinskya (2001) (Paper II) have shown that the second empirical orthogonal function (EOF) of total ozone for November-April (TOMS, 1979-1992) has some similarities with the AO structure which is defined as the first EOF of geopotential, and coefficients of these EOFs are anticorrelated. The second EOF (Fig 4.1) represents a positive zonal ring with a discontinuity over the western coast of North America and a maximum over eastern Siberia.

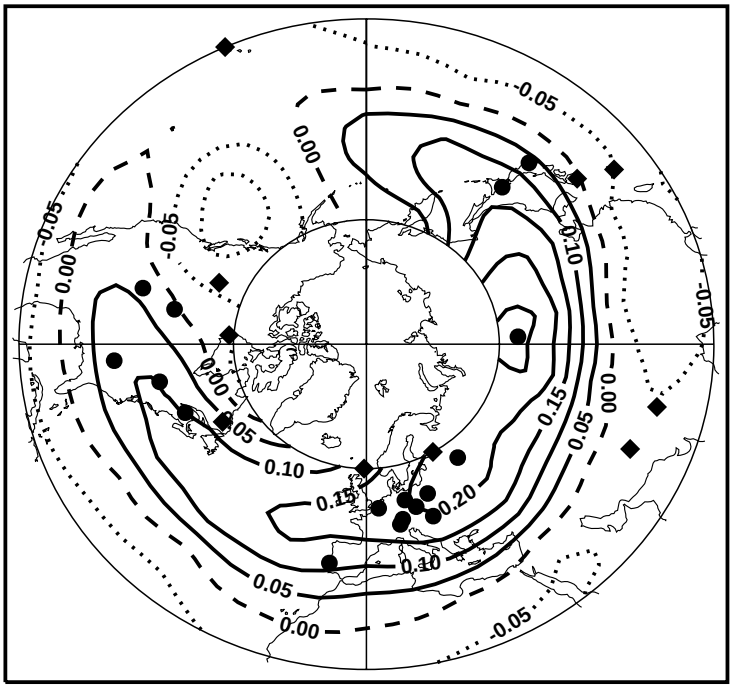

Figure 4.1. Second EOF of the monthly mean total ozone anomalies over the time period 1979–1992 (November–April). Circles and squares indicate the ozonometric stations with statistically significant and insignificant correlations (at the 95% confidence level), respectively, between the NAO index and total ozone anomalies (both averaged over December–March).

The high positive AO index is associated to lower-than-usual ozone values within the positive zonal ring in Fig. 4.1 with the lowest anomalies over eastern Siberia and vice versa. The strongest correlation between the AO index and total ozone in March was also found over eastern Siberia (Thompson and Wallace, 2000, Fig. 12b). Since the 14 years of the TOMS total ozone series are a rather short period, the relationship between total ozone the AO has been studied on the basis of longer series of measurements from the groundbased ozonometric network. Stations situated in the latitudinal belt 20°-60°N are shown in Fig. 4.1 and separated according to significant (circles) or insignificant (squares) correlation between total ozone and the NAO index averaged for December-March. It is seen that the stations with significant correlation (see Table 2, Paper II) lie within the zonal semi-ring determined by EOF2 of total ozone. The correlation between the NAO index and total ozone is strongest at stations located in the region of maximum positive values of EOF2 and decreases on the periphery of the zonal semi-ring. On average, the correlation coefficient for stations situated within the maximum of EOF2 is -0.6 which gives about 35% of variance in total ozone coupled to the NAO. Low-pass filtered total ozone and the NAO index show similar antiphase behaviour on a decadal timescale. Since the late 1960s, when the AO and NAO indexes were minimal, both indexes started to increase and reached abnormally high positive values in the mid 1990s. Simultaneously with an increase in the NAO and AO indexes, total ozone started to decrease in mid and high latitudes of the NH.

Anticorrelation between total ozone and the AO and NAO indexes has been related to the tropopause height, which varies synchronously with both indexes with distinct geographical patterns (Appenzeller et al., 2000; Brönnimann et al., 2000; Thompson et al., 2000). In addition during winter, the AO and NAO are coupled to the strength of the polar vortex above: a positive (negative) phase of both modes corresponds to a strong (weak) polar vortex. In turn, variability

in the strength of the polar vortex reflects variability in wave forcing and consequently is related to the Brewer-Dobson circulation. Hence anticorrelation between total ozone and the AO and NAO indexes should also mirror variations in the poleward ozone transport (Nikulin and Repinskya, 2001) (Paper II). The anomalous values of the AO index are found to appear in the stratosphere first and then propagate downward over periods of several weeks (Baldwin and Dunkerton, 1999). Polvani and Waugh (2004) have shown that anomalous low (high) upward wave activity fluxes at 100 hPa precede the high (low) AO index near the surface by up to 60 days. Therefore the observed relation between total ozone and the AO index may be caused by preceding upward wave activity propagation from the troposphere into stratosphere. One question which is needed to be clarified is a link between upward wave activity and the following response in the tropopause height.

After the mid 1990s, the NAO and AO indexes showed a tendency to the negative phase (Overland and Wang, 2005) while total ozone in the NH midlatitudes began to increase (Reinsel et al., 2002). This latest change in long-term ozone behaviour, so called "turnaround" may be linked to the beginning of ozone recovery due to decline of ozone-depleting substances in the atmosphere. However, the increase in total ozone coincides with a cluster of warm stratospheric winters (Manney et al., 2004) with much lower (or almost none) than usual potential for PSC formation and ozone loss. Such warm winters with a weak and disturbed polar vortex are a result of stronger wave activity propagating into the stratosphere and consequently stronger poleward ozone transport. Modelling results with fixed halogen loading at the 1980s levels showed that all of the observed upward total ozone trends from 1994 to 2003 in the NH midlatitudes are reproduced by the model which is forced only by transport changes (Hadjinicolaou et al., 2005). Hence the recent upward ozone trend is most probably influenced to a larger extent by changes in dynamics than by decline of ozone-depleting substances.

4.3 Midlatitude ozone buildup and the Brewer-Dobson circulation

Seasonal variations in midlatitude total ozone reflect a balance between transport and photochemical loss with a remarkable buildup through winter when poleward ozone transport is dominant. Anomalies established in the wintertime midlatitude ozone buildup persist (with photochemical decay) until the end of the following autumn, and then are rapidly erased once the next winter's buildup begins (Fioletov and Shepherd, 2003). It is recognized that the wintertime ozone buildup in the extratropics results from the Brewer-Dobson circulation which is driven by upward propagating waves from the troposphere. The positive correlation between wave forcing and extratropical ozone has been demonstrated by several authors (Nagatani and Miller, 1987; Fusco and Salby, 1999; Randel et al., 2002; Salby and Callaghan, 2002; Weber et al., 2003). A close correlation ($r \approx 0.8$-0.9) exists between wintertime total ozone tendency ($\Delta O_3 / \Delta t$) over mid and high latitudes and wave forcing accumulated during winter (Salby and Callaghan, 2002; Weber et al., 2003). Midlatitude $\Delta O_3 / \Delta t$ shows weaker correlation ($r \leq 0.6$) in January-March while a lack of correlation is observed in November-December (Randel et al., 2002). Since the midlatitude ozone buildup starts between October and November (Fioletov and Shepherd, 2003) and this is thought to result from the meridional stratospheric transport, the lack of correlation in November-December seems somewhat surprising.

Nikulin and Karpechko (2005) (Paper V) have shown that the NH midlatitude ozone buildup has a stable relationship with the mean meridional circulation in all months from October to March, though in October this relation is regional and in December it is somewhat questionable. The buildup begins locally in October with positive ozone tendencies over the North Pacific, which spread eastward and westward in November and finally cover all midlatitudes in December. During October-January a longitudinal distribution of the ozone tendencies mirrors a

structure of quasi-stationary planetary waves in the lower stratosphere and has less similarity with this structure in February-March when chemistry begins to play a more important role. Eddy heat flux, the residual velocities and temperature tendency are used as proxies to estimate the contribution from the mean meridional circulation to interannual variability of monthly $\Delta O_3/\Delta t$. On average, for all months from November to March, absolute values of correlation coefficients between zonal mean $\Delta O_3/\Delta t$ (50°-60°N) and HF, $\Delta T/\Delta t$ or $\overline{w}^*$ are close to 0.7. However, the correlation patterns between $\Delta O_3/\Delta t$ and HF are not uniform during the buildup (Fig. 3, Paper V) and maximal values of correlations are often located above 100 hPa and at different latitudes. That is the opposite to correlation patterns of $\Delta O_3/\Delta t$ with $\Delta T/\Delta t$ and $\overline{w}^*$ which are almost homogeneous from month to month. Hence HF averaged over the usual region 45°-75°N, 100 hPa is not always an optimal proxy for total ozone variability in midlatitudes. One partial exception is December, in the middle stage of the buildup, when $\Delta T/\Delta t$ and HF have weaker correlation (r_{max}=0.45) with $\Delta O_3/\Delta t$ while the $\overline{w}^*$ correlation coefficient (r_{min}=-0.7) is similar to that in other months. No explanation has been found for this feature. In October, zonal mean ozone tendencies have no coupling with the proxies. However, positive tendencies averaged over the North Pacific (60°-70°N, 105°-225°E) correlate well, with all of them suggesting that intensification of northward ozone transport starts locally over the Pacific already in October.

Assuming a linear relation, half of the interannual variability in the midlatitude ozone buildup for 1980-2002 can be linked to the mean meridional circulation. The obtained half of observed variance in $\Delta O_3/\Delta t$ is lower than in the results of Salby and Callaghan (2002) and Weber et al. (2003) for total ozone averaged over extratropics. At the same time 50% of explained variance is higher than the results of Randel et al. (2002) and Hood and Soukharev (2005) for zonal mean $\Delta O_3/\Delta t$ at different latitudes in the 35°-60°N region where the explained variance is less than 50%. Hence the obtained results correspond with the previous results according to the chosen latitude belt (50°-60°N).

5. Early winter upward wave activity flux as a precursor of midwinter circulation

It has been demonstrated that interannual variability of the Arctic stratosphere temperature and extratropical ozone is strongly correlated with strength of the Brewer-Dobson circulation (e. g. Newman et al., 2001; Salby and Callaghan, 2002; Nikulin and Karpechko, 2005 (Paper V)). The primary forcing of the Brewer-Dobson circulation originates from upward-propagating, tropospherically generated waves. Since trends have been documented in both the stratospheric temperature (Ramaswamy et al., 2001) and the total ozone (Staehelin et al., 2001) a lot of effort has been made to connect these changes to the changes in wave forcing. Several studies (Newman and Nash, 2000; Randel et al., 2002; Hu and Tung, 2002, 2003) have led to conclusions about significant negative trends in planetary wave forcing averaged for January-February (JF) or January-March and insignificant positive trends in November-December (ND). However, in separate months only negative trends in January are close to statistical significance. The obtained results suggest that the behaviour of the upward wave propagation in the stratosphere on decadal time scales differs between early and midwinter.

Differences in wave propagation behaviour between early and midwinter are also found in interannual variations (Karpetchko and Nikulin, 2004) (Paper IV). Figure 5.1 shows one-point correlations of the 20-hPa ND total heat flux averaged over 45°-75°N with the JF total heat flux for 1979-2005. Two distinct minima are evident: one in the troposphere at 400 hPa, 55°N and another in the stratosphere at 10 hPa, 50°N. Positive correlations cover the region from 300 to 30 hPa between 30° and 45°N. Spectral analysis revealed that in the midlatitude stratosphere the

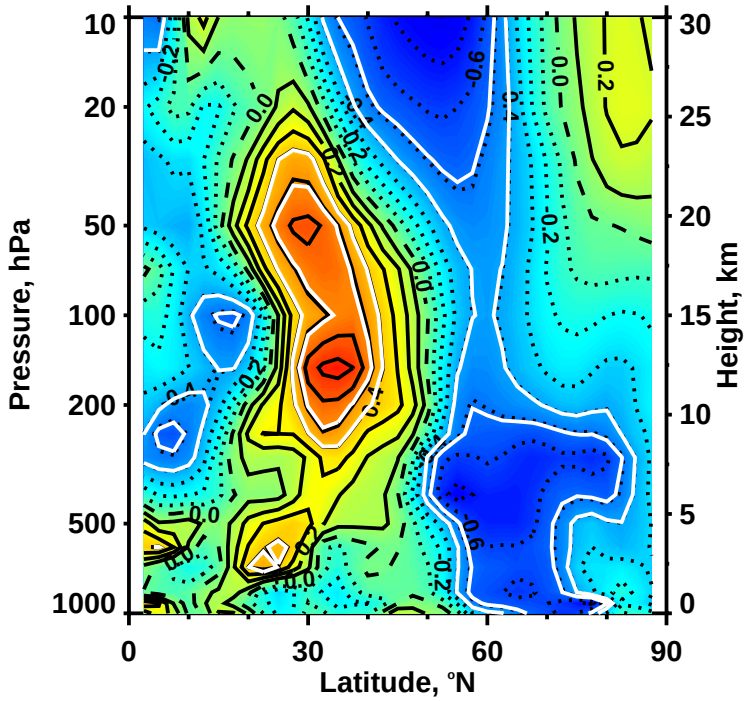

Figure 5.1. Correlation between the November-December heat flux at 20 hPa averaged over 45°-75°N and the January-February heat flux (1979-2005). Positive contour values are solid, negative values are dotted and zero contours are dashed. The first and second white lines are the 95% and 99% confidence levels.

ND heat fluxes mainly anticorrelate with the JF heat fluxes due to planetary waves (zonal wavenumbers 1-3) while in the midlatitude troposphere they anticorrelate better with total flux. The JF heat flux due to waves 4-7 mainly contributes to the positive correlation area near and above the subtropical jet stream. According to Fig 5.1, upward wave activity flux during midwinter is weaker throughout the majority of the midlatitude stratosphere and troposphere in years with strong wave activity flux during the early winter and vice versa. These intraseasonal variations are actually related to the stratospheric vacillations (Holton and Mass, 1976) and their period is determined by the time that the stratosphere takes to relax to radiative equilibrium.

Anomalous wave activity fluxes in early winter also strongly influence the subsequent evolution of the midwinter circulation in the stratosphere and troposphere. Schematically, two scenarios of the midwinter circulation corresponding to anomalous weak and strong wave fluxes in early winter are presented in Fig. 5.2. It is known that zonal wind anomalies in the winter stratosphere propagate downward and poleward (Kodera et al., 1990). In early winter zonal wind anomalies in the midlatitude stratosphere are created by anomalous wave activity flux and downward propagation of these anomalies is initialised by the early winter wave forcing (Fig. 5, Paper III). The vertical wind shear (U_z) changes are an integral part in the mechanism for intraseasonal heat flux anticorrelation. According to analysis by Hu and Tung (2002), stronger U_z increases the refractive index and therefore enhances upward wave propagation. In contrast, the strengthened polar night jet tends to refract planetary waves equatorward. Presumably, increased wave fluxes from the troposphere overcompensate the effect of increased equatorward wave reflection. The increased wave fluxes from the troposphere could be explained by enhanced generation of wave activity. However, direct estimation of wave activity from data is difficult and verification of this hypothesis is a subject for model experiments.

The earlier reported trends in wave activity flux have been confirmed by Karpetchko and Nikulin, (2004) (Paper III) for 1979-2002: 1) significant negative trends in the JF heat flux

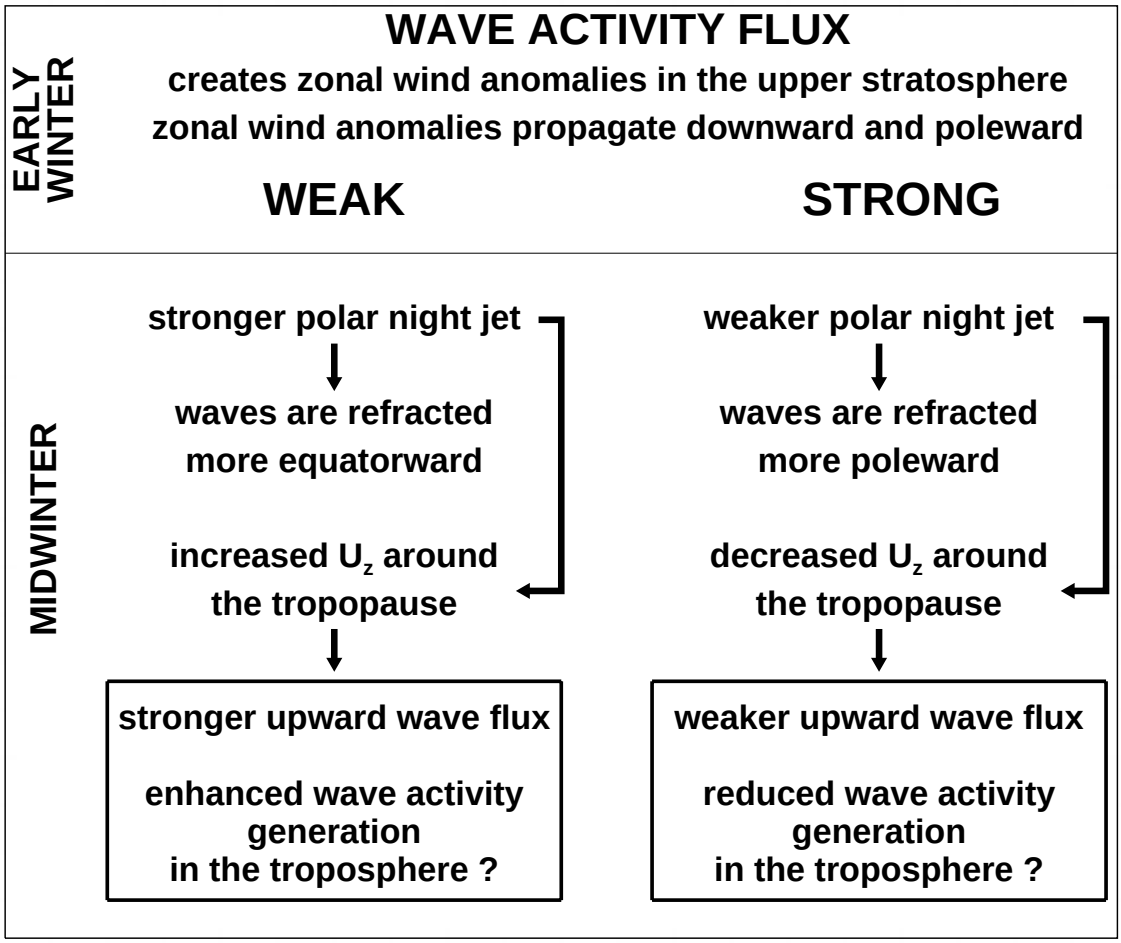

Figure 5.2. Schematical diagram showing influence of anomalous early winter wave activity fluxes on the midwinter circulation in the troposphere and stratosphere.

north of 60°N spreading from the lower stratosphere to middle troposphere, 2) positive trends at the edge of statistical significance in the ND heat flux in the polar stratosphere. The opposite heat flux trends in early and midwinter are not a result of the intraseasonal heat flux anticorrelation because spatial patterns of anticorrelation and trends do not coincide. The origin of the significant negative trends in midwinter wave fluxes is still not clear. One proposed mechanism (e. g. Shindell, 1998, Hu and Tung, 2003) is that an enhanced meridional temperature gradient, related to increase in CO_2 or decrease in O_3 (or both together), leads to strengthened zonal winds, which consequently refract planetary waves away from the high latitudes. However, for the 1979-2002 period when the negative trends are observed in the JF heat flux, no significant trends were found in either stratospheric zonal winds nor in U_z. The modelling results with realistic changes in CO_2 and O_3 have revealed an increase in zonal winds and a decrease in eddy heat flux (Langematz et al., 2003) but these changes are not statistically significant. It appears that other processes (for example, from the troposphere) contribute to the observed wave flux trends. Finally it should be noted that trend estimations are very sensitive to the choice of period and removing or adding one year can appreciable change the results obtained.

Summary of the included papers

Paper I. Roldigin, V. C., Nikulin, G. N., and Henriksen, K., Wave-like ozone movement, Phys. Chem. Earth (B), 25, 511-514, 2000.

The Paper I examines wave-like total ozone variations occurring during summer over Northern Scandinavia and Middle Asia. The waves have periods of 10-20 days and eastward phase speeds of 11-15 °/day with typical amplitudes in total ozone of about 20-50 DU. Similar waves are found in geopotential and the tropopause pressure. The observed total ozone variations result from redistribution of ozone in the lower stratosphere by eastward travelling waves. The passing of wave crests causes the convergence of ozone-poor air under the tropopause and the divergence of ozone-rich air above leading to local increase in total ozone. Wave trough passage has the opposite effect. Meridional advection associated with crests (northward) and troughs (southward) work in the same direction: bringing ozone-poor air in crests and ozone-rich air in troughs, because of the northward ozone gradient.

Paper II. Nikulin, G. N., and Repinskya R. P., Modulation of total ozone anomalies in the midlatitude Northern Hemisphere by the Arctic oscillation, Izvestia - Atmospheric and Oceanic Physics, 37, 633-643, 2001.

The statistical relationship between midlatitude total ozone in the NH and the Arctic and North Atlantic oscillations is studied in Paper II. On the basis of empirical orthogonal functions, it is shown that a part of interannual variability in total ozone is coupled to the AO and NAO indexes. The second EOF of total ozone (1979-1992) has some similarities with the structure of the AO, defined as the first EOF of geopotential in the 1000-50 hPa layer, and the coefficients of these EOFs are anticorrelated. The use of longer total ozone series from the ground-based network revealed similar anticorrelation on interannual and decadal scales between total ozone and the index of the NAO, which is a regional part of the AO. The strongest anticorrelations are found at stations located in the region of maximal positive values of EOF2 of total ozone (Siberia, Europe). Since the late 1960s the NAO index started to increase and reached abnormally high values in the mid 1990s. Simultaneously with increase in the NAO index, total ozone started to decrease in the middle and high latitude of the NH. The antiphase behaviour of total ozone and AO and NAO indexes can be related to decrease in wave activity propagating from the troposphere into the stratosphere. Such a decrease leads to a stronger polar vortex (higher indexes of the AO and NAO) as well as to weaker poleward ozone transport. In addition a strong and cold vortex is preferable for triggering chemical ozone loss inside vortex that can influence midlatitude ozone through export of ozone depleted air from the vortex.

Paper III. Karpetchko, A., and Nikulin G., Influence of early winter upward wave activity flux on midwinter circulation in the stratosphere and troposphere, J. Climate, 17, 4443-4452, 2004.

Paper III presents evidence that upward wave activity fluxes in early winter to a substantial extent defines the midwinter circulation of the stratosphere and troposphere. The November-December stratospheric eddy heat flux (45°-75°N) is anticorrelated with several parameters in January-February, namely: eddy heat flux in the midlatitude stratosphere and troposphere, zonal wind north of 50°N in the 1000-10 hPa layer and the vertical wind shear near and above the tropopause (50-70°N). Hence weaker wave fluxes in early winter are associated with stronger wave fluxes, the well developed polar night jet and increased vertical wind shear in midwinter.

Stronger early winter wave fluxes have the opposite effect on the midwinter circulation. Intraseasonal anticorrelation of wave fluxes results from changes in the upward wave propagation in the troposphere which is sensitive to the vertical shear of zonal wind. The observed intraseasonal variations are actually related to the stratospheric vacillations and their period is determined by the time that the stratosphere takes to relax to radiative equilibrium. Trends in early and midwinter wave fluxes (1979-2002) are in agreement with the trends reported earlier: positive trends at the edge of statistical significance in November-December and significant trends in January-February. However, the origin of the trends is not clear since no significant trends were found in the zonal wind and the vertical wind shear for the same period.

Paper IV. Orsolini, Y. J., and Nikulin, G., A low ozone episode during the European heat wave of August 2003, Quart. J. Roy. Meteor. Soc., in press, 2005.

Paper IV studies the dynamical origins of formation of a low ozone episode over Scandinavia and the North Sea coinciding with the European heat wave of August 2003. The LOE results from the conjunction of a deep tropospheric blocking over Europe and a displaced Arctic pool of low-ozone air in the stratosphere at 30 hPa, aloft of the blocking. The blocking anticyclone developed as a part of a Rossby wave train originated from the Western Atlantic and its influence is seen up to the 50 hPa level. At the same time the disturbances have weak influence at 30 hPa where low ozone concentration is found. The wavenumber-frequency analysis of geopotential at 60°N and 30 hPa reveals westward propagating wave-1 and 2, with respective periods of 15 and 20 days. These waves are not related to the wave train since they exist during the whole summer and may be identified as free Rossby waves (normal modes) also observed in stratospheric ozone. Intense LOEs occur several times during summer depending on the formation and intensity of tropospheric anticyclones, and their position with respect to westward travelling mid-stratospheric ozone waves.

Paper V. Nikulin, G., and Karpechko, A., The mean meridional circulation and midlatitude ozone buildup, Atmos. Chem. Phys. Discuss., 5, 4223-4256, 2005.

Paper V deals with the development of wintertime ozone buildup over the NH midlatitudes from October to March and its statistical connection with the mean meridional circulation in the stratosphere. The buildup begins locally in October with positive ozone tendencies over the North Pacific, which spread eastward and westward in November and finally cover all midlatitudes in December. Eddy heat flux, the residual velocities and temperature tendency are used as proxies to estimate the contribution from the mean meridional circulation to interannual variability of monthly $\Delta O_3/\Delta t$. On average for all months from November to March (1979-2002), absolute values of correlation coefficients between zonal mean $\Delta O_3/\Delta t$ (50°-60°N) and HF, $\Delta T/\Delta t$ or $\overline{w}^*$ are close to 0.7. December, when strong correlation found only for $\overline{w}^*$ is a partial exception. Also HF averaged over the usual region 45°-75°N, 100 hPa is not always an optimal proxy for total ozone variability in midlatitudes because the strongest correlations do not coincide well with the mentioned region. Similar correlation was found for local positive $\Delta O_3/\Delta t$ over the North Pacific in October and the zonal mean proxies. The NH midlatitude ozone buildup has a stable statistical relationship with the mean meridional circulation in all months from October to March and half of interannual variability in monthly ozone tendencies can be explained by applying different proxies of the mean meridional circulation.

References

Akiyoshi, H., Sugita, T., Kanzawa, H., and Kawamoto, N., Ozone perturbations in the Arctic summer lower stratosphere as a reflection of NO_X chemistry and planetary scale wave activity, J. Geophys. Res., 109, doi:10.1029/2003JD003632, 2004.

Allen, D. R., and Nakamura, N., Dynamical reconstruction of the record low column ozone over Europe on 30 November 1999, Geophys. Res. Lett., 29, 1362, doi:10.1029/2002GL014935, 2002.

Andrews, D. G., and McIntyre, M. E., Planetary waves in horizontal and vertical shear: the generalised Eliassen-Palm relation and the mean zonal acceleration, J. Atmos. Sci., 33, 2031-2048, 1976.

Andrews, D. G., and McIntyre, M. E., Generalised Eliassen-Palm and Charney-Drazin theorems for waves on axisymmetric mean flows in compressible atmosphere, J. Atmos. Sci., 35, 175-185, 1978.

Andrews, D. G., Holton, J. R., and Leovy C. B., Middle Atmosphere Dynamics, Academic Press, 489 p., 1987.

Appenzeller, C., Weiss, A. K., and Staehelin, J., North Atlantic Oscillation modulates total ozone winter trends, Geophys. Res. Lett., 27, 1131-1134, 2000.

Baldwin, M. P., and Dunkerton, T. J., Propagation of the Arctic Oscillation from the stratosphere to the troposphere. J. Geophys. Res., 104, 30937-30946, 1999.

Baldwin, M. P., Thompson, D. W. J., Shuckburgh, E. F., Norton, W. A., and Gillett, N. P., Weather from the Stratosphere?, Science, 301, 317-318, 2003.

Bekoryukov, V. I., Bugaeva, I. V., Zakharov, G. R., Koshel'kov, Yu. P., and Tarasenko, D.A., Study of the parameters of the Azores High affecting ozone variations in Western Europe, Izv. Akad. Nauk, Fiz. Atmos. Okeana, 31, 41–45, 1995.

Black, E., Blackburn, M., Harrison, G., Hoskins, B. J., and Methven, J., Factors contributing to the summer 2003 european heat wave, Weather, 59, 217-222, 2004.

Blinova, E. N., Hydrodynamic theory of pressure waves, temperature wave and atmospheric actions centres, Dokl. Akad. Nauk SSSR, 39, 284-287, 1943.

Brasseur, G., and Solomon, S., Aeronomy of the middle atmosphere, Reidel Publish., Dordrecht, 452 pp., 1986.

Brewer, A. E., Evidence for a world circulation provided by the measurements of helium and water vapour distribution in the stratosphere, Q. J. Roy. Meteorol. Soc., 75, 351-363, 1949.

Brönnimann, S., Luterbacher, J., Schmutz, C., Wanner, H., and Staehelin, J., Variability of total ozone at Arosa, Switzerland, since 1931 related to atmospheric circulation indices, Geophys. Res. Lett., 27, 2213–2216, 2000.

Canziani, P. O., and Legnani, W. E., Tropospheric-stratospheric coupling: extratropical synoptic systems in the lower stratosphere, Q. J. Roy. Meteorol. Soc., 129, 2315-2329, 2003.

Chang, E. K. M., Downstream development of baroclinic waves as inferred from regression analysis, J. Atmos. Sci., 50, 2038-2053, 1993.

Charney, J. G., and Drazin, P. G., Propagation of planetary-scale disturbances from the lower into the upper atmosphere, J. Geophys. Res., 66, 83-109, 1961.

Chipperfield, M. P., and Pyle, J. A., Model sensitivity studies of Arctic ozone depletion, J. Geophys. Res., 103, 28389-28403, 1998.

Chipperfield, M. P., A three-dimensional model study of long-term mid-high latitude lower stratosphere ozone changes, Atmos. Chem. Phys., 3, 1253-1265, 2003.

Christiansen, B., Downward propagation of zonal mean zonal wind anomalies from the stratosphere to the troposphere: Model and reanalysis, J. Geophys. Res., 106, 27307-27322, 2001.

Christiansen, B., Downward propagation and statistical forecast of the near surface weather, in press, J. Geophys. Res., 2005.

Dobson, G. M. B., Harrison, D. N., and Lawrence, J., Measurements of amount of ozone in the earth's atmosphere and its relation to other geophysical conditions, Proc. Roy. Soc., 122A, 456-486, 1929.

Dobson, G. M. B., Origin of distribution of the polyatomic molecules in the atmosphere, Proc. Roy. Soc. London, 236A, 187-193, 1956.

Dunkerton, T., On the mean meridional mass motions of the stratosphere and mesosphere, J. Atmos. Sci., 35, 2325-2333, 1978.

Farman, J. C., Gardiner, B. G., and Shanklin, J. D., Large losses of total ozone in Antarctica reveal seasonal ClO_x/NO_x interaction, Nature, 315, 207-210, 1985.

Fioletov, V. E. and Shepherd, T. G., Seasonal persistence of midlatitude total ozone anomalies, Geophys. Res. Lett., 30(7), 1417, doi:10.1029/2002GL016739, 2003.

Fusco, A. C. and Salby, M. L., Interannual variations of total ozone and their relationship to variations of planetary wave activity, J. Climate, 12, 1619-1629, 1999.

Hadjinicolaou, P. and Pyle, J. A.: The impact of Arctic ozone depletion on northern middle latitudes: interannual variability and dynamical control, J. Atmos. Chem., 47, 25-43, 2004.

Hadjinicolaou, P., Pyle, J. A., and Harris, N. R. P., The recent turnaround in stratospheric ozone over northern middle latitudes: A dynamical modeling perspective, Geophys. Res. Lett., 32, L12821, doi:10.1029/2005GL022476, 2005.

Hakim, G. J., Developing wave packets in the North Pacific storm track, Mon. Weather Rev., 131, 2824-2837, 2003.

Hartmann, D. L., Wallace, J. M., Limpasuvan, V., Thompson, D. W. J., and Holton, J. R., Can Ozone Depletion and Greenhouse Warming Interact to Produce Rapid Climate Change?, Proc. Nat. Acad. Sci., 97, 1412-1417, 2000.

Hayashi, Y., and Golder, D. G., Transient planetary waves simulated by GFDL spectral general circulation models. Part I: Effects of mountains, J. Atmos. Sci., 40, 941-950, 1983.

Haynes, P. H., Marks, C. J., McIntyre, M. E., Shepherd, T. G., and Shine K. P., On the "downward control" of extrotropical diabatic circulation by eddy-induced mean zonal forces, J. Atmos. Sci., 49, 651-678, 1991.

Hitchman, M. H., Buker, M. L., and Tripoli, G. J., Influence of synoptic waves on column ozone during Arctic summer 1997, J. Geophys. Res., 104, 25547-26563, 1999.

Holton, J. R., An introduction to dynamical meteorology, Academic Press, 511 pp., 1992.

Holton, J. R., Haynes, P. H., McIntyre, M. E., Douglass, A. R., Rood, R. B., and Pfister, L., Stratosphere-troposphere exchange, Rev. Geophys., 33, 403-439, 1995.

Hood, L. L., and Zaff, D. A., Lower stratospheric stationary waves and the longitude dependence of ozone trends in winter, J. Geophys. Res., 100, 25791-25800, 1995.

Hood, L. L., Rossi, S., and Baulen, M., Trends in the lower stratosphere zonal winds, Rossby wave breaking behaviour, and column ozone at northern midlatitudes, J. Geophys. Res., 104, 24321-24339. 1999.

Hood, L. L., Soukharev, B. E., Fromm, M., and McCormack, J. P., Origin of extreme ozone minima at middle to high northern latitudes, J. Geophys. Res., 106, 20925-20940, 2001.

Hood, L. L., and Soukharev, B. E., Interannual variations of total ozone at northern midlatitudes correlated with stratospheric EP flux and potential vorticity, J. Atmos. Sci., in press, 2005.

Hoppel, K. W., Bowman, K. P., and Bevilacqua, R. M., Northern hemisphere summer ozone variability observed by POAM II, Geophys. Res. Lett., 26, 827-830, 1999.

Hoskins, B. J., Towards a PV-theta view of the general circulation, Tellus, Ser. A, 43, 27-35, 1991.

Hu, Y., and Tung, K. K., Interannual and decadal variations of planetary wave activity, stratospheric cooling, and Northern hemisphere annular mode, J. Climate, 15, 1659–1673, 2002

Hu, Y., and Tung, K. K., Possible ozone-induced long term changes in planetary wave activity in late winter, J. Climate, 16, 3027-3038, 2003.

Hurrell, J. W., Decadal trends in the North Atlantic Oscillation: regional temperature and precipitation, Science, 269, 676-679, 1995.

Karpetchko, A., and Nikulin G., Influence of early winter upward wave activity flux on midwinter circulation in the stratosphere and troposphere, J. Climate, 17, 4443-4452, 2004.

Knudsen, B. M., and Andersen, S. B., Longitudinal variation in springtime ozone trends, Nature, 413, 699-700, 2001.

Koch, G., Wernli, H., Schwierz, C., Staehelin, J., and Peter, T., A composite study on the structure and formation of ozone miniholes and minihighs over central Europe, Geophys. Res. Lett., 32, L12810, doi:10.1029/2004GL022062, 2005.

Kurzeja, R. J., Spatial variability of total ozone at high latitudes in winter, J. Atmos. Sci., 41, 695-697, 1984.

Lloyd, S., Swartz, W. H., Kusterer, T., et al., Intercomparison of total ozone observations at Fairbanks, Alaska, during POLARIS, J. Geophys. Res., 104, 26767–26778, 1999.

Manney, G. L., Krüger, K., Sabutis, J. L., Sena, S. A., and Pawson, S., The remarkable 2003–2004 winter and other recent warm winters in the Arctic stratosphere since the late 1990s, J. Geophys. Res., 110, D04107, doi:10.1029/2004JD005367, 2005.

Matsuno, T., A dynamical model of the stratospheric sudden warming, J. Atmos. Sci., 28, 1479-1494, 1971.

McIntyre, M. E., How well do we understand the dynamics of stratospheric warmings?, J. Meteorol. Soc. Japan, 60, 37-65, 1982.

McIntyre, M. E., and Palmer, T. N., The “surf zone” in the stratosphere, J. Atmos. Terrest. Phys., 46, 825-849, 1984.

McIntyre, M. E., On global-scale atmospheric circulation, pp. 557-625 in Perspectives of fluid dynamics, edited by Batchelor, G. K., Moffatt, H. K., and Worster, M. G., Cambridge university press, 631 p., 2000.

McKenna, D. S., Jones, R. L., Austin, J., Browell, E. V., McCormick, M. P., Krueger, A. J., and Tuck, A. F., Diagnostic studies of the Antarctic vortex during the 1987 airborne Antarctic ozone experiment: ozone miniholes, J. Geophys. Res., 94, 11641–11668, 1998.

Nagatani, R. M., and Miller, A. J., The influence of lower stratosphere forcing on the October Antarctic ozone decrease, Geophys. Res. Lett., 14, 202-205, 1987.

Nakamura, H., Nakamura, M., and Anderson, J. L., The role of high and low-frequency dynamics in blocking formation, Month. Wea. Rev., 125, 2074-2093, 1997.

Newman, P. A., Lait, L. R., and Schoeberl, M. R., The morphology and meteorology of southern hemisphere spring total ozone miniholes, Geophys. Res. Lett., 15923-15926, 1998.

Newman, P. A., Nash, E. R., and Rosenfield, J. E., What controls the temperature of the Arctic stratosphere during the spring?, J. Geophys. Res., 106, 19999-20010, 2001.

Newman, P. A., and Nash, E. R., The unusual Southern Hemisphere stratosphere winter 2002, J. Atmos. Sci., 62, 614-628, 2005.

Nikulin, G. N., and Repinskya R. P., Modulation of total ozone anomalies in the midlatitude Northern Hemisphere by the Arctic oscillation, Izvestia - Atmospheric and Oceanic Physics, 37, 633-643, 2001.

Nikulin, G., and Karpechko, A., The mean meridional circulation and midlatitude ozone buildup, Atmos. Chem. Phys. Discuss., 5, 4223-4256, 2005.

Orsolini, Y. J., Eskes, H., Hansen, G., Hoppe, U-P., Kylling, A., Kyro, E., Notholt, J., Van der A, R., and Von der Gathen, P., Summertime low ozone episodes over northern high latitudes, Quart. J. Roy. Meteor. Soc., 129, 3265-3276, 2003.

Orsolini, Y. J., and Nikulin, G., A low ozone episode during the European heat wave of August 2003, Quart. J. Roy. Meteor. Soc., in press, 2005.

Overland, J. E., and Wang, M., The Arctic climate paradox: The recent decrease of the Arctic Oscillation, Geophys. Res. Lett., 32, L06701, doi:10.1029/2004GL021752, 2005.

Pawson, S., and Kubitz, T., Climatology of planetary waves in the northern stratosphere, J. Geophys. Res., 101, 16987-16996, 1996.

Polvani, L. M., and Waugh, D. W., Upward wave activity flux as precursor to extreme stratospheric events and subsequent anomalous surface weather regimes. J. Climate., 17, 3548-3554, 2004.

Rabbe, Å, and Larsen, S. H. H., On the low ozone values over Scandinavia during the winter of 1991-1992, J. Atmos. Terr. Phys., 57, 367-373, 1995.

Ramaswamy, V., Chanin, M.-L., Angell, J., et al., Stratospheric temperature trends: observations and model simulations, Rev. Geophys., 39, 71-122, 2001.

Randel, W. J., and Stanford, J. L., An observation study of medium-scale wave dynamics in the Southern Hemisphere summer. Part I: Wave structure and energetics, J. Atmos. Sci., 42, 1172-1188, 1985.

Randel, W. J., Wu, F., and Stolarski, R., Changes in column ozone correlated with the stratospheric EP flux, J. Meteorol. Soc. Japan, 80, 849-862, 2002.

Reed, R. J., The role of vertical motions in ozone –weather relationship, J. Meteorology, 7, 263-267, 1950.

Reinsel, G. C., Weatherhead, E., Tiao, G. C., Miller, A. J., Nagatani, R. M., Wuebbles, D. J., and Flynn, L. E., On detection of turnaround and recovery in trend for ozone, J. Geophys. Res., 107, 4078, doi:10.1029/2001JD000500, 2002.

Roldigin, V. C., Nikulin, G. N., and Henriksen, K., Wave-like ozone movement, Phys. Chem. Earth (B), 25, 511-514, 2000.

Rossby, C.-G., Relation between variations in the intensity of the zonal circulation of the atmosphere and the displacement of the semipermanent centers of action, J. Mar. Res., 2, 38-55, 1939.

Salby, M. L. and Callaghan, P. F., Fluctuations of total ozone and their relationship to stratospheric air motions, J. Geophys. Res., 98, 2715-2727, 1993.

Salby, M. L., Fundamentals of atmospheric physics, Academic Press, 627 pp., 1995.

Schoeberl, M. R., and Kruger, A. J., Medium scale disturbances in total ozone during Southern Hemisphere summer, Bull. Amer. Meteor. Soc., 64, 1358-1365, 1983.

Simmons, A. J., and Hoskins, B. J., The downstream and upstream development of unstable baroclinic waves, J. Atmos. Sci., 36, 1239-1254, 1979.

Solomon, S., Progress toward a quantitative understanding of Antarctic ozone depletion, Nature, 347, 347-354, 1990.

Solomon, S., Portmann, R. W., Garcia, R. R., Thomason, L. W., Poole, L. R., and McCormick, M. P., The role of aerosol variations in anthropogenic ozone depletion at northern midlatitudes, J. Geophys. Res., 101, 6713-6727, 1996.

Solomon, S., Portmann, R. W., Garcia, Randel, W., Wu, F., Nagatani, R., Gleason, J., Thomason, L. W., Poole, L. R., and McCormick, M. P., Ozone depletion at midlatitudes: Coupling of volcanic aerosol and temperature variability to anthropogenic chlorine. Geophys. Res. Lett., 25, 1871-1874, 1998.

Solomon, S., Stratospheric ozone depletion: A review of concepts and history, Rev. Geophys. 37, 275-316, 1999.

Staehelin, J., Harris, N. R. P., Appenzeller, C., and Eberhard, J., Ozone trends: a review. Rev. Geophys., 39, 231-290, 2001.

Standford, J. L., Ziemke, J. R., McPeters R. D., Krueger, R. D., and Bhartia P. K., Spectral analyses, climatology, and interannual variability of Nimbus-7 TOMS version 6 total ozone content. NASA reference publication 1360, 1995.

Stolarski, R. S., Bloomfield, P., McPeters, R. D., and Herman, J. R., Total ozone trends deduced from NIMBUS 7 TOMS data, Geophys. Res. Lett., 18, 1015-1018, 1991.

Stone, E. M., Randel, W. J., Stanford, J. L., Read, W. G., and Waters, J. W., Baroclinic wave observation observed in MLS upper tropospheric water vapour, Geophys. Res. Lett., 23, 2967-2970, 1996.

Takaya, K., and Nakamura, H., A formulation of a phase-independent wave-activity flux for stationary and migratory quasigeostrophic eddies on a zonally varying basic flow, J. Atmos. Sci., 58, 608-627, 2001.

Thompson, D. W. J, and Wallace, J. M., The Arctic Oscillation signature in the wintertime geopotential height and temperature fields, Geophys. Res. Lett., 25, 1297-1300, 1998.

Thompson, D. W. J, and Wallace, J. M., Annular modes in the extratropical circulation. Part I: Month-to-month variability, J. Climate, 13, 1000-1016, 2000.

Thompson, D. W. J., Wallace, J. M., and Hegerl, G. C., Annular modes in the extratropical circulation. Part II: Trends. J. Climate, 13, 1018-1036, 2000.

Vincent, D. G., Mean meridional circulation in the Northern Hemisphere lower stratosphere during 1964 and 1965, Quart. J. Roy. Meteor. Soc., 94, 333-349, 1968.

Walker, G. T., and Bliss, E. W., World Weather V, Mem. Roy. Meteor. Soc., 4, No. 36, 53-84, 1932.

Weber M., Dhomse, S., Wittrock, F., Richter, A., Sinnhuber, B.-M., and Burrows, J. P., Dynamical control of NH and SH winter/spring total ozone from GOME observations in 1995-2002, Geophys. Res. Lett., 30(11), 1583, doi:10.1029/2002GL016799, 2003.

Wirth, V., Quasi-stationary planetary waves in total ozone and their correlation with lower stratospheric temperature, J. Geophys. Res., 98, 8873-8882, 1993.

World Meteorological Organization (WMO), Scientific assessment of ozone depletion 2002, Report No 47, Geneva, 2003.

Yu, W., Stanford, J. L., and Martin R. L., Some interhemispheric comparisons of medium-scale waves in the lower stratosphere, J. Atmos. Sci., 41, 2084-2088, 1984.

Zvyagintsev, A. M., and Kruchenitskii, G. M., Connections between the total ozone in the midlatitude Northern Hemisphere and the North Atlantic Oscillation, Meteorol. Gidrol., No. 7, 65–70, 1996.

List of Acronyms

AO	Arctic Oscillation
BD	Brewer-Dobson
CFC	Chlorofluorocarbons
CPC	Climate Prediction Center
DU	Dobson Units
ECMWF	European Centre for Medium-Range Weather Forecasts
EOF	Empirical Orthogonal Function
EP	Eliassen-Palm
ERA	ECMWF Re-Analysis
HF	Heat Flux
LM	Lagrangian Mean
LOE	Low Ozone Episode
MSISE	Mass Spectrometer Incoherent Scattered Model
NAM	Northern Annular Mode
NAO	North Atlantic Oscillation
NCAR	National Center for Atmospheric Research
NCEP	National Centers for Environmental Prediction
NH	Northern Hemisphere
PSC	Polar Stratospheric Clouds
SH	Southern Hemisphere
TEM	Transformed Eulerian Mean
TOMS	Total Ozone Mapping Spectrometer
UTLS	Upper Troposphere Lower Stratosphere
UV	Ultra Violet
WAF	Wave Activity Flux
WKB	Wentzel-Kramer-Brillouin
WMO	World Meteorological Organization

Acknowledgements

I would like to thank to Professor Raisa P. Repinskya (Russian State Hydrometeorological University) who was the first one to interest me in atmospheric science. My special thanks go to Dr. Mikhail I. Beloglazov and Dr. Valentin C. Roldugin (Polar Geophysical Institute) for supporting me at the beginning of my scientific career. I am greatly in debt to my supervisor Professor Sheila Kirkwood for support and independence that I have received during my studies. I also want to thank Swedish Institute of Space Physics, Umeå University and Swedish Research Council for funding of my research. My thanks are extended to Dr. Alexey Karpechko (Finish Meteorological Institute) and Dr. Yvan Orsolini (Norwegian Institute for Air Research) who provided helpful scientific discussions and comments.

It has been a pleasure to work at IRF with the really friendly and comfortable working environment created here. I very much appreciate all my colleagues and friends at IRF in Kiruna with special thanks to Evgenia Belova, Tima Sergienko, Alexander Grigoriev, Daria Mikhaylova.

The TOMS science team (NASA/GSFC), ECMWF, CPC and FMI are gratefully acknowledged for providing data.

Finally, I am forever indebted to my parents for their continuous support, understanding and endless patience when it was most required.

Paper I

Wave-like ozone movements

V. C. Roldigin, G. N. Nikulin, and K. Henriksen

Phys. Chem. Earth (B), 25, 511-514, 2000

Pergamon

Phys. Chem. Earth (B), Vol. 25, No. 5–6, pp. 511–514, 2000

1464-1909/00/$ - see front matter

PII: S1464-1909(00)00055-1

Wave-Like Ozone Movements

V. C. Roldugin[1], G. N. Nikulin[1] and K. Henriksen[2]

[1]Polar Geophysical Institute, Academy, Apatity, Murmansk Region, Russia
E-mail: roldugin@pgi.kolasc.net.ru
[2]The Auroral Observatory, University of Tromso, 9037 Tromso, Norway

Received 8 November 1999; accepted 29 February 2000

Abstract. The wave-like character of the total ozone variations is examined from the Aral Sea and Karaganda observatories in Middle Asia, and from Tromsø and Murmansk in the Arctic. The waves have a period of 10-20 days and an amplitude of about 20-50 DU. They are seen practically every year when the ozone data do not contain too many gaps. In Middle Asia waves with the same periods are found in geopotential height and tropopause pressure variations. The ozone waves are caused by dynamic meteorological disturbances near the tropopause. The passing of a wave crest in the pressure field causes the convergence of ozone poor air under the tropopause and the divergence of ozone rich air above the tropopause giving rise to a total ozone content decrease. The passing of a wave trough stimulates the opposite process. By crosscorrelation analysis the wave-like movement was determined as eastward for both pairs of stations with a velocity of 11 - 15 °/day.

1 Introduction

Temporal variations of the total ozone, such as long-term trends or seasonal variations, are studied most often. Quasi-periodic oscillations of about ten days duration attract interest in connection with the development of weather phenomena, such as cyclones and anticyclones. Fishbein et al. (1993) reported waves in the stratospheric ozone content and temperature in the Southern Hemisphere from UARS satellite data. In one 40 day winter interval they observed a 9-day eastward travelling wave for the 5 hPa height level. Mote et al. (1991) used regression analysis to compare global distributions of total ozone for the 500 hPa height. They found a wave-like pattern of their covariance, and the wave structure moves eastward at a rate of about 15 degrees per day.

Correspondence to: V.C. Roldugin

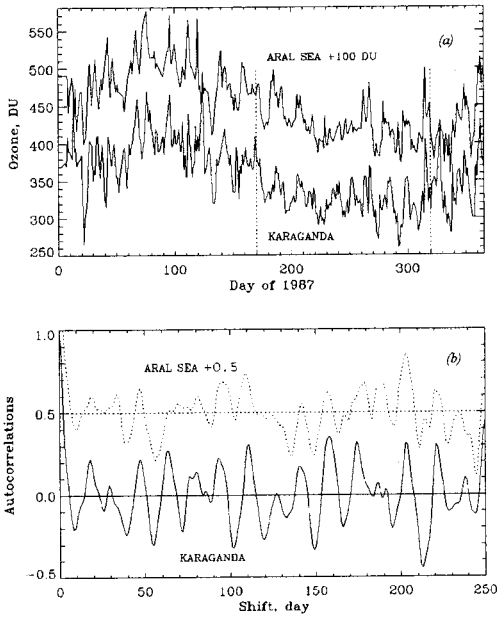

Fig. 1. (a) Total ozone variations for the middle Asian stations Aral Sea and Karaganda in 1987, and (b) their autocorrelation functions.

Here we try to consider ozone variations with a characteristic time of the order of 10-20 days as an independent geophysical phenomenon.

2 Ozone data

We have picked out for primary analysis the total ozone data for two stations: Aral Sea (46.8° N, 61.7° E) and Karaganda (49.8° N, 73.1° E) from year books published continuously in Leningrad (Gushchin, 1978-1992). The stations are situated near the same latitude with a distance of about 1000 km between them. The top panel (a) of Figure 1 shows the mean daily total ozone variations for these two stations during 1987. Except for seasonal variations, some quasi-periodic oscillations with a period of 15-25 days are seen at both stations and their amplitudes

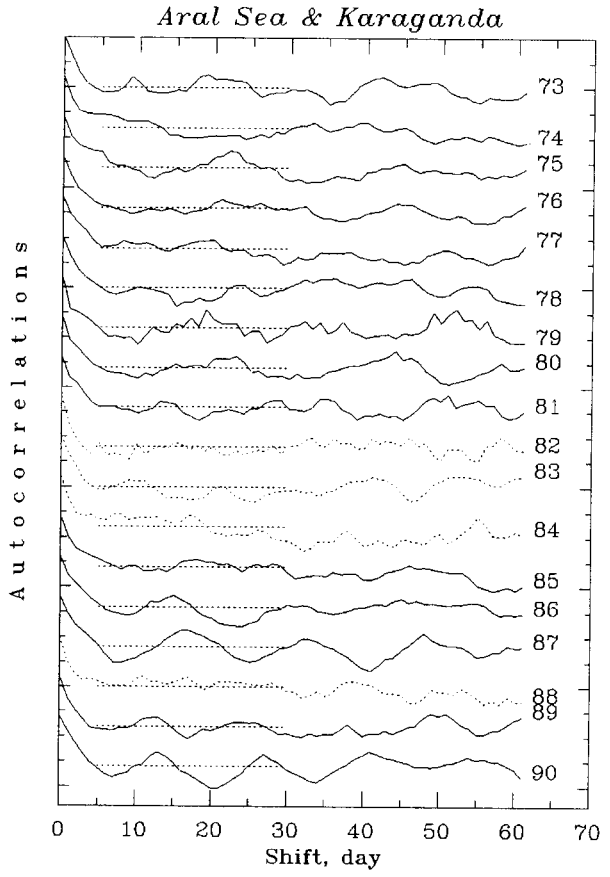

Fig. 2. Autocorrelation functions for averaged data sets of total ozone from the Aral Sea and Karaganda. Years are marked on the right side. The dashed curves are calculated for cases with single observatory data set.

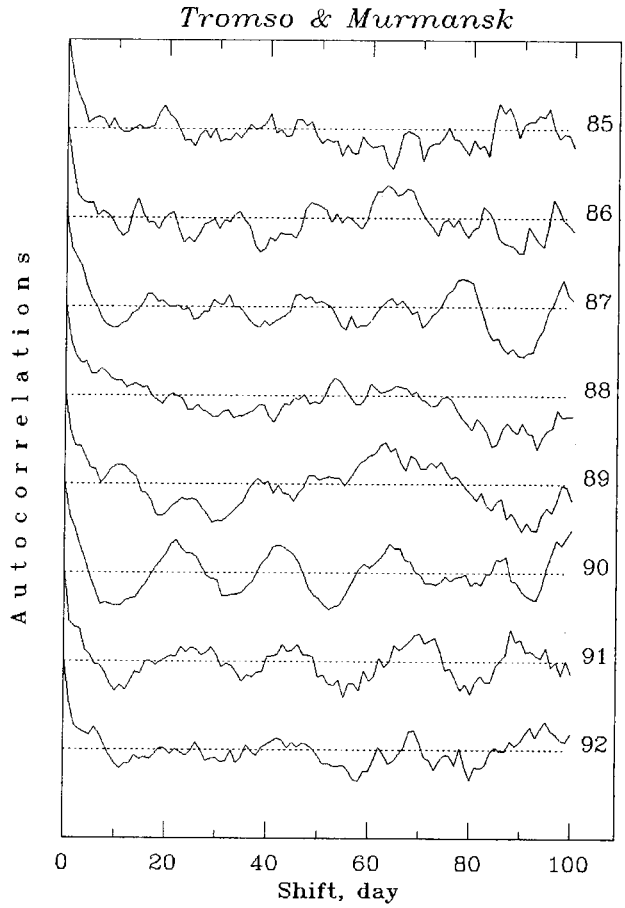

Fig. 3. Autocorrelation functions for averaged data sets of total ozone from Murmansk an Tromsø.

are of the order 50 DU. This dynamic feature is the object of our investigation. To see the oscillations more distinctly, the seasonal variation is eliminated from the primary ozone data sets by filtering. The autocorrelation functions for these resulting sets are shown in Fig.1 (b). The periodicity appears better here than in the primary curves, and the periods are identical for both stations and close to 16 days. We may conclude that these total ozone changes oscillate nearly simultaneously at both stations.

To investigate how often the periodicity occurs, we have treated all the data for both stations from 1973 to 1990. We combine two data sets into an averaged one because of data gaps from several days to several months. To eliminate seasonal variations and avoid too long intervals, we have picked out the data for only 151 days for day numbers 170-320, or 19 June - 16 November. This is shown in Fig. 1 (a) by the dashed vertical lines. The seasonal ozone variation is small during this time. The autocorrelation functions, shown in Fig. 2, reveal the quasi-periodic component of the ozone variations in many cases. The regular character of the oscillation is seen quite distinctly in 1986, 1987, 1989 and 1990.

These quasiperiodic oscillations of the total ozone have been investigated also in data from the high-latitude stations Tromsø (69.6° N, 19.0° E) and Murmansk (69.0° N, , 33.0° E) for eight years. As before, we have averaged together data from both stations and the time interval 170-320 days (151 days after 19th June) was used again. The result is presented in Fig.3. The quasi-periodic character of the total ozone variations at Tromsø and Murmansk can also be seen, barring 1985 and 1988. We have compared the periods at both pairs of stations for four years in Table 1. In three years the periods are equal, but in 1990 they differ significantly.

Table 1 .Mean periods of total ozone waves at Aral Sea and Karaganda and at Tromsø and Murmansk obtained by autocorrelation analysis.

Year	Period, day	
	Aral Sea Karaganda	Tromso Murmansk
1986	15	15
1987	16	16
1989	12	12
1990	14	21

3 Meteorological wave processes

The ozone may be considered as a trace gas, and so these ozone waves perform some wave processes in the atmospheric motion. The ozone variations at Middle Asia in 1986, 1987 and 1988, when the periodic nature was shown convincingly, were compared with the variations of

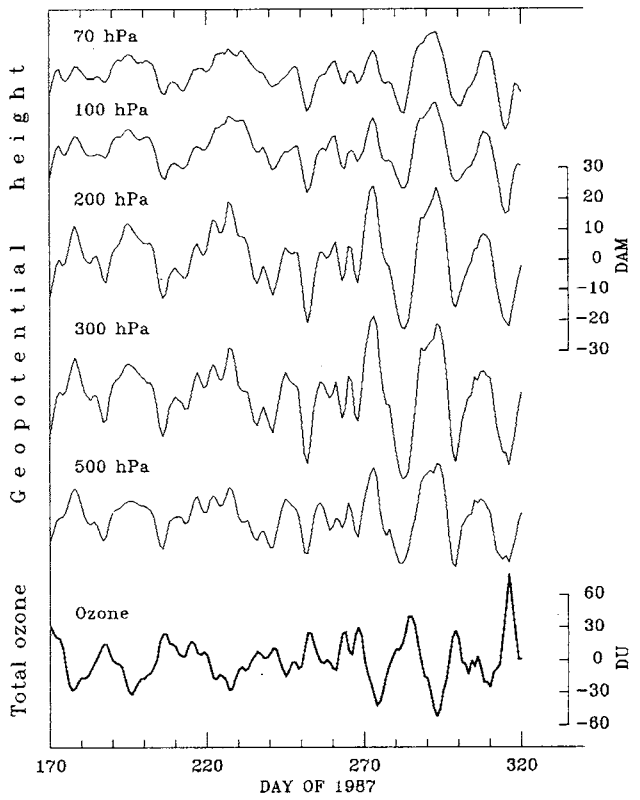

Fig. 4. Time variations of geopotential heights and the total ozone at Karaganda in 1987.

geopotential heights of 500, 300, 200, 100 and 70 hPa. The long-period oscillations are excluded by subtracting a 51-day running mean. Short-period oscillations are smoothed also. The variations of all 5 geopotential levels over Karaganda during the same 151 days of 1987 are shown in Fig. 4 together with the ozone variations. Here we used TOMS ozone data. A good negative correlation between the changes of ozone and all geopotential levels takes place. The periods of ozone variations are seen well in the day-to-day values of isobaric heights too. The mean square deviation of the geopotential height variations is about 8 dam at 500 hPa, 12.5 and 11.5 dam at 300 and 200 hPA, respectively, and goes down to 6.5 dam at 70 hPa. The tropopause is situated in the region between 200 hPa and 300 hPa, therefore the biggest amplitude of geopotential level variations occurs at this altitude. The variations of the tropopause pressure and the TOMS total ozone at Karaganda for 1987 are shown in Fig. 5 after some filtering. There is a good positive correspondence between them: when the pressure at the tropopause rises, i.e. the tropopause falls, the total ozone increases. The same pattern in ozone, geopotential height and tropopause pressure is observed for 1986 and 1988 at Karaganda and Aral Sea. As an example, Fig.6 shows the autocorrelation functions of the TOMS total ozone, 500 hPa geopotential height and the tropopause pressure over Aral Sea for days 170-320 days of 1986. The 15 days variation is present for all three phenomena.

These wave-like oscillations presuppose some movement and its direction may be found by crosscorrelation. We

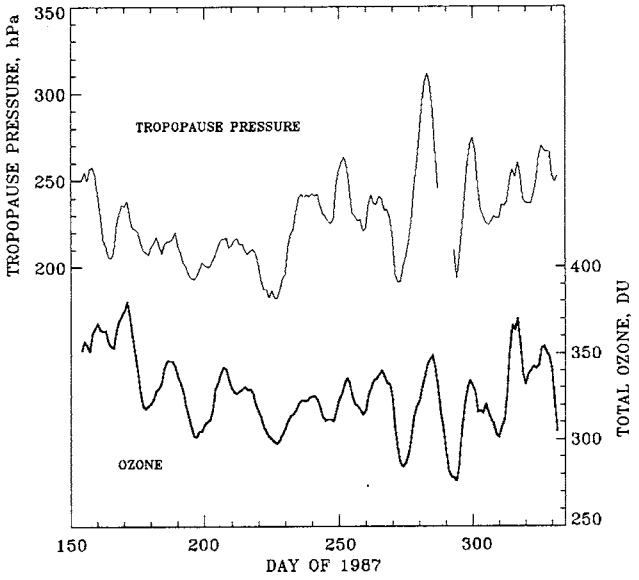

Fig. 5. Variations of the total ozone and tropopause pressure at Karaganda in 1987.

choose two geographic points in this region with coordinates 48° N, 65° E and 48° N, 80° E, and take both ozone and geopotential height data for the three years 1986-1988. In all the examined years a disturbance of both geopotential and of ozone moves from 48° N, 65° E to 48° N, 80° E, i.e. the displacement of the wave occurs from the west to the east with a latitudinal velocity of about 15 deg/day or 13 m/sec.

We may conclude that these ozone waves bring to light some wave processes in the atmospheric motion near the tropopause. The global weather pattern has a general eastward motion in the troposphere and lower stratosphere at middle latitudes, and it is therefore likely that horizontal motion in the ozone layer has the same direction.

4 Dynamics of ozone variations near the tropopause

We may suppose that these waves in Tromsø and Murmansk are generated by the Scandinavian mountains, and in Middle Asia by the Caucasus or by convective motions over the hot Kara Kum desert.

Quasi-periodic oscillations of the total ozone are determined by dynamic wave-like motions in the upper troposphere and lower stratosphere. Both horizontal advection and vertical movement near the tropopause change the total ozone content. When a wave crest passes, the air moves upwards adiabatically. Wirth (1993) showed that this causes convergence in the upper troposphere and divergence in the lower stratosphere. Therefore the movement of a crest causes the convergence of ozone poor air under the tropopause and the divergence of ozone rich air over the tropopause, as a result of which the total ozone content decreases. When a trough passes, the reverse process occurs, and the total ozone increases. At high levels the horizontal air movement is parallel to the isobars, so the air mass passing westerly through a trough is displaced to

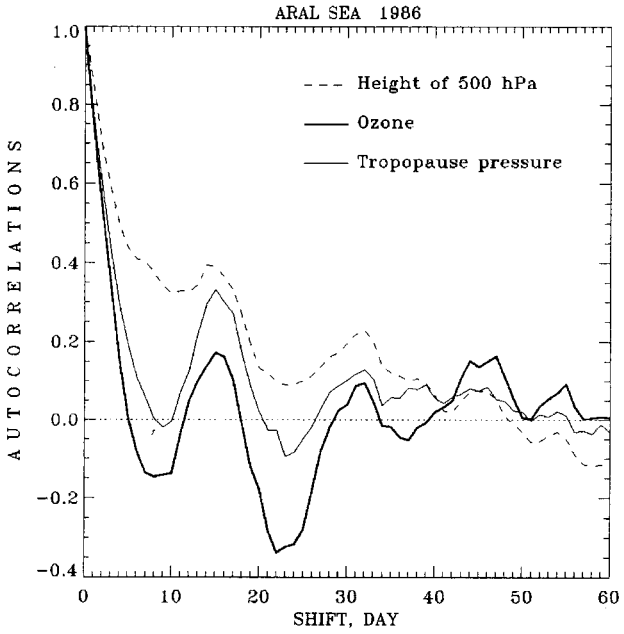

Fig. 6. Autocorrelation functions of total ozone, tropopause pressure and the geopotential height of 500 hPa at Aral Sea in 1986.

the South, and one passing through a crest is displaced to the North.

Reed, as early as (1950), revealed the importance of horizontal advection for ozone changes. The southward air displacement causes removal of more ozone rich air into the trough, and vice versa, the northward movement brings ozone poor air to the crest. Our analysis of June monthly averaged ozone values of TOMS data shows a 20% increase of the total ozone between 35° and 55° latitude along the 67° longitude meridian. This region of high ozone gradient coincides with the region of maximum negative correlation between ozone and geopotential heights (see Stanford et al., 1995). These authors also note the strong "tropopause effect": the most close coupling between ozone and air motion occurs near the tropopause, below the ozone maximum.

The jointed effect of vertical motion and horizontal advection considered above, produces growth of the ozone in troughs and reduction in crests. Note that the horizontal advection makes a more sizeable input in volume above the tropopause.

Acknowledgement. This work has been supported by the grants N 99-05-64979 and 00-05-64152 from the Russian Foundation for Basic Research.

References

Fishbein, E.F., Elson L.S., Froidevaux L., Manney G.L., Read W.G., Waters J.W., and Zurek R.W., MLS observations of stratospheric waves in temperature and O3 during the 1992 southern winter, *Geophys. Res. Lett., 20,* 1255-1258, 1993.

Gushchin, G.P. (editor). *Common content of atmospheric ozone and spectral transparency of atmosphere. Annual data report* (in Russian). Leningrad, Hidrometeoizdat, 1978-1992.

Mote, W.R., Holton J.R., and Sallace J.N., Variability in total ozone associated with baroclinic waves, *J. Atmos. Sci., 48,* 1900-1903, 1991.

Reed, R.J., The role of vertical motions in ozone-weather relationships, *J. Meteorology, 7,* 263-267, 1950.

Stanford, J.L., Ziemke J.R., McPeters R.D., Krueger R.D., and Bhartia P.K., *Spectral analyses, climatology, and interannual variability of Nimbus-7 TOMS version 6 total ozone content.* NASA reference publication 1360, 1995.

Wirth, V., Quasi-stationary planetary waves in total ozone and their correlation with lower stratospheric temperature, *J. Geophys. Res., 98,* 8873-8882, 1993.

Paper II

Modulation of total ozone anomalies in the midlatitude Northern Hemisphere by the Arctic oscillation

G. N. Nikulin and R. P. Repinskya

Izvestia - Atmospheric and Oceanic Physics, 37, 633-643, 2001

Izvestiya, Atmospheric and Oceanic Physics, Vol. 37, No. 5, 2001, pp. 633–643. Translated from Izvestiya AN. Fizika Atmosfery i Okeana, Vol. 37, No. 5, 2001, pp. 681–691.

Modulation of Total Ozone Anomalies in the Midlatitude Northern Hemisphere by the Arctic Oscillation

G. N. Nikulin* and R. P. Repinskaya**

** Polar Geophysical Institute, Kola Scientific Center, Russian Academy of Sciences, ul. Fersmana 14, Apatity, Murmansk oblast, 184200 Russia*
e-mail: nikulin@pgi.kolasc.net.ru
*** Russian State Hydrometeorological University, Malookhtinskii proezd 98, St. Petersburg, 195196 Russia*
e-mail: hydrodyn@hm.sici.ru

Received June 20, 2000; in final form, December 7, 2000

Abstract—On the basis of expanding random geophysical fields in terms of empirical orthogonal functions (EOFs), it is shown that winter monthly mean total ozone (TO) anomalies in the midlatitude Northern Hemisphere (TOMS, 1979–1992) are associated with a large-scale mode of atmospheric variability—the Arctic Oscillation (AO). The second TO EOF has a spatial structure similar to the AO structure, which is determined by the first EOF of the sea-level pressure, and the coefficients of these EOFs are anticorrelated. An analysis of a longer TO series obtained from the data of ground-based stations (1958–1998) has shown that a similar anticorrelation occurs between the index of the North Atlantic Oscillation (NAO), which is a regional part of the AO, and the TO anomalies averaged over December–March. A portion of a negative TO trend in the middle and high latitudes of the Northern Hemisphere can be attributed to a decrease in wave activity in the lower stratosphere. This decrease is associated with AO and NAO intensification started in the late 1960s. AO and NAO decay after 1995 resulted in a TO increase in the midlatitude Northern Hemisphere. This increase was especially noticeable in 1998–1999.

INTRODUCTION

A significant part of spatiotemporal variations in total ozone (TO) in the middle and high latitudes can be attributed to dynamic processes. A mechanism of TO relationship to vertical transfer and advection on time scales of a few days was considered in [1]. The theory of advection is based on the fact that the TO increases northward on average, and, consequently, meridional motions of air masses will cause the TO either to decrease or to increase. The main contribution of advection to TO variations occurs over the tropopause, in the lower stratosphere, where the ozone concentration is significantly greater than that in the troposphere. Rising motions in the tropopause region lead to the convergence of ozone-depleted air below the tropopause and to the divergence of ozone-enriched air above it. As a result, the TO in an air column decreases. Under descending motions, a reverse process is observed. More recently, it has been shown in [2] that about 80% of TO variability on time scales shorter than two weeks is due to ozone redistribution in the vertical and horizontal directions during air motion along isentropic surfaces in the lower stratosphere. A similar relationship between atmospheric dynamics and the TO can be followed from disturbances caused by baroclinic [3] and planetary [4] waves to anomalies associated with decadal variations in geopotential [5].

Statistical relations between TO anomalies and the characteristics of the Azores High—the surface pressure p at its center and the geographical latitude of the center φ—were studied in [6]. It has been found that a negative trend of the TO over western Europe is associated with a positive trend of the quantities p and φ, especially in winter. A possible relationship between a positive trend of the 300-hPa surface geopotential and a negative trend of the TO over the North Atlantic and Europe was shown in [7].

The main source of the interannual variability of atmospheric circulation in the above region is the North Atlantic Oscillation (NAO), which controls the large-scale motion of air masses between subtropical and high latitudes over the Atlantic and which has a strong effect on the climate of Europe [8]. With regression analysis, a feedback is obtained between the TO in the midlatitude Northern Hemisphere and the NAO index [9]. This index is defined as the difference of surface-pressure anomalies between the Azores High and the Icelandic Low. In winter, the NAO is a regional part of a global hemispheric mode, which includes the feedback between the Arctic basin and the zonal ring surrounding it [10]. This mode, which is determined by the first empirical orthogonal function (EOF) of the sea-level pressure, was termed the Arctic Oscillation (AO) in [10], where it was shown that it propagates through the entire troposphere and the lower stratosphere up to the 50-hPa level. According to [10], the AO can be interpreted as a surface structure reflecting the force of the circumpolar vortex at the top. In winter, when the

AO and the NAO are most clearly defined, the largest negative TO trends are observed in the latitudinal belt 30°–60° N [11]. This belt coincides with the zonal ring being the spatial part of the AO. Specifically, it is shown in [12] that about 40% of the negative TO trend in March (1979–1993) to the north of 40° N can be attributed to AO index variations. It is also known that, since the late 1960s, a positive NAO index trend with abnormally high values in the 1990s has appeared [8]. Since the same time, negative TO trends have been observed [11].

The aim of this work is to study the spatiotemporal relationship between atmospheric general circulation variability modes (such as the AO and the NAO) and TO anomalies in the midlatitude Northern Hemisphere and to answer the question as to whether a TO decrease in the 1980s–1990s could be associated with AO and NAO intensification.

METHOD OF STUDY AND INITIAL DATA

The expansion of random geophysical fields in terms of EOFs was used to analyze TO and geopotential anomalies. This approach makes it possible to derive the most essential information about their spatiotemporal variability [13–15]. For the initial data, we used the TO monthly means (TOMS, *Nimbus 7*) over 1979–1992 taken on a 1° × 1.25° latitude–longitude grid and the monthly mean heights of the 1000-, 500-, 300-, 100-, and 50-hPa pressure surfaces ($H_{1000–50}$) with 2.5° × 2.5° spatial resolution (US National Center for Environmental Predictions). The initial grid leads to a very large dimension of correlation matrices (8928 for ozone and 3600 for geopotential), which hinders the determination of matrix eigenvalues. At the same time, deriving the largest modes in the fields in question does not require high-resolution grids. For this reason, the $H_{1000–50}$ and TO values are presented by us on a coarser grid (10° × 20°) in the latitudinal belts 20°–90° N for $H_{1000–50}$ and 20°–60° N for the TO. The choice of the latitudinal range for the TO is due to the availability of data for the region south of 60° N during the whole year. As a rule, studies discussing the effect of the NAO on climate consider winter months, when the NAO is most clearly pronounced. In order to obtain a more complete picture, we will first analyze the data without their seasonal separation, and, then, we will analyze them separately for the summer and winter months. Thus, the initial correlation matrices have the dimensions 127 (points including the pole) × 168 (months) for the $H_{1000–50}$ fields and 90 × 168 for the TO fields. For all the fields, the monthly mean anomalies are obtained by subtracting the climatic values taken for the corresponding months over the period 1979–1992 at each grid point. Since sample inhomogeneity (the presence of decadal trends) can affect the EOF form, the linear trend determined by the least-squares method is removed from the resulting anomalies at each grid point.

The data of the ground-based ozonometric network are taken from the World Ozone and Ultraviolet Radiation Data Centre, Canada. The corrected complete TO series at Aroza (1926–1999) is given by the Swiss Meteorological Office [16]. The surface pressure values at Gibraltar (36° N, 5° W) and Reykjavik (64° N, 22° W) obtained from the Climatic Research Unit, University of East Anglia, England, are used to determine the NAO index.

RESULTS OF ANALYSIS

The first EOFs (EOF1) of anomalies in the geopotential at 1000-, 500-, 100-, and 50-hPa pressure surfaces are shown in Fig. 1. At the 1000-hPa surface (Fig. 1a), EOF1 is responsible for 18% of the total variance (TV) of the initial sample and derives a negative region in the Arctic, with minimum values over Greenland, and two positive regions in the middle latitudes, one of which, more intense, is situated over the Atlantic, western Europe, and the Mediterranean, and the other is situated over the Pacific and eastern Eurasia. The pattern of EOF1 of H_{1000} anomalies is obtained at different samples [10, 15, 17] and determines two major oscillations in the Northern Hemisphere: the North Atlantic and North Pacific oscillations. A similar pattern holds in the troposphere at 500- (Fig. 1b) and 300-hPa heights and has a more clearly defined character. In this case, the contribution of the first mode to the TV decreases to 13%. At the 100-hPa height in the lower stratosphere (Fig. 1c), the positive regions become close to one another over the western coast of North America and form a zonal ring with a discontinuity over eastern Europe and western Siberia. The center of the negative region is located over the pole. The EOF1 contribution increases and amounts to 23% of the TV. At the 50-hPa height (Fig. 1d), the positive zonal ring closes around the negative region over the Arctic, and the EOF1 contribution reaches 39% of the TV. Thus, during the 14-year period under consideration, a spatial structure similar to an oscillatory mode obtained for the winter months [10] exists in the troposphere and the lower stratosphere. Since this mode encompasses the lower stratosphere, where the effect of dynamic factors on ozone is most significant, one can believe that one of the first EOFs of TO anomalies can be similar to EOF1 of H_{100} anomalies, and the expansion coefficients (ECs), which carry information about their evolution, will be correlated with each other.

Let us consider the results of expanding the fields of TO anomalies in the latitudinal belt 20°–60° N in terms of EOFs. Figure 2 shows the first four EOFs of TO anomalies. These EOFs are responsible for 30, 11, 8, and 7% of the TV, respectively. Table 1 presents the correlations between the first four ECs of TO anomalies, EC1 of $H_{1000–50}$ anomalies, and the NAO. The first EOF of TO anomalies is positive over the entire territory; i.e., TO variations associated with EOF1 occur in phase over the entire region in question. The first EOF of TO

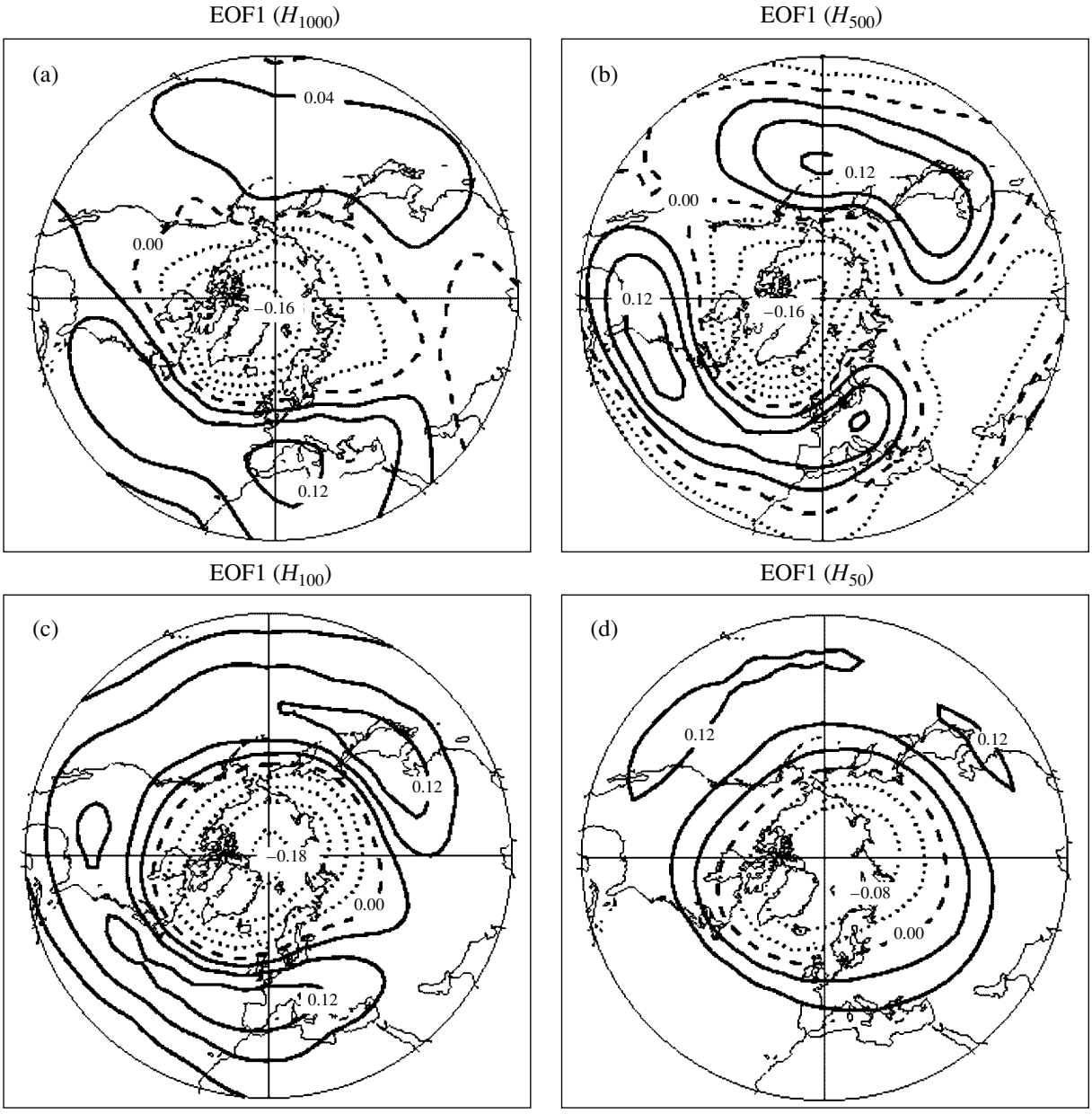

Fig. 1. Patterns of the first EOFs of the monthly mean (a) H_{1000}, (b) H_{500}, (c) H_{100}, and (d) H_{50} anomalies over the time period 1979–1992. Isolines are drawn in ±0.04 intervals: zero, positive, and negative isolines are shown by dashed, solid, and dotted lines, respectively.

anomalies is characterized by a clearly defined zonal distribution with maximum values in the subtropics and values close to zero in the zone 50°–60° N (correspondingly, one can assume the presence of a tropical source of disturbances). No significant correlations are observed between EC1 of TO anomalies and EC1 of $H_{1000–50}$ anomalies. On the other hand, EC1 of TO anomalies is anticorrelated with the index of the quasi-biennial oscillation (QBO), which is defined as anomalies in the zonal wind at the 30-hPa height over Singapore. The correlation is equal to –0.29 ($r_{99\%} = \pm 0.2$), and it reaches –0.39 at a time shift of three months; i.e., the disturbance in the TO field lags behind the QBO by three months. The second EOF (EOF2) represents a positive zonal ring in the middle latitudes with a discontinuity over the western coast of North America and with a maximum over eastern Siberia. A closed ring of negative values is observed south of 30° N. It can be seen that EOF2 of TO anomalies bears some similarities to the spatial pattern of EOF1 of $H_{1000–50}$ anomalies, and EC2 of TO anomalies is anticorrelated with EC1 of $H_{1000–50}$ anomalies. Figure 3 shows the temporal behav-

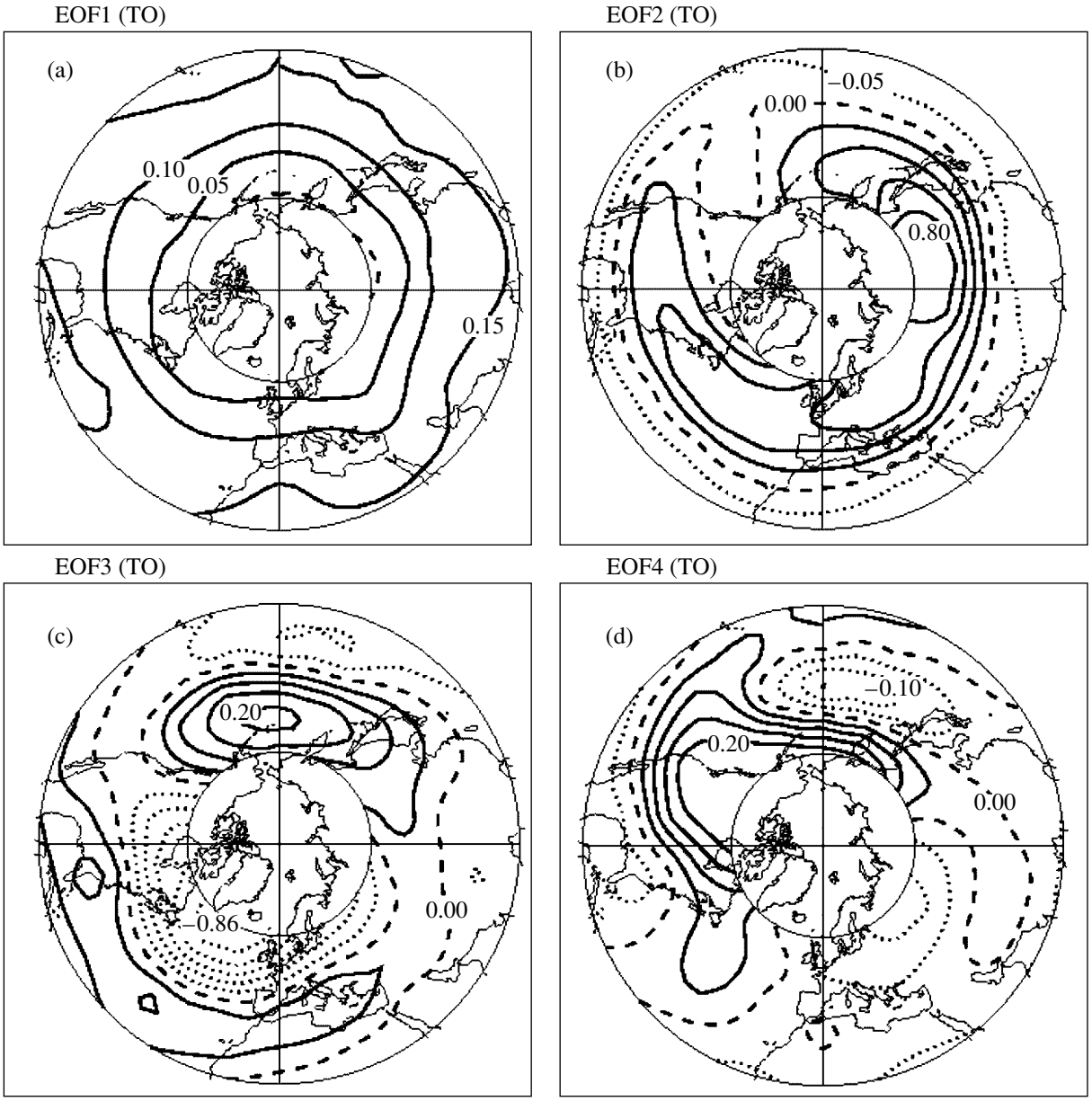

Fig. 2. Patterns of the (a) first, (b) second, (c) third, and (d) fourth EOFs of the monthly mean TO anomalies. Isolines are drawn in ±0.05 intervals: zero, positive, and negative isolines are shown by dashed, solid, and dotted lines, respectively. The NO data are unavailable in the region north of 60° N.

iors of the NAO index and the normalized EC1 of $H_{1000–50}$ anomalies and EC2 of TO anomalies (the data are smoothed by a three-point triangular filter). In months with high positive values of the NAO index and EC1 of $H_{1000–50}$ anomalies, the TO decreases in the region determined by positive values of EOF2 of TO anomalies. The largest absolute values of the NAO index and of EC1 of $H_{1000–50}$ anomalies occur in December–March. Correspondingly, the most significant midlatitude TO variations, which are determined by EOF2, are observed at the same time. It is believed that a low correlation between the NAO index and EC2 of TO anomalies is associated with the presence of high-frequency components in the spectrum of the NAO index, which are absent in the spectrum of EC2 of TO anomalies. After the time series are filtered by a three-point triangular filter, the correlation becomes equal to –0.61. The third EOF (EOF3) of TO anomalies has a dipole pattern with a clearly defined negative region over the north Atlantic and a clearly defined positive region over the midlatitude Pacific (Fig. 2c). In the south Atlantic, a weakly pronounced positive zonal band encompassing America and the Mediterranean is observed. The spatial pattern of EOF3 of TO anomalies

Table 1. Correlations between the first EOF expansion coefficients of the monthly mean fields of $H_{1000, 500, 300, 100, 50}$ anomalies, the NAO index, and the first–to–fourth expansion coefficients of the monthly mean fields of TO anomalies over the period from 1979 to 1992 ($r_{99\%} = \pm 0.2$)

	EC1 H_{50}	EC1 H_{100}	EC1 H_{300}	EC1 H_{500}	EC1 H_{1000}	NAO	EC1 TO	EC2 TO	EC3 TO	EC4 TO
EC1 H_{50}	1.00	0.95	0.52	0.50	0.60	0.45	0.16	−0.44	0.17	−0.01
EC1 H_{100}		1.00	0.69	0.68	0.73	0.52	0.11	−0.50	0.07	−0.02
EC1 H_{300}			1.00	0.98	0.82	0.57	0.07	−0.46	−0.27	0.06
EC1 H_{500}				1.00	0.89	0.59	0.05	−0.48	−0.18	0.09
EC1 H_{1000}					1.00	0.64	0.03	−0.51	−0.07	0.04
NAO						1.00	−0.01	−0.31	−0.13	−0.06
EC1 TO							1.00	0.00	0.00	0.00
EC2 TO								1.00	0.00	0.00
EC3 TO									1.00	0.00
EC4 TO										1.00

bears some similarities to EOF1 $H_{500, 300}$. However, the only significant coefficient of correlation between EC3 of TO anomalies and EC1 of H_{300} anomalies is too small (–0.27) to indicate the presence of correlation. The fourth EOF (EOF4) of TO anomalies is determined by a positive region over northwestern North America and by two weakly pronounced negative regions (Fig. 2d). No correlation is observed between EC4 of TO anomalies and EC1 of $H_{1000–50}$ anomalies. Thus, among the above EOFs of TO anomalies, only EOF2 has a spatial pattern similar to that of EOF1 of $H_{1000–50}$ anomalies, and the correlation between EC2 of TO anomalies and EC1 of $H_{1000–50}$ anomalies is, on average, –0.5 and is statistically significant.

To analyze seasonal features, the initial samples were separated into winter (November–April) and summer (May–October) ones. In this case, the length of a sample (84 months) turns out to be smaller than the dimension of the spatial basis (90 and 127 grid points for the TO and geopotential fields, respectively). The correlation matrices will be special (the rank of a matrix is smaller than the number of field points), and some higher-order EOFs will be equal to zero. However, this fact does not significantly affect the form of the first few EOFs, which are mainly responsible for the variance [18]. For the winter season, the spatial pattern of EOF1 of $H_{1000–50}$ anomalies remains unchanged, and the EOF contribution to the TV increases by 1 to 2% at each height. The first four EOFs of TO anomalies also retain their form, and, only in EOF2, a closed negative region over the western coast of North America appears. The contribution of the above EOFs of TO anomalies to the TV increases only slightly. In the summer season, the patterns of EOF1 of $H_{1000–50}$ anomalies turn out to be smaller scale and are represented by a few weakly pronounced positive regions. The EOF1 contributions to the TV also decrease (15, 11, 12% for $H_{1000, 500, 300}$, respectively). In the lower stratosphere, the negative region over the Arctic disappears, and the functions EOF1 of $H_{100, 50}$ anomalies become positive over the entire hemisphere. Their contributions to the TV remain as before. The first EOF of TO anomalies (responsible for 31% of the TV) does not change significantly in form, while, in the pattern of EOF2 (10% of the TV), the zonal ring is not observed, and EOF3 and EOF4 (6 and 5% of the TV, respectively) decay into a

Table 2. Significant correlations (at the 95% significance level) between the NAO index (averaged over December–March) and the TO anomalies (averaged over December–March) obtained at the ozonometric stations of the Northern Hemisphere

Station (coordinates)	*R*
Sapporo (43°N 141°E)	−0.49
Tateno (36°N 140°E)	−0.40
Krasnoyarsk (56°N 93°E)	−0.60
Moscow (56°N 37°E)	−0.58
Belsk (53°N 21°E)	−0.51
Hradec Kralove (50°N 16°E)	−0.56
Hohenpeissenberg (48°N 11°E)	−0.64
Ucle (51°N 4°E)	−0.49
Aroza (47°N 10°E)	−0.64 −0.40
Potsdam (52°N 13°E)	−0.40
Lisbon (39°N 9°W)	−0.43
Budapest (47°N 19°E)	−0.60
Toronto (44°N 79°W)	−0.46
Bismarck (47°N 101°W)	−0.49
Cariboo (46°N 68°W)	−0.49
Boulder (40°N 105°W)	−0.53
Nashville (36°N 87°W)	−0.52
Wallops Island (38°N 76°W)	−0.53

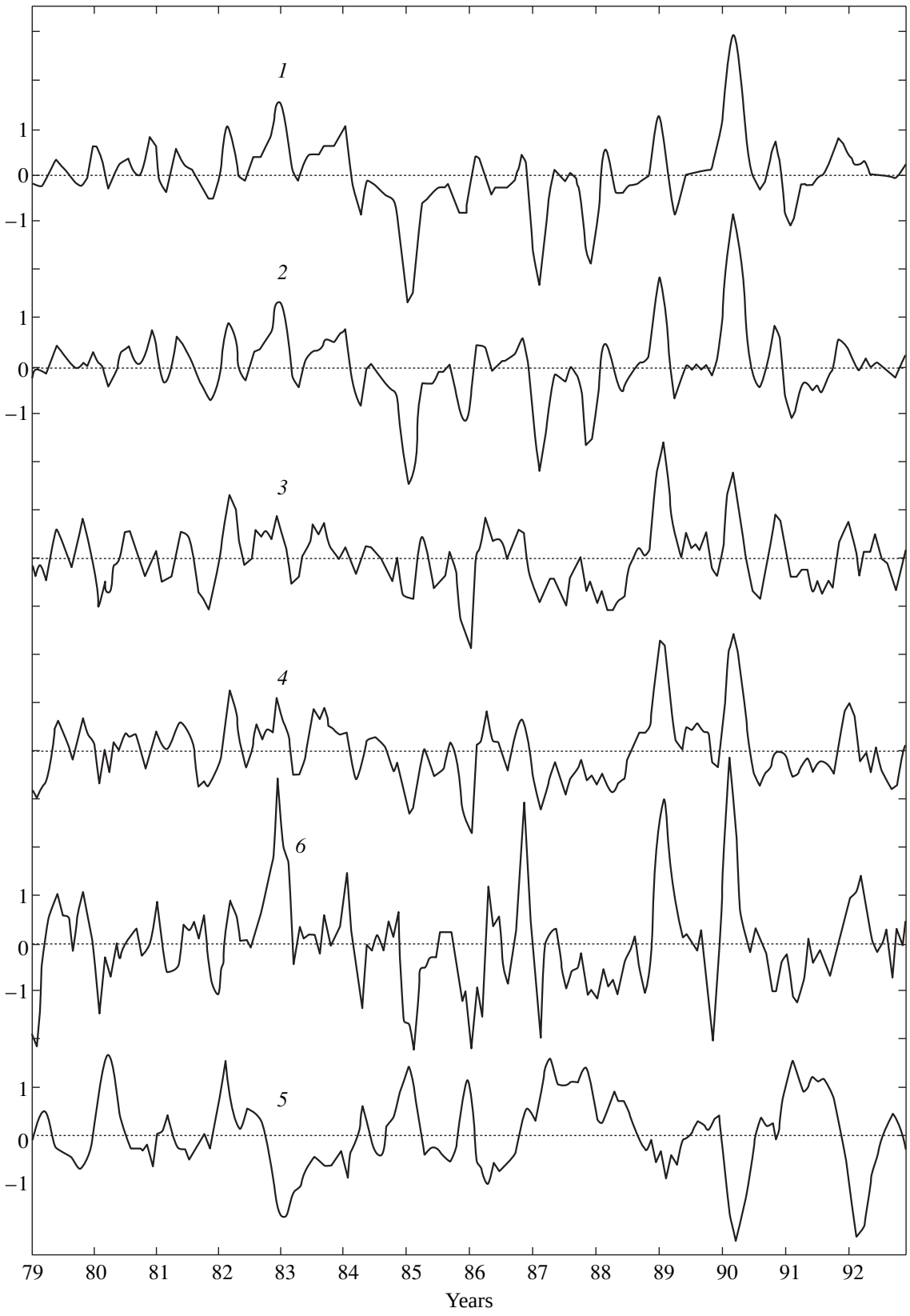

Fig. 3. Time behaviors of the expansion coefficients of the fields of the monthly mean (*1*) H_{50}, (*2*) H_{100}, (*3*) H_{500}, and (*4*) H_{1000} anomalies, (*5*) the second expansion coefficient of the fields of the monthly mean TO anomalies, and (*6*) the NAO index over the time period 1979–1992. Each time series is normalized by the variance.

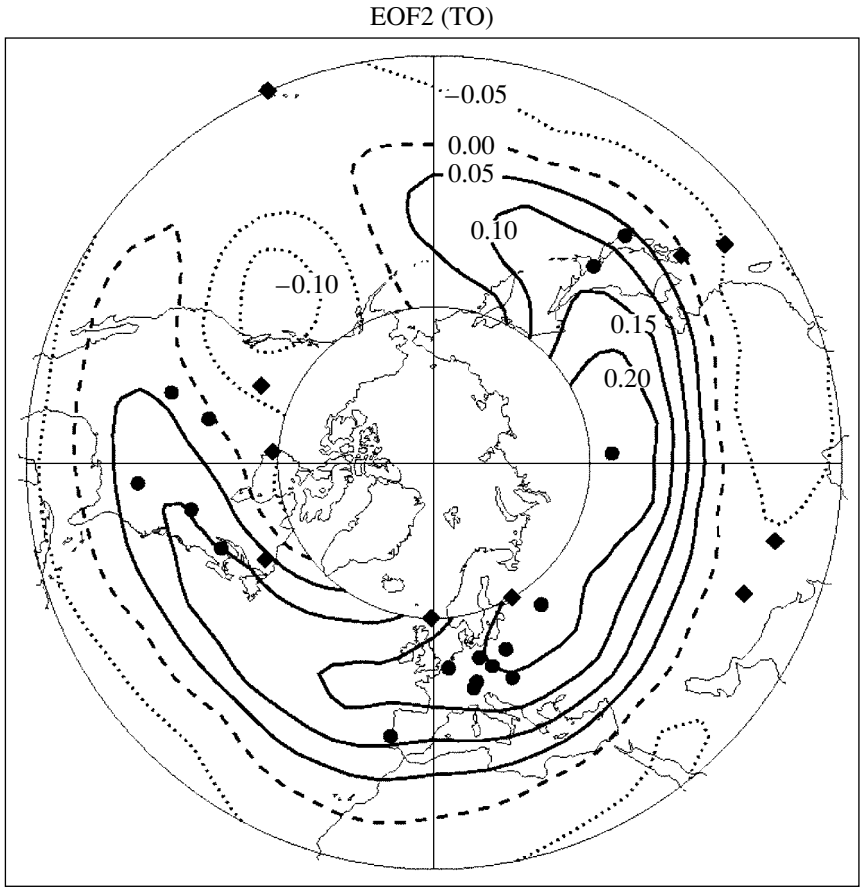

Fig. 4. Second EOF of the monthly mean TO anomalies over the time period 1979–1992 (November–April). Circles and squares indicate the ozonometric stations with statistically significant and insignificant correlations (at the 95% significance level), respectively, between the NAO index (averaged over December–March) and TO anomalies (averaged over December–March).

few small regions opposite in sign. Consequently, EOF1 of $H_{1000–50}$ anomalies and EOF2–EOF4 of TO anomalies are unstable when seasons change. Winter months make the main contribution to the form of the EOF when the expansion in the complete sample is used. This is due to a higher variability of meteorological quantities in winter than in summer. For example, the ratio of the variances of EC1 of H_{100} anomalies for winter and summer samples is 3.6, and the corresponding ratio of the variances of EC2 of TO anomalies is 2. It is seen that the functions EOF1 of $H_{1000–50}$ anomalies are similar to EOF2 of TO anomalies only in winter months, and changes in circulation that are due to the AO can make a partial contribution to midlatitude TO variations.

The initial data in this case were also presented on a $5° \times 10°$ grid, so that the dimension of the basis (505 for $H_{1000–50}$ and 324 for the TO) was greater than the sample length. The results of expanding in terms of EOFs have shown that EOF1 of $H_{1000–50}$ anomalies and EOF1–EOF4 of TO anomalies are insensitive to a basis change; i.e., these functions retain their form, and their contributions to the TV vary by 1 to 2%.

Since TO series obtained with the TOMS (14 years) are limited, we will study the relationship between the TO and the AO on the basis of the data of the ground-based ozonometric network. For our analysis, we took stations situated in the latitudinal belt 20°–60° N, which were used in [11] to determine TO trends in the Northern Hemisphere. As shown in [10], the winter means of the NAO and AO indices are in phase; therefore, the NAO index is used by us as the criterion of AO intensity. For each station, the December–March means of TO anomalies and the NAO index were obtained for the period from the starting time of measurements at the station to 1998. Figure 4 shows EOF2 of TO anomalies for the winter months (November–April) and the locations of the ground-based stations. The stations are separated according to the significance of correlation between TO anomalies and the NAO index (at the 95% significance level). It is seen that the stations with significant correlations (see Table 2) lie within the zonal semiring determined by EOF2 of TO anomalies over the period 1979–1992. The exceptions are two stations

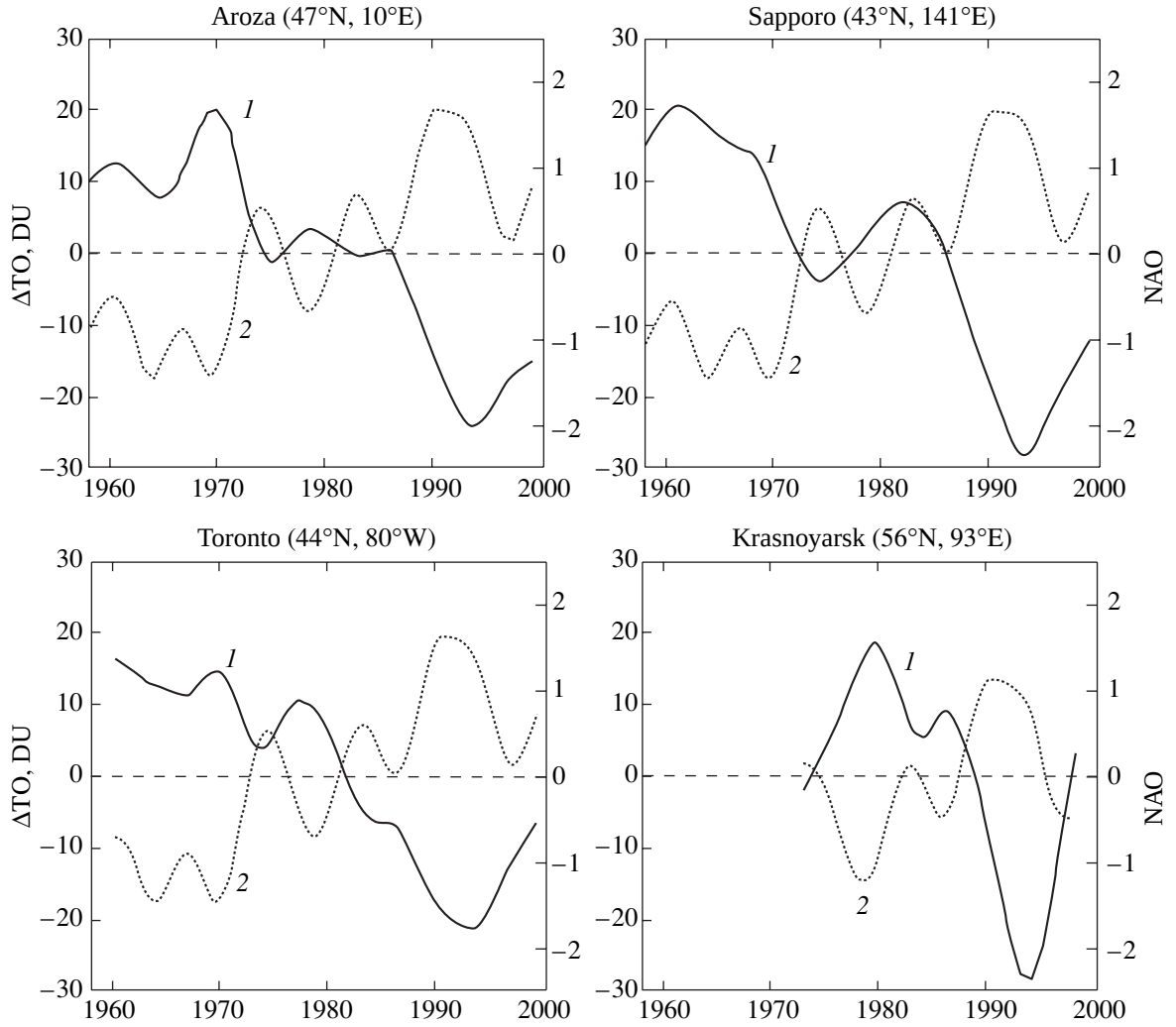

Fig. 5. December–March mean (*1*) TO anomalies smoothed by a seven-point filter (with weights of 1, 3, 5, 6, 5, 3, 1) and (*2*) NAO index for Aroza, Sapporo, Toronto, and Krasnoyarsk.

in Europe: St. Petersburg (60° N, 30° W) and Lerwick (60° N, 1° W), and one station in North America: Goose Bay (53° N, 60° W). This can be explained by the fact that these stations are located close to the center of the negative region over the north Atlantic determined by EOF3 of TO anomalies (Fig. 2c). In this region, the contribution of processes associated with EOF3 to TO anomalies becomes comparable to that corresponding to EOF2. Since the correlations were calculated using both TO anomalies including variations associated with the QBO [19] and local features of each station, we consider the initial data smoothed by a low-frequency filter with seven weights (1, 3, 5, 6, 5, 3, 1) [8]. Such a filter efficiently suppresses high-frequency components with periods less than four years. Figure 5 shows the temporal behaviors of the smoothed TO anomalies and NAO index at four stations located within the positive zonal semiring of EOF2 of TO anomalies at different longitudes. At each station, the temporal behaviors of the TO anomaly and NAO index are in antiphase. This phenomenon is most clearly defined at the Krasnoyarsk and Aroza stations, which are located in the region of high positive values of EOF2 of TO anomalies. At the Sapporo and Toronto stations, located on the periphery of the EOF2 positive semiring, NAO index variations do not all manifest themselves in TO anomalies; however, the general trend holds. In Aroza and Toronto, a decrease in the TO started simultaneously with an increase in the NAO index in 1970 and ceased in 1993–1995. The TO change over this period of time amounts to about 53 DU in Aroza and 34 DU in Toronto. In Sapporo, a decrease in the TO began somewhat earlier (~1962), its increase also began in 1993–1995, and the TO change over the period of time from 1970 to 1994 amounts to about 36 DU. In Krasnoyarsk, for which the series of data is shorter (1973–1998), a decrease in the TO is observed from 1980 to 1993–1995, and its change amounts to about 47 DU. Figure 6 shows the

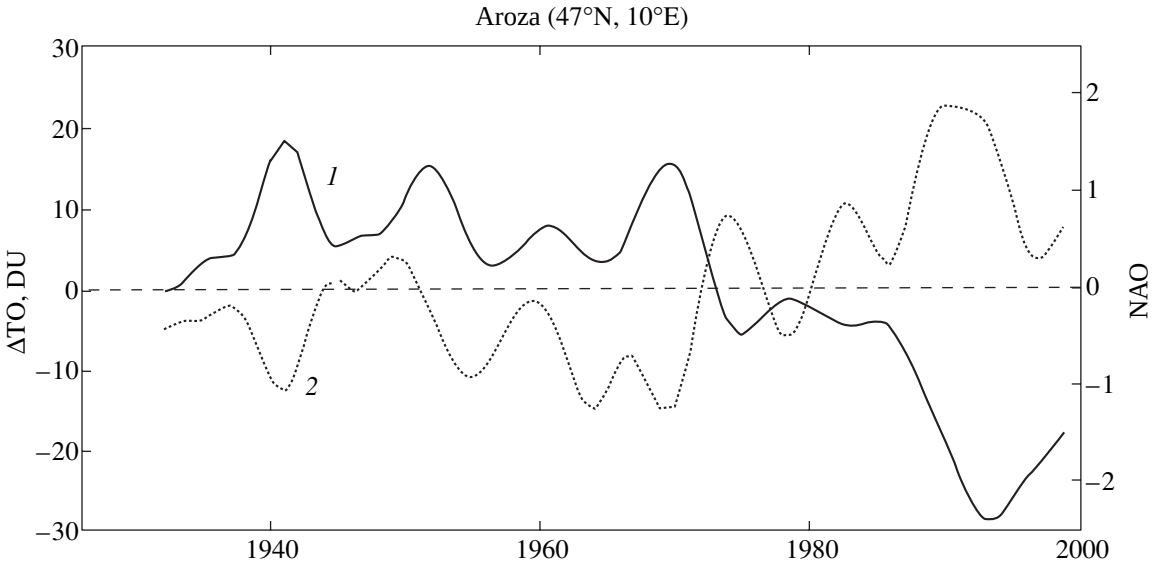

Fig. 6. December–March mean (*1*) TO anomalies smoothed by a seven-point filter (with weights of 1, 3, 5, 6, 5, 3, 1) and (*2*) NAO index for Aroza over the time period 1932–1999.

temporal behavior of the smoothed winter TO anomalies and NAO index in Aroza since 1932, because there were many gaps in data during the first observation years 1926–1931. Two periods of time when TO anomalies and the NAO index are in antiphase are prominent: from 1935 to 1945 and from 1965 to 1999. No clear-cut connection between them is observed from 1945 to 1965. However, it is seen that from the 1930s to the early 1970s, when the NAO index was basically negative, TO anomalies were positive. After the phase of the NAO index became positive, TO anomalies went negative. During the past few years after the time of high positive values of the NAO index in the early 1990s, the NAO index decreased to zero. Simultaneously, the TO increased gradually in the winter–summer period in the middle latitudes of the hemisphere, which was especially noticeable in 1998–1999, when the TO regained its value of the mid-1970s [20].

CONCLUSIONS

This work examines the spatial pattern of the largest scale mode (EOF1) for the monthly mean anomalies of the heights of the 1000-, 500-, 300-, 100, and 50-hPa pressure surfaces and the spatial patterns of the first four modes (EOF1–EOF4) for the monthly mean TO anomalies over the time period 1979–1992. It is found that, in the troposphere and lower stratosphere in this period, there is a spatial pattern similar to the Arctic Oscillation (AO) pattern obtained from a longer series of winter data [10]. Among the first four EOFs of TO anomalies, EOF2, which has the form of a positive zonal semiring in the middle latitudes, is similar in form to EOF1 of $H_{1000–50}$ anomalies. The correlation between the corresponding expansion coefficients (EC2 of TO anomalies and EC1 of $H_{1000–50}$ anomalies) is close to –0.5 and is statistically significant. There is a certain correlation between EOF3 of TO anomalies and EOF1 of $H_{500, 300}$ anomalies. However, a small statistically significant correlation occurs only between the third and first expansion coefficients of the fields of TO and H_{300} anomalies. The separation of the initial data into two seasonal samples (November–April and May–October) indicates that the resulting forms of EOF1 of $H_{1000–50}$ anomalies and EOF2 of TO anomalies are similar only in the cool season. In the warm season, the EOFs in question become somewhat smeared; i.e., they decay into a number of small, unclearly defined regions, and no similarity is observed between them. The use of a longer TO series obtained at ozonometric stations indicates the presence of statistically significant correlations (see Table 2) between the index of the North Atlantic Oscillation (NAO), which is an AO regional mode, and the December–March means of TO anomalies observed at stations located within a positive zonal semiring, which is determined by EOF2 of TO anomalies over 1979–1992. The NAO effect on the winter means of TO anomalies is strongest at stations located in the region of maximum positive values of EOF2 of TO anomalies (Siberia, Europe), and it decreases on the periphery of the zonal semiring. Since the late 1960s, when the NAO index was minimum, it started to increase and reached abnormally high positive values that were not encountered previously. In calculating trends for the stations at which observations have been carried out since 1958, a trend of the "ice-stick" type (with a constant level until December 1969, followed by a linear function) was used. Simulta-

neously with an increase in the NAO index, the TO started to decrease in the middle and high latitudes of the Northern Hemisphere. The maximum negative TO trends occur in the winter and spring months, when the AO and NAO spatial patterns are most clearly defined. It is believed that a significant part of the negative trend of TO anomalies in the middle latitudes of the hemisphere can be attributed to long-period variations in the circulation of the lower stratosphere. In years with high positive AO and NAO indices, positive and negative $H_{1000-50}$ anomalies are observed in the middle latitudes and over the Arctic, respectively. On time scales of about several decades, this is confirmed by the fact that, starting in the mid-1960s, a negative H_{50} trend north of 60° N and a positive trend north of 50° N were present in the winter season [21]. As a result, a gradual increase in the meridional gradient in the geopotential field and, correspondingly, an intensification of the zonal westerly flow are observed in the lower stratosphere in the latitudinal belt 45°–80° N [22]. The intensification of the westerly flow hinders the penetration of large-scale quasi-stationary waves, which represent the main source of meridional ozone transport in the lower stratosphere in winter, from the troposphere into the stratosphere [23]. The decrease of the wave activity and the intensification of the zonal circulation are responsible for the blocking of ozone transport from the tropical region into the middle and high latitudes in the lower stratosphere [24, 25].

Thus, in addition to the connection between the phase of the quasi-biennial oscillation and the wave activity (increasing at an easterly phase and decreasing at a westerly phase) in the middle and high latitudes [26], one can observe long-period variations in the wave activity that are modulated by a large-scale atmospheric circulation mode—the Arctic Oscillation. A positive trend in the AO index since the late 1960s [12] led to a decrease in the wave activity in the lower stratosphere and, correspondingly, to negative TO anomalies in the middle and high latitudes of the Northern Hemisphere. Up to now, there has been no unified view of the processes responsible for the low-frequency AO variability, including a positive trend over the last 30 years. The proposed hypotheses involve the effect of anthropogenic forcings [27], the natural atmospheric variability [28], and the interaction of the atmosphere with the ocean surface layer [29]. Many research programs are aimed at studying dynamical–chemical processes affecting large-scale modes of atmospheric variability and the possibilities of forecasting the behavior of such modes. However, nonlinear interactions between the above factors make the elucidation of a unified physical mechanism controlling interseasonal and decadal AO variations very difficult. If an increase in the AO (and, correspondingly, NAO) index will follow its low values observed in the late 1990s, one can expect a decrease in the TO in the middle latitudes in comparison with relatively high TO values observed in 1998–1999.

ACKNOWLEDGMENTS

This work was supported by the Russian Foundation for Basic Research, project no. 99-05-64979.

REFERENCES

1. Reed, R.J., The Role of Vertical Motions in Ozone–Weather Relationships, *J. Meteorol.*, 1950, vol. 7, pp. 263–267.
2. Salby, S. and Callaghan, P.F., Fluctuations of Total Ozone and Their Relationship to Stratospheric Air Motion, *J. Geophys. Res. D*, 1993, vol. 88, no. 2, pp. 2715–2727.
3. Mote, W.R., Holton, J.R., and Wallace, J.M., Variability in Total Ozone Associated with Baroclinic Waves, *J. Atmos. Sci.*, 1991, vol. 48, no. 16, pp. 1900–1903.
4. Wirth, W., Quasi-Stationary Planetary Waves in Total Ozone and Their Correlation with Lower Stratospheric Temperature, *J. Geophys. Res. D*, 1993, vol. 98, no. 5, pp. 8873–8882.
5. Hood, L.L., McCormack, J.P., and Labitzke, K., An Investigation of Dynamical Contributions to Midlatitude Ozone Trends in Winter, *J. Geophys. Res. D*, 1997, vol. 102, no. 11, pp. 13079–13093.
6. Bekoryukov, V.I., Bugaeva, I.V., Zakharov, G.R., Koshel'kov, Yu.P., and Tarasenko, D.A., Study of the Parameters of the Azores High Affecting Ozone Variations in Western Europe, *Izv. Akad. Nauk, Fiz. Atmos. Okeana*, 1995, vol. 31, no. 1, pp. 41–45.
7. Entzian, G. and Peters, D., Very Low Zonally Asymmetric Ozone Values in March 1997 above the North Atlantic-European Region, Induced by Dynamic Processes, *Ann. Geophys.*, 1999, vol. 17, no. 7, pp. 933–940.
8. Hurrell, J.W., Decadal Trend in the North Atlantic Oscillation: Regional Temperatures and Precipitation, *Science*, 1995, vol. 296, pp. 676–679.
9. Zvyagintsev, A.M. and Kruchenitskii, G.M., Connections between the Total Ozone in the Midlatitude Northern Hemisphere and the North Atlantic Oscillation, *Meteorol. Gidrol.*, 1996, no. 7, pp. 65–70.
10. Thompson, D.W. and Wallace, J.M., The Arctic Oscillation Signature in the Wintertime Geopotential Height and Temperature Fields, *Geophys. Res. Lett.*, 1998, vol. 25, no. 9, pp. 1297–1300.
11. Bojkov, R., Bishop, L., Hill, W.J., Reinsel, G.C., and Tiao, G.C., A Statistical Trend Analysis of Revised Dobson Total Ozone Data over the Northern Hemisphere, *J. Geophys. Res. D*, 1990, vol. 95, no. 7, pp. 9785–9807.
12. Thompson, D.W.J., Wallace, J.M., and Hegerl, G.C., Annular Modes in the Extratropical Circulation, Part II: Trends, *J. Clim.*, 2000, vol. 13, no. 5, pp. 1018–1036.
13. Bagrov, N.A., Analytical Representation of a Sequence of Meteorological Fields in Terms of Empirical Orthogonal Functions, *Tr. TsIP*, 1959, no. 74, pp. 3–24.
14. Oboukhov, A.M., Statistical Orthogonal Expansions of Empirical Functions, *Izv. Akad. Nauk SSSR, Ser. Geofiz.*, 1960, no. 3, pp. 432–439.
15. Meshcherskaya, A.V., Rukhovets, L.V., Yudin, M.I., and Yakovleva, N.I., *Estestvennye sostavlyayushchie meteorologicheskikh polei* (Empirical Components of Meteorological Fields), Leningrad: Gidrometeoizdat, 1970.

16. Staehelin, J., Renaud, A., Bader, J., McPeters, R., Viatte, P., Hoegger, B., Bugnion, V., Giroud, M., and Schill, H., Total Ozone Series at Aroza (Switzerland): Homogenization and Data Comparison, *J. Geophys. Res. D*, 1998, vol. 103, no. 5, pp. 5827–5841.

17. Lorenz, E.N., Seasonal and Irregular Variations of the Northern Hemisphere Sea-Level Pressure Profile, *J. Meteorol.*, 1951, vol. 8, pp. 52–59.

18. Rinne, J. and Jarvenoja, S., Accuracy of the Series Given in EOFs, *E.C.M.W.F. Workshop on the Use of Empirical Orthogonal Functions in Meteorology*, Reading, UK, 1977, pp. 97–111.

19. Hollandsworth, S.M., Bowman, K.P., and McPeters, R.D., Observational Study of the Quasi-Biennial Oscillation in Ozone, *J. Geophys. Res. D*, 1995, vol. 100, no. 5, pp. 7347–7361.

20. Chernikov, A.A., Borisov, Yu.A., Zvyagintsev, A.M., Kruchenitskii, G.M., and Perov, S.P., Variability if the Ozone Layer in the period 1979–1999, *Opt. Atmos. Okeana*, 2000, vol. 13, no. 1, pp. 100–105.

21. Perlwitz, J. and Graf, H.F., On the Statistical Connection between Tropospheric and Stratospheric Circulation of the Northern Hemisphere in Winter, *J. Clim.*, 1995, vol. 8, no. 9, pp. 2281–2295.

22. Kodera, K. and Koide, H., Spatial and Seasonal Characteristics of Recent Decadal Trends in the Northern Hemispheric Troposphere and Stratosphere, *J. Geophys. Res. D*, 1997, vol. 102, no. 16, pp. 19433–19447.

23. Charney, J.G. and Drazin, P.G., Propagation of Planetary-Scale Disturbances from the Lower into the Upper Atmosphere, *J. Geophys. Res.*, 1961, vol. 66, no. 1, pp. 83–109.

24. Zhadin, E.A., Planetary Waves and Interannual Anomalies of Ozone in Polar Regions, *Izv. Akad. Nauk SSSR, Fiz. Atmos. Okeana*, 1990, vol. 26, no. 11, pp. 1156–1160.

25. Hood, L. and Zaff, D., Lower Stratospheric Stationary Waves and the Longitude Dependence of Ozone Trends in Winter, *J. Geophys. Res. D*, 1995, vol. 100, no. 12, pp. 25 791–25 800.

26. Zhadin, E.A., Resonance of Planetary Waves and Sudden Stratospheric Warmings, *Izv. Akad. Nauk SSSR, Fiz. Atmos. Okeana*, 1988, vol. 24, no. 1, pp. 30–34.

27. Corti, S., Molteni, F., and Palmer, T.N., Signature of Recent Climate Change in Frequencies of Natural Atmospheric Circulation Regimes, *Nature*, 1999, vol. 398, pp. 799–802.

28. Osdorne, T.J., Briffa, K.R., Tett, S.F.B., Jones, P.D., and Trigo, R.M., Evaluation of the North Atlantic Oscillation as Simulated by a Coupled Climate Model, *Clim. Dyn.*, 1999, vol. 15, no. 9, pp. 685–702.

29. Kushnir, Y., Interdecadal Variations in North Atlantic Sea Surface Temperature and Associated Atmospheric Conditions, *J. Clim.*, 1994, vol. 7, no. 1, pp. 142–157.

Translated by Z. Feizulin

Paper III

Influence of early winter upward wave activity flux on midwinter circulation in the stratosphere and troposphere

A. Karpetchko and G. Nikulin

J. Climate, 17, 4443-4452, 2004

Influence of Early Winter Upward Wave Activity Flux on Midwinter Circulation in the Stratosphere and Troposphere

ALEXEI KARPETCHKO

Finnish Meteorological Institute, Arctic Research Centre, Sodankylä, Finland

GRIGORY NIKULIN

Swedish Institute of Space Physics, Atmospheric Research Programme, Kiruna, Sweden

(Manuscript received 22 October 2003, in final form 23 April 2004)

ABSTRACT

Using NCEP–NCAR reanalysis data the authors show that the November–December averaged stratospheric eddy heat flux is strongly anticorrelated with the January–February averaged eddy heat flux in the midlatitude stratosphere and troposphere. This finding further emphasizes differences between early and midwinter stratospheric wave flux behavior, which has recently been found in long-term variations. Analysis suggests that the intraseasonal anticorrelation of stratospheric heat fluxes results from changes in the upward wave propagation in the troposphere. Stronger (weaker) upward wave fluxes in early winter lead to weaker (stronger) upward wave fluxes from the troposphere during midwinter. Also, enhanced equatorward wave refraction during midwinter (due to the stronger polar night jet) is associated with weak heat flux in the early winter. It is suggested that the effect of enhanced midwinter upward wave flux from the troposphere in the years with weak early winter heat flux overcompensates the effect of increased equatorward wave refraction in midwinter, leading to a net increase of midwinter upward wave fluxes into the stratosphere.

1. Introduction

Large-scale waves propagating from the troposphere into the stratosphere during winter decelerate the stratospheric westerly winds, and it is recognized that this wave forcing drives the diabatic circulation in the stratosphere. This circulation is responsible, in particular, for wintertime adiabatic warming of the polar stratosphere and poleward ozone transport. It has been demonstrated that interannual variability of the Arctic stratospheric temperature and extratropical ozone is strongly correlated with strength of the meridional circulation (Newman et al. 2001; Salby and Callaghan 2002). Since trends have been documented in both the stratospheric temperature (Ramaswamy et al. 2001) and the total ozone (Staehelin et al. 2001), a lot of effort has been made to connect these changes to the changes in wave forcing. The vertical component of the Eliassen–Palm (EP) flux (F_z), which is proportional to the zonal mean eddy heat flux, is widely used as a proxy of wave forcing of the diabatic circulation. Fusco and Salby (1999) found a decrease of F_z in January (1979–93) and suggested that the negative trends of midlatitude total ozone are, to a large extent, explained by the negative trends of F_z. Newman and Nash (2000) compared the heat flux based on different datasets and found statistically significant negative trends in the January–February averaged heat flux (1979–99). The subsequent work by Randel et al. (2002) confirmed the negative trends separately in January and February for the period 1979–2000, but they pointed out that the February trend is not significant and the January trend is on the edge of statistical significance. They also found weak insignificant positive trends in early winter [November–December (ND)], whereas winter-averaged November–March heat flux trends are far from statistically significant. Hu and Tung (2002) did not find evidence for a decrease of the November–January upward EP flux from the troposphere and divergence of the EP flux in the stratosphere in recent decades. However in their follow-up paper Hu and Tung (2003) confirmed the negative trends in the January–March mean of the vertical EP flux component as well as weak positive insignificant trends in November–December.

The observed decline of the upward wave flux in the January–March period may be caused by some forcing that is not effective in the early winter. For example, Hu and Tung (2003) presented evidence that Arctic ozone depletion, which is the severest in late winter and early spring, could result in such a forcing. They pro-

Corresponding author address: Dr. A. Karpetchko, Finnish Meteorological Institute, Arctic Research Centre, Tähteläntie 62, FIN-99600 Sodankylä, Finland.
E-mail: alex.karpetchko@fmi.fi

posed that ozone decline leads to an enhanced meridional temperature gradient in the subpolar stratosphere that in turn strengthens the polar night jet and increases wave refraction away from the high latitudes.

The results described above suggest that behavior of the upward wave propagation in the stratosphere on decadal time scales differs between early and midwinter. In the present paper we further document the intraseasonal differences in wave activity propagation. Attention is focused on the question of whether or not differences in wave propagation behavior in early and midwinter are revealed in intraseasonal variations. First, we show that the early winter heat flux is, in fact, strongly anticorrelated with the midwinter heat flux in the midlatitude troposphere and stratosphere, and we propose a mechanism for the intraseasonal heat flux anticorrelation. Then we discuss decadal trends in the early and midwinter heat fluxes.

2. Data

We use temperature and wind fields from the NCEP–NCAR-reanalysis database, a joint product of National Centers of Environmental Prediction (NCEP) and National Center for Atmospheric Research (NCAR) (Kalnay et al. 1996). The quality of the NCEP–NCAR reanalysis in the stratosphere in the pre-1979 period before the inclusion of satellite data is questionable. Therefore we use the pre-1979 data only for a comparison with the results obtained on the basis of the 1979–2002 period. To take into account both transient and quasi-stationary eddies, all calculations of the eddy heat flux were performed on daily means and then monthly averaged. Weighting with the cosine of the latitude is applied for averaging in latitudinal belts.

3. Heat fluxes in early and midwinter

We separate a whole winter into the November–December (ND) and January–February (JF) periods, which are described hereafter as early and midwinter. The year for winter denotes the year of the JF period. Figure 1a shows one-point correlations of the 20-hPa ND total heat flux averaged over 45°–75°N with the JF total heat flux for 1979–2002. An area of negative correlations is located north of 45°N throughout the majority of the stratosphere and the troposphere with two minima, one at 10 hPa, 50°N and another at 400 hPa, 55°N. Both minima are significant at the 99% level with minimum correlation coefficients −0.72 at 10 hPa and −0.8 at 400 hPa. Positive correlations cover the region from 300 to 30 hPa between 30° and 45°N with maximum correlation significant at the 99% level. Another area of insignificant positive correlations is located in the polar stratosphere higher than 50 hPa north of 70°N. According to Fig. 1a, upward wave flux during the JF period is weaker (stronger) throughout the majority of the midlatitude stratosphere and troposphere in years

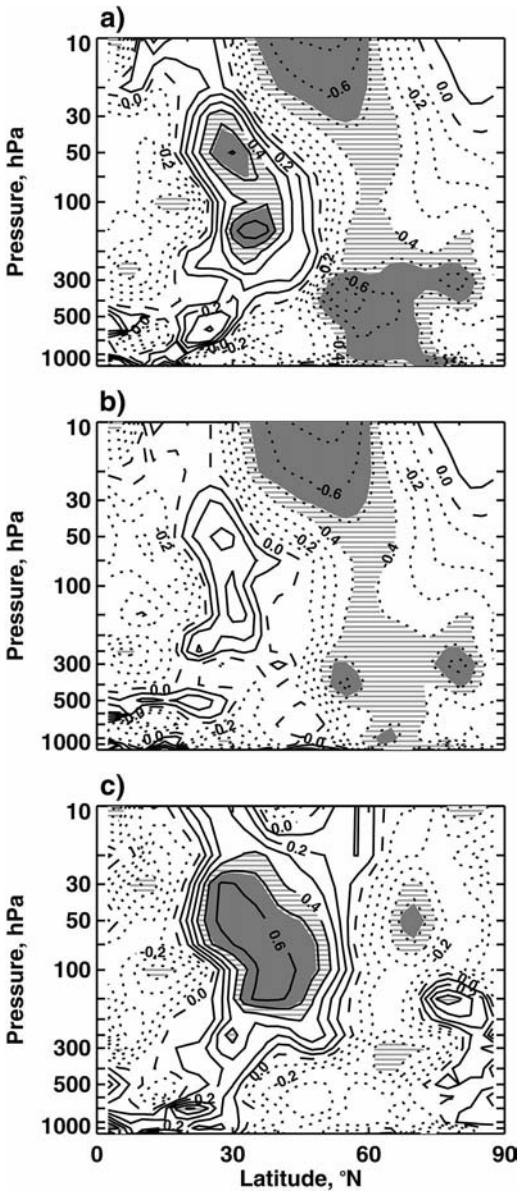

FIG. 1. Correlation between the ND total heat flux at 20 hPa averaged over 45°–75°N and JF (a) total heat flux, (b) heat flux for waves 1–3, and (c) heat flux for waves 4–7. Positive contour values are solid, negative values are dotted, and zero contours are dashed. The 95% (lines) and 99% (solid) confidence levels are shaded.

with strong (weak) heat flux during early winter. The upper troposphere and lower stratosphere region at the edge of the Tropics and extratropics near and above the subtropical jet stream shows opposite behavior. The results presented in Fig. 1a are not sensitive to the level at which the early winter heat flux is taken. Similar results with just slight differences are obtained if the early winter heat flux is taken at the 50 or 100 hPa level.

Planetary-scale waves dominate in the stratospheric eddy heat flux while in the troposphere a contribution from the shorter waves should also be expected. It is

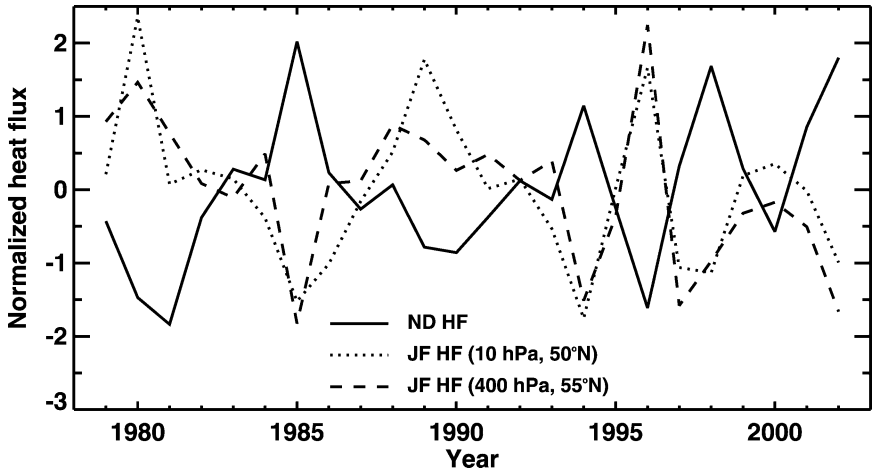

FIG. 2. Time series of normalized heat flux anomalies averaged for 15 Nov–31 Dec at 20 hPa over 45°–75°N (solid) and for 1 Jan–28 Feb at 10 hPa, 50°N (dotted) and 400 hPa, 55°N (dashed).

interesting to partition the total midwinter heat flux into the flux due to zonal waves 1–3 and the flux due to waves 4 and higher in order to see which waves contribute to the correlation with the early winter heat flux and where this occurs. Figure 1b shows correlation of the same ND total heat flux as in Fig. 1a, but with the JF heat flux for waves 1–3. The comparison of Figs. 1b and 1a shows that restricting the eddy heat flux to the planetary waves leads to a slight strengthening of the anticorrelation in the midlatitude stratosphere. The anticorrelation in the troposphere is, however, noticeably weakened, suggesting that waves 1–3 are not the only contributors to the observed tropospheric anticorrelation. The area of significant positive correlation near the subtropical jet stream, evident in Fig. 1a, does not appear in Fig. 1b. Correlation of the ND total heat flux with the JF heat flux for waves 4–7 is presented in Fig. 1c. Negative correlation is evident in the midlatitude troposphere though it is at the edge of statistical significance. It is interesting to note that the area of significant positive correlation near the subtropical jet stream reappears in Fig. 1c. Moreover, there is a noticeable improvement in the correlation with the maximum correlation coefficient reaching 0.68, which is significant at the 99% level. The correlation pattern for the midwinter heat flux due to waves 1–7 (not shown) differs insignificantly from the one for the total flux, which implies that flux due to waves 1–7 can virtually be regarded as the total heat flux. The ND total heat flux does not correlate with the JF heat flux due to waves higher than 8. Analysis of Figs. 1a–c suggests that in the midlatitude stratosphere early winter heat fluxes mainly anticorrelate with midwinter heat fluxes due to planetary waves, while in the midlatitude troposphere, they anticorrelate better with total fluxes. The planetary waves, however, are the main contributor to the observed anticorrelation in the troposphere. The midwinter heat flux due to waves 4–7 mainly contributes to the positive correlation area near and above the subtropical jet stream.

The results presented in Fig. 1 are not restricted to the 1979–2002 period. The correlation patterns for 1958–2002 (not shown here) are very similar to the patterns in Figs. 1a–c, with slightly lower but significant absolute values of correlation coefficients. This result suggests that the anticorrelation between the heat fluxes is not due to trends but rather due to year-to-year variations. This statement is further illustrated by Fig. 2, which shows the anomalies of the 20-hPa latitudinal averaged ND heat flux together with the JF heat flux anomalies taken from two grid points where the best anticorrelation is observed. The anomalies are normalized by their standard deviations. It is clearly seen that a maximum in ND usually corresponds to a minimum in JF. In Fig. 2 we use early winter heat fluxes averaged for 15 November to 31 December. This period differs slightly from the one used in Fig. 1 but, as we found experimentally, gives the best correlation coefficients. It is worth mentioning that heat flux averaging periods close to 45 days were also used by Newman et al. (2001), giving remarkably high correlation with averaged temperature of the following period. They pointed out that the duration of the periods is determined by thermal damping times. In the next section we will discuss how the period of the heat flux anticorrelation is related to relaxation of the stratosphere to the radiative equilibrium.

4. Midwinter EP flux and zonal mean circulation

Figures 1 and 2 suggest that wave fluxes in the midlatitude stratosphere vary during winter with a period of weak fluxes following a period of strong fluxes and vice versa. These variations are actually related to the stratospheric vacillations, which were first modeled by Holton and Mass (1976) in their quasigeostrophic β-

plane channel model. They found that, when wave forcing at the lower boundary is raised beyond a critical amplitude, the eddy components and mean zonal flow in the stratosphere oscillate quasiperiodically. In their model vertically propagating planetary waves 1 and 2 decelerate westerly zonal flow until it turns into easterlies. Since planetary waves cannot propagate in easterlies (Charney and Drazin 1961), this results in trapping of the waves. In the absence of wave forcing the stratosphere relaxes to the radiative equilibrium, westerlies are recovered, and waves can again propagate into the stratosphere. This mechanism suggests that the period of oscillations is determined by the time that the stratosphere takes to relax to the radiative equilibrium. The period of the vacillations is roughly 2–3 months, which coincides with the period of the heat flux anticorrelation found here.

A connection between eddy components and mean zonal flow oscillations was afterward found in general circulation models and in observations (Cristiansen 1999, 2001). Cristiansen (2001) pointed out that these oscillations originate from competition between zonal wind deceleration caused by vertical convergence of the vertical component of the EP flux and zonal wind acceleration caused by relaxation toward the radiative equilibrium. Figure 3 shows the JF wind anomalies for years with the weak and strong ND heat flux as well as their differences. Only winters when the ND normalized latitudinal averaged heat flux anomalies at 20 hPa were more (1985, 1994, 1998, 2001, 2002) or less (1980, 1981, 1989, 1990, 1996, 2000) than 1 σ were included in these statistics. It is seen that, when wave flux is weak in the early winter, the midwinter polar night jet is well developed between 60° and 70°N (Fig. 3a). In contrast, when the early winter heat flux is strong, the midwinter polar night jet is decelerated between 60° and 70°N with a secondary maximum appearing at about 30°N (Fig. 3b). The positive JF wind speed differences between the winters with weak and strong ND heat fluxes are statistically significant throughout the majority of the extratropical stratosphere (Fig. 3c). There is also a negative statistically significant wind speed anomaly in the upper part of the plot at about 30°N. To see the wave propagation behavior for these periods, we calculated the EP fluxes (see Andrews et al. 1987) and superimposed them on the wind fields. The arrows of the EP flux vector are scaled by density to make the stratospheric part of the picture more readable. The JF EP flux differences between the winters with weak and strong ND heat flux are shown in Fig. 3c. It is seen that the direction of the anomalous EP flux is consistent with the correlation pattern shown in Fig. 1a. It is directed upward throughout the midlatitude stratosphere and troposphere on the southern part of the positive wind difference, where significant anticorrelation between the heat fluxes is observed (Fig. 1a). The anomalous EP flux is directed downward in the polar stratosphere in the upper part of the plot on the northern side of the positive wind difference. The statistical significance of the differences between the EP flux components during midwinter in the years with weak and strong ND heat flux can be seen in Fig. 4. The picture for the vertical component (Fig. 4a) is essentially the same as that for the heat flux correlation (Fig. 1a). It shows that the vertical component of the EP flux is stronger in the midlatitude troposphere and stratosphere and weaker in the vicinity of the subtropical jet stream in the years

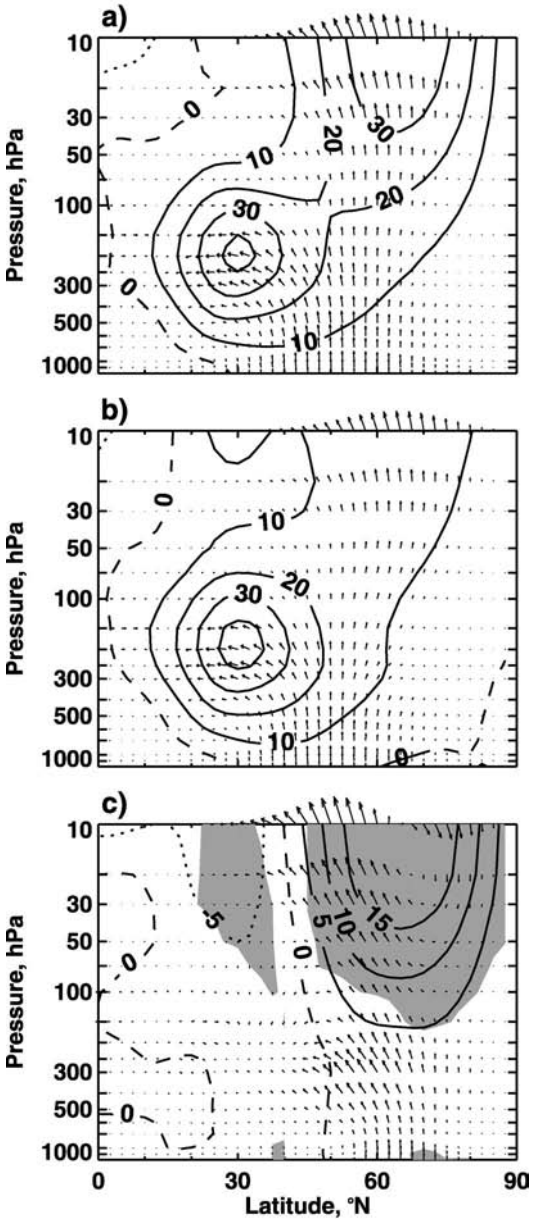

FIG. 3. Composite means of the JF zonal-mean zonal wind (m s^{-1}) and EP flux vectors in the years with (a) weak and (b) strong wave activity during the ND period and (c) their difference. Positive contour values are solid, negative values are dotted, and zero contours are dashed. The arrow scale is four times larger in (c) than in (a) and (b). The 99% confidence level for zonal wind is shaded.

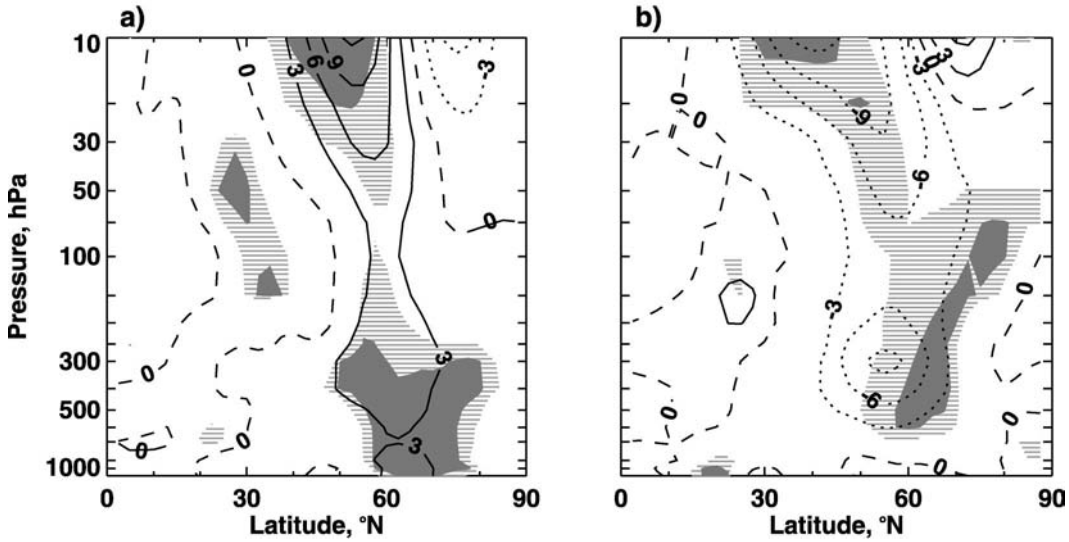

FIG. 4. The difference between the composite means of (a) vertical component (b) meridional component of the JF EP flux in the years with weak and strong wave activity during the ND period. Units are 10^5 m^3 s^{-2} for the vertical component and 10^7 m^3 s^{-2} for the meridional component. Positive contour values are solid, negative values are dotted, and zero contours are dashed. The 95% (lines) and 99% (solid) confidence levels are shaded.

with weak ND heat flux. The meridional component of the EP flux (Fig. 4b) is smaller during midwinter in the midlatitude troposphere and stratosphere in the years with weak ND heat flux. Since weaker early winter heat flux leads to a stronger polar night jet during midwinter (Fig. 3), this implies that waves are refracted more equatorward in the case of the stronger polar night jet. Detailed inspection of Fig. 3 leads to the conclusion that waves are refracted more poleward in the lower stratosphere (below 50 hPa) in the years with strong ND heat flux and more equatorward south of the polar night jet in the years with weak ND heat flux.

Figure 3 suggests that both zonal wind and EP flux anomalies in January–February are connected to the anomalous ND heat flux. It is known that zonal wind anomalies in the winter stratosphere propagate downward and poleward (Kodera at al. 1990). This propagation is closely related to downward propagation of the Arctic Oscillation (AO) signal (Kodera at al. 2000). Figure 5 shows the correlation of the ND heat flux with (a) December and (b) JF zonal winds. The wind anomaly caused by wave forcing appears in December in the stratosphere at 100–10 hPa and in the 40°–60°N latitudinal belt. According to Fig. 5a, stronger wave flux

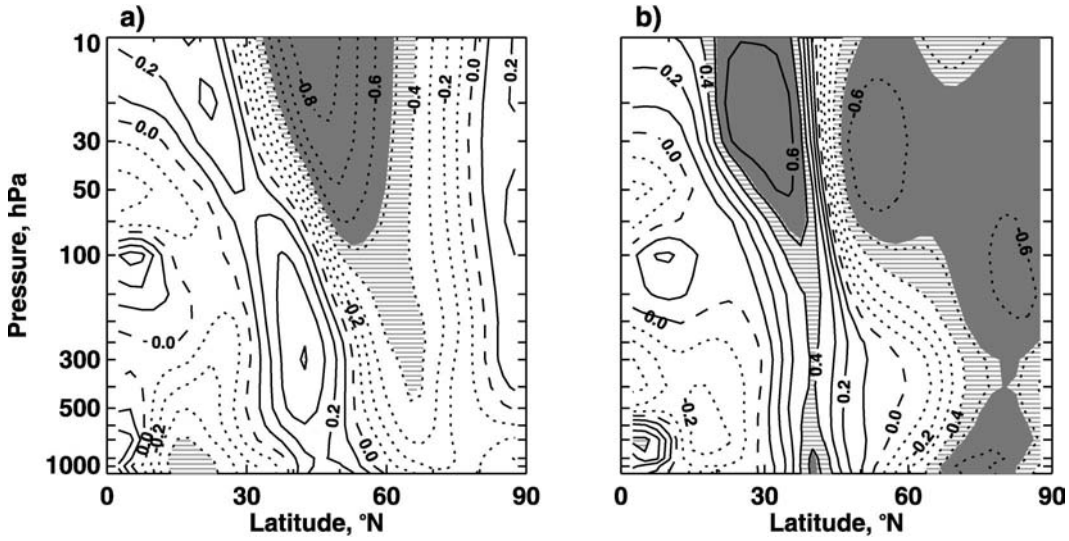

FIG. 5. Correlation between the ND total heat flux at 20 hPa averaged over 45°–75°N and (a) Dec and (b) JF zonal-mean zonal wind. Positive contour values are solid, negative values are dotted, and zero contours are dashed. The 95% (lines) and 99% (solid) confidence levels are shaded.

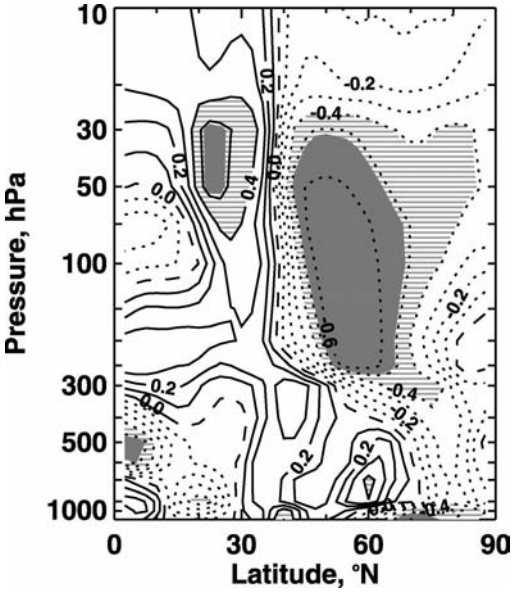

FIG. 6. Correlation between the ND total heat flux at 20 hPa averaged over 45°–75°N and zonal mean zonal wind shear for JF. Contours and shading as in Fig. 5.

causes weaker winds in that region. The area of statistically significant wind anomalies in January–February moves poleward and downward and even reaches the lower troposphere (Fig. 5b). Figure 5 is quite similar to the results of Kodera at al. (1990, Fig. 2). The key difference is that the zonal wind anomaly in the early winter centered at 10 hPa, 45°N is shown to be created by the anomalous wave activity flux. The downward zonal wind anomaly propagation is therefore initialized by the early winter wave forcing.

Additionally, it is interesting to note that the dipole structure evident in Fig. 5b is similar to the correlation pattern between the AO index and zonal mean wind (Baldwin and Dunkerton 1999, Fig. 2a) but with opposite signs. The high phase of the AO seems to correspond to increased zonal winds north of a node line and decreased winds south of it. Therefore, our results suggest that the high phase of the AO more likely follows a period of weak wave fluxes into the stratosphere and vise versa, similar to the results of Polvani and Waugh (2004).

5. Mean flow–wave propagation feedback

The model results by Chen and Robinson (1992) suggest that wave propagation between the troposphere and stratosphere is not sensitive to the zonal winds in the stratosphere but depends on the vertical derivative of the zonal-mean zonal wind (U_z) at the tropopause level. Figure 6 shows the ND heat flux correlation with the January–February-averaged U_z. It is seen that there is an area of statistically significant negative correlation in the midlatitude lower stratosphere and tropopause

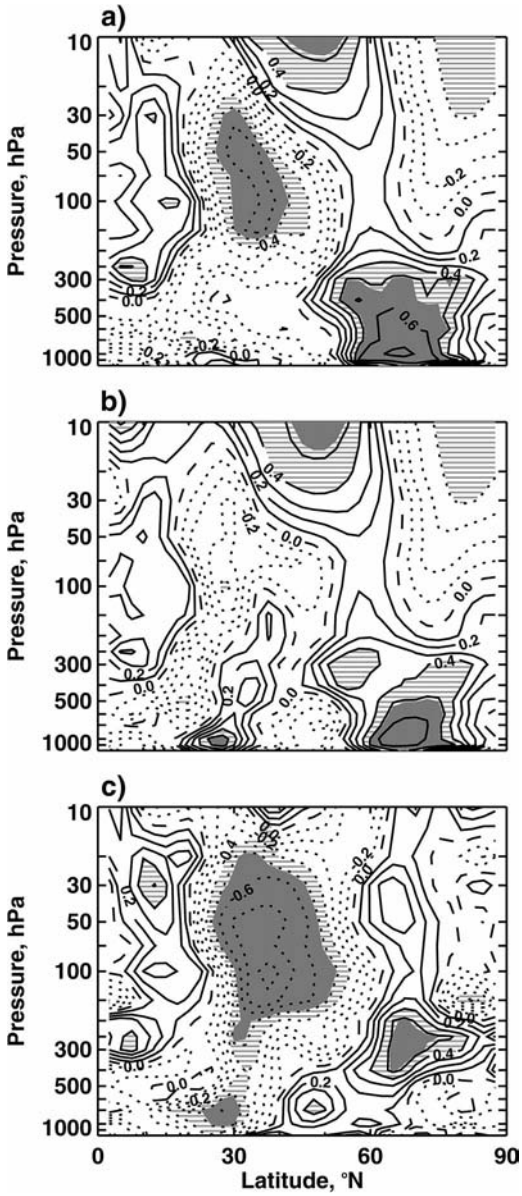

FIG. 7. Correlation between the JF zonal mean zonal wind shear at 250 hPa averaged over 50°–70°N and JF (a) total heat flux, (b) heat flux for waves 1–3, and (c) heat flux for waves 4–7. Contours and shading as in Fig. 5.

region that means that the early winter upward wave flux decreases U_z in that region in the following period. Comparison of Fig. 6 with Fig. 1 shows that decreased U_z at the tropopause level in midwinter corresponds to decreased upward wave flux in the midlatitude stratosphere. This is clearly seen from Fig. 7, which shows correlation of the JF wind shear at 250 hPa averaged over 50°–70°N latitudes with the JF (Fig. 7a) total heat flux as well as heat flux due to (Fig. 7b) waves 1–3 and (Fig. 7c) waves 4–7. Figure 7 closely repeats all the main features evident in Fig. 1, suggesting that U_z changes at the tropopause level are involved in the

mechanism for the intraseasonal heat flux anticorrelation. A noticeable difference between Fig. 1 and Fig. 7 is that the area of correlation north of 70°N between 10 and 30 hPa (positive in Fig. 1 and negative in Fig. 7) becomes significant at the 95% level. This suggests that increased wind shear at the tropopause is related to suppression of the wave propagation into the polar stratosphere that is in agreement with results by Chen and Robinson (1992). However, increasing U_z at the tropopause also leads to increasing planetary wave propagation into the midlatitude stratosphere south of 60°N (Fig. 7b). This was not described by Chen and Robinson (1992), but their results are derived under the assumption that the amount of wave activity generated in the troposphere is independent of changes in the wind shear at the tropopause. Additionally, Hu and Tung (2002) have shown that the wind shear tends to enhance upward wave propagation whereas the zonal wind and second vertical derivative of the zonal wind tend to impede upward propagation.

Enhanced upward wave flux in the troposphere (Fig. 7b) could be directly related to enhanced generation of wave activity. However, wave activity is a highly derivative quantity given by the formula $A = 0.5\rho_0 \cdot \overline{q'^2}/\overline{q}_y$, where ρ_0 is the basic air density, $\overline{q'^2}$ is the zonal-mean squared eddy quasigeostrophic potential vorticity (QGPV), and $\overline{q}_y$ is the meridional gradient of the zonal mean QGPV (Andrews et al. 1987). Direct calculation of the wave activity from the data show that A is very sensitive to small changes in the zonal wind, and therefore the results obtained are noisy and hardly reliable. Therefore, model experiments are required to investigate the relationship between wave activity generation in the troposphere and the mean flow in the stratosphere and at the tropopause level.

Our results also suggest that enhanced upward wave propagation into the stratosphere can be coupled with enhanced equatorward wave refraction. Indeed, waves are refracted more equatorward during midwinter in years when the ND heat flux is weaker and the midwinter polar night jet is stronger (Fig. 4b). This results in insignificant weakening of the upward wave flux into the polar stratosphere north of 65°N, but at the same time the upward EP flux into the stratosphere south of 65°N is stronger (Fig. 4a). This can be explained by taking into account that the midwinter upward EP flux is also enhanced in the troposphere in the years with weak ND heat flux. Enhanced upward wave fluxes from the troposphere can overcompensate the effect of the stronger equatorward wave refraction. In addition, waves refracted away from the polar stratosphere can also contribute to enhancement of the midlatitude upward wave flux. The important inference is that the stronger polar night jet does not necessarily imply a weaker upward planetary wave flux into the stratosphere.

In contrast to the planetary waves, waves 4–7 almost do not propagate into the midlatitude stratosphere, undergoing strong equatorward refraction in the upper troposphere. The remarkable decrease of the upward wave propagation in the subtropical stratosphere in years with weak ND heat fluxes (Fig. 7c) is caused by enhancement of the equatorward refraction, with less wave activity left to propagate upward. Stronger refraction is probably related to the stronger zonal winds in the midlatitude stratosphere in years with weak ND heat flux (Fig. 3). This mechanism can also explain the observed positive correlation between the ND total heat flux and the JF heat flux due to waves 4–7 in the subtropical upper troposphere/lower stratosphere region (Fig. 1c). Another mechanism was proposed by a reviewer who suggested that weakened planetary waves (Fig. 1b) might result in stronger small-scale waves in that region, which is a residual of planetary wave breaking effects.

6. Long-term wave activity variations

Finally, in Fig. 8 we show in more detail an altitude–latitudinal cross section of decadal trends in the early and midwinter heat fluxes for the 1979–2002 period. In early winter (Fig. 8a), an area of positive heat flux trends significant at the 95% level appears in the polar stratosphere and upper troposphere. During midwinter (Fig. 8b) one area of negative significant heat flux trends is confined within the polar lower stratosphere and middle troposphere. Another area is located in the midlatitude lower troposphere. To be sure that the significant patterns have not occurred by chance we perform a field significance test using Monte Carlo simulations (Chu and Wang 1997). The patterns are significant at the 95% level for both early and midwinter. Figure 8 illustrates that trend signs are opposite in these two seasons. These opposite trends might be a result of the intraseasonal heat flux anticorrelation. The area of the significant positive trends in Fig. 8a partly overlaps the region (20 hPa, 45°–75°N) that was used for averaging the ND heat fluxes to calculate correlations in Fig. 1, but the 20-hPa ND heat flux does not show any trend in Fig. 2. A part of the significant negative trends in the JF polar upper troposphere corresponds with the area of negative correlation shown in Figs. 1a,b. However there are no significant trends in the midlatitude stratosphere where strong anticorrelation was found. These arguments do not support the assumption that the opposite heat flux trends in early and midwinter result from the intraseasonal heat flux anticorrelation. Trend estimates are very sensitive to the choice of period and removing or adding one year can appreciably change the results obtained. If we calculate heat flux trends after removing 2002 from the statistics, there are no longer any significant positive trends in the early winter. In fact, excluding only one year with the early-winter low heat flux from the beginning of the sample (e.g. 1981, see Fig. 2) or a year with high heat flux from the end of the sample (1998) gives similar results. Thus, the trends in the early winter heat flux for 1979–2002 are positive, but the

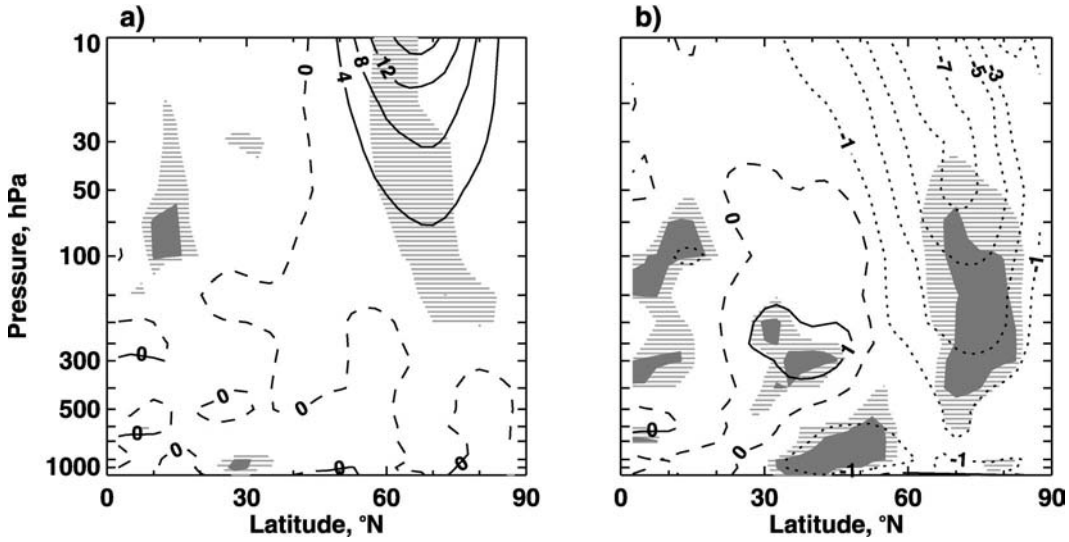

FIG. 8. Decadal trends in heat flux averaged for (a) ND and (b) JF for 1979–2002. Units are in K m s^{-1} per decade. Shading as in Fig. 5.

significance of them is strongly influenced by changing the sample by only one year and should be interpreted very carefully. At the same time the significant negative trends in the midwinter heat flux are not so sensitive to such small changes as mentioned above. However, the largest decline of the JF heat flux occurred before 1997 with no significant decline afterward.

As far as statistical trend estimations are concerned, our results are in agreement with estimations made in previous studies (Newman and Nash 2000; Randel et al. 2002; Hu and Tung 2003). Hu and Tung showed that decreasing upward wave activity fluxes is related to a decrease in the refraction index and enhancement of the equatorward wave refraction away from the polar night jet. These changes, however, are not coupled with statistically significant strengthening of the stratospheric westerly winds. Figure 9 shows decadal trends in zonal-mean zonal wind and U_z for the period 1979–2002. As can be seen (Fig. 9a), there is no strengthening of the zonal winds in the lower stratosphere. Only the area in the midlatitude troposphere between 50° and 60°N and below 200 hPa shows positive trends significant at 95%. A strengthening of the stratospheric winds from the end of the 1970s to the second half of the 1990s found previously (see, e.g., Hood et al. 1999) is not confirmed in the extended time series. Moreover, zonal winds show

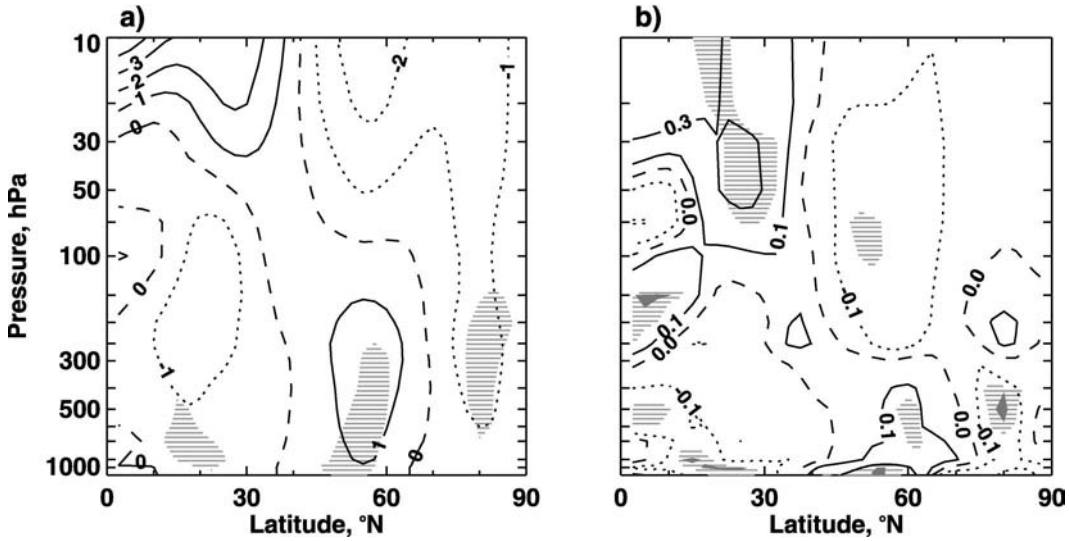

FIG. 9. Decadal trends in the JF (a) zonal mean zonal wind and (b) zonal mean zonal wind shear for 1979–2002. Units are in (a) m s^{-1} $decade^{-1}$ and (b) m s^{-1} km^{-1} $decade^{-1}$. The 95% (lines) and 99% (solid) confidence levels are shaded.

insignificant negative trends in the extratropics at levels higher than 70 hPa that are mainly due to recent winters 2000/01 and 2001/02. The observed decline of the midwinter upward wave activity flux could also be related to trends in U_z. However, calculations of trends in U_z for the same period (Fig. 9b) show only weak insignificant negative trends throughout the stratosphere and upper troposphere north of 40°N and insignificant positive trends in the midlatitude troposphere below 300 hPa. Only a small area with significant negative U_z trends is evident in the midlatitude stratosphere between 70 and 100 hPa, but it comprises only a few points. Insignificant strengthening of the lower stratospheric zonal wind coupled with insignificant decreasing of the U_z could result in statistically significant decreasing of the refractive index in the lower stratosphere, as was found by Hu and Tung (2003). However, in this case the trends in both the refractive index and the upward wave flux cannot be directly connected to the changes in the zonal winds, so physical interpretation of the trends is not very clear.

7. Conclusions

We have shown that the November–December averaged stratospheric total eddy heat flux is strongly anticorrelated with the January–February averaged total eddy heat flux in the midlatitude stratosphere and troposphere. It has also been shown that anticorrelation in the stratosphere is related to a part of the JF total heat flux that is due to planetary waves. This finding further demonstrates differences between the behavior of upward wave activity propagation in early compared to midwinter, as previously observed in the long-term variations by Hu and Tung (2003). The observed stratospheric heat flux anticorrelation is similar to the well-known stratospheric vacillations (Holton and Mass 1976).

According to our results, stronger upward wave fluxes in early winter lead to weaker upward wave fluxes from the upper troposphere in January–February. This ultimately leads to decreased wave flux into the stratosphere, thus providing a mechanism for the intraseasonal heat flux anticorrelation in the stratosphere. The observed heat flux anticorrelation is essentially related to the changes in both zonal wind and wind shear. Wind shear at the tropopause level is positively correlated with upward wave fluxes in the midlatitude troposphere and stratosphere. According to analysis by Hu and Tung (2002), positive wind shear increases the refractive index and therefore enhances upward wave propagation into the stratosphere. In contrast, the strengthened midwinter stratospheric jet, which is observed in years with weak ND heat flux, tends to refract planetary waves equatorward. Presumably, increased wave fluxes from the troposphere overcompensates, the effect of increased equatorward wave refraction. The increased wave fluxes in the troposphere could be explained by enhanced generation of the wave activity. However, direct calculations of the wave activity from data are difficult due to the high sensitivity of the calculation to small changes in initial data. Therefore, verification of this hypothesis is a subject for model experiments.

It should be mentioned, however, that the observed heat flux anticorrelation does not imply functional dependence between early and midwinter heat fluxes since moderate early winter heat fluxes may have no effect on the midwinter circulation and consequently on wave propagation. Rather, our results statistically demonstrate that strong (weak) early winter heat fluxes can hardly be followed by strong (weak) heat fluxes in the midwinter.

We have also presented a closer look at the long-term behavior of heat fluxes in early and midwinter by showing a latitude–height cross section of the heat flux trends in these seasons. While statistically significant negative trends exist in the lower polar stratosphere and midlatitude troposphere in midwinter, there are no negative trends in early winter. In fact, there is even an area of the polar stratosphere with positive trends in the period 1979–2002, which are at the edge of statistical significance. Trend significance depends essentially, however, on the period and is sensitive to small changes in the sample. Moreover, attributing negative trends in the midwinter upward wave flux to the changes in stratospheric winds is hardly possible since no statistically significant trends are found either in extratropical stratospheric zonal winds or in wind shear.

Acknowledgments. We are grateful to Prof. W. Robinson for helpful comments and two anonymous reviewers for suggested improvements. The authors also thank the Climate Prediction Center for providing NCEP–NCAR reanalysis data. The work of AK is supported by the EU Commission under project CANDIDOZ. The work of GN is supported by the Swedish Research Council.

REFERENCES

Andrews, D. G., J. R. Holton, and C. B. Leovy, 1987: *Middle Atmosphere Dynamics.* Academic Press, 489 pp.

Baldwin, M. P., and T. J. Dankerton, 1999: Propagation of the Arctic Oscillation from the stratosphere to the troposphere. *J. Geophys. Res.,* **104,** 30 937–30 946.

Charney, J. G., and P. G. Drazin, 1961: Propagation of planetary-scale disturbances from the lower into the upper atmosphere. *J. Geophys. Res.,* **66,** 83–109.

Chen, P., and W. A. Robinson, 1992: Propagation of planetary waves between the troposphere and stratosphere. *J. Atmos. Sci.,* **49,** 2533–2545.

Christiansen, B., 1999: Stratospheric vacillations in a general circulation model. *J. Atmos. Sci.,* **56,** 1858–1872.

——, 2001: Downward propagation of zonal mean zonal wind anomalies from the stratosphere to the troposphere: Model and reanalysis. *J. Geophys. Res.,* **106,** 27 307–27 322.

Chu, P. S., and J. B. Wang, 1997: Recent climate change in the tropical western Pacific and Indian Ocean regions as detected by outgoing longwave radiation records. *J. Climate,* **10,** 636–646.

Fusco, A. C., and M. L. Salby, 1999: Interannual variations of total ozone and their relationship to variations of planetary wave activity. *J. Climate,* **12,** 1619–1629.

Holton, J. R., and C. Mass, 1976: Stratospheric vacillation cycles. *J. Atmos. Sci.,* **33,** 2218–2225.

Hood, L., S. Rossi, and M. Beulen, 1999: Trends in lower stratospheric zonal winds, Rossby wave breaking behavior, and column ozone at northern midlatitudes. *J. Geophys. Res.,* **104,** 24 321–24 339.

Hu, Y., and K. K. Tung, 2002: Interannual and decadal variations of planetary wave activity, stratospheric cooling, and Northern Hemisphere annular mode. *J. Climate,* **15,** 1659–1673.

——, and ——, 2003: Possible ozone-induced long-term changes in planetary wave activity in late winter. *J. Climate,* **16,** 3027–3038.

Kalnay, E., and Coauthors, 1996: The NCEP/NCAR 40-Year Reanalysis Project. *Bull. Amer. Meteor. Soc.,* **77,** 437–471.

Kodera, K., K. Yamazaki, M. Chiba, and K. Shibata, 1990: Downward propagation of upper stratospheric mean zonal wind perturbation to the troposphere. *Geophys. Res. Lett.,* **17,** 1263–1266.

——, Y. Kuroda, and S. Pawson, 2000: Stratospheric sudden warmings and slowly propagating zonal-mean zonal wind anomalies. *J. Geophys. Res.,* **105,** 12 351–12 359.

Newman, P. A., and E. R. Nash, 2000: Quantifying the wave driving of the stratosphere. *J. Geophys. Res.,* **105,** 12 485–12 497.

——, ——, and J. E. Rosenfield, 2001: What controls the temperature of the Arctic stratosphere during the spring? *J. Geophys. Res.,* **106,** 19 999–20 010.

Polvani, L. M., and D. W. Waugh, 2004: Upward wave activity flux as precursor to extreme stratospheric events and subsequent anomalous surface weather regimes. *J. Climate,* **17,** 3547–3553.

Ramaswamy, V., and Coauthors, 2001: Stratospheric temperature trends: Observations and model simulations. *Rev. Geophys.,* **39,** 71–122.

Randel, W. J., F. Wu, and R. Stolarski, 2002: Changes in column ozone correlated with the stratospheric EP flux. *J. Meteor. Soc. Japan,* **80,** 849–862.

Salby, M. L., and P. F. Callaghan, 2002: Interannual changes of the stratospheric circulation: Relationship to ozone and tropospheric structure. *J. Climate,* **15,** 3673–3685.

Staehelin, J., N. R. P. Harris, C. Appenzeller, and J. Eberhard, 2001: Ozone trends: A review. *Rev. Geophys.,* **39,** 231–290.

Paper IV

A low ozone episode during the European heat wave of August 2003

Y. J. Orsolini and G. Nikulin

Quart. J. Roy. Meteor. Soc., in press, 2005

A low-ozone episode during the European heat wave of August 2003

Yvan J. ORSOLINI[1] and Grigory NIKULIN[2]

(1) Norwegian Institute for Air Research, Kjeller, Norway

(2) Swedish Institute for Space Research, Kiruna, Sweden

Quarterly Journal of the Royal Meteorological Society, in press, 2005

SUMMARY

An intense low-ozone episode (LOE) was observed over Scandinavia and the North Sea in the middle of August 2003. The LOE occurred under exceptional meteorological conditions, associated with a severe heat wave over Europe. The column ozone summer (June-July-August) minimum for 2003 was reached during the event.

Using meteorological analyses, satellite ozone observations from the Total Ozone Mapping Spectrometer (TOMS) and the Michelson Interferometer for Passive Atmospheric Sounding (MIPAS) aboard the ENVIronment SATellite (ENVISAT), we demonstrate that the LOE results from the conjunction of a deep tropospheric blocking over Europe, and a displaced Arctic pool of low-ozone air in the stratosphere, aloft of the anticyclone. The anticyclonic anomaly is part of a Rossby wave train, that is apparent throughout the troposphere, and whose influence is felt up to 50mb. In the midstratosphere (e.g. 30 mb), long-period westward-propagating planetary waves dominate, a ridge extending over northern Europe in mid-August.

We band-passed the geopotential field to isolate sub-monthly fluctuations, and calculated threedimensional wave activity fluxes for quasi-stationary, quasi-geostrophic disturbances embedded in a zonally asymmetric basic state. Results clearly indicate that upward wave fluxes in the lower stratosphere originate from the Atlantic sector, upstream of the maturing blocking.

KEYWORDS : stratosphere / atmospheric blocking / summer heat wave / ozone mini-holes /

1. INTRODUCTION

Transient column ozone decreases associated with anticyclonic weather systems occur at mid and high latitudes year-round. There have been many studies of intense low-ozone episodes (LOE) occurring in the winter season in conjunction with travelling, anticyclonic synoptic systems, or “ozone mini-holes” (Newman et al., 1988; McKenna, 1989; Peters and Waugh, 1996; Orsolini et al., 1998; Hood et al., 2000; James et al., 2000; Orsolini and Limpasuvan, 2001; Allen and Nakamura, 2002). Such events occur in both hemispheres. Large, summertime transient ozone lowerings were also observed at high northern latitudes by Lloyd et al. (1999). Orsolini et al. (2003a) studied the formation of two summertime LOEs over northern Europe in the summer 2000, using ozone observations from lidar, sondes and satellite instruments, as well as model results. They demonstrated that each pronounced summertime LOE resulted from the conjunction of two factors: first, the occurrence of an anticyclonic centre in the troposphere. Second, the displacement aloft of the anticyclone, of the mid-stratospheric pool of low-ozone air which develops over the Arctic in summer, due to the ozone gas phase destruction acting during long sunlit hours. Both factors combine to strongly decrease the ozone column. Orsolini et al. (2003a) showed an enhancement in ultraviolet (UV) radiation reaching the

ground by 15% over northern Scandinavia during the summertime LOEs in 2000. The enhancements resulted from the reduced ozone column and cloud-free anticyclonic conditions.

We hereby show evidence of a LOE event over northern Europe in mid-August 2003, when Europe experienced a strongly blocked circulation and an exceptional heat wave (Schär et al., 2004; Stott et al., 2004). Anticyclonic conditions persisted over Europe during most of the summer 2003, which was the warmest summer on record. In addition, several heat waves led to soaring ground temperatures in August. The hottest period was around the middle of August, during a highly anomalous blocking event centred over France (Grazzini et al., 2003; Black et al., 2004; Fink et al., 2004). All-time temperature records then tumbled over much of Europe. The heat waves caused large agricultural and forestry damages, and had devastating health impacts. The World Health Organisation estimated that the extreme heat caused 15000 excess deaths (WHO, 2003).

The LOE over Scandinavia and the North Sea occurred around August 10, at the peak of the central Europe heat wave. We will demonstrate that low-ozone stratospheric air extended southwards from the Arctic toward northern Europe, as the large-scale circulation in the lower and mid-stratosphere was perturbed by large-scale waves. Combined to the column ozone lowering by the anticyclonic conditions, this southward displacement of stratospheric Arctic air led to a column abundance as low as 250 Dobson Units (DU) over the North Sea and parts of Scandinavia[1].

2. OZONE OBSERVATIONS IN AUGUST 2003

We investigate the stratospheric ozone distribution in the summer 2003, using two satellite data sets: i) the daily column ozone from the TOMS (Version 7), at a spatial resolution of 1.25 degree longitude by 1 degree latitude, ii) the three-dimensional ozone derived from the limb-scanning MIPAS instrument. Characteristics of MIPAS are briefly described in ESA (2000). The along-track resolution is nearly 500 km, and the vertical resolution nearly 3 km. Near-real-time (NRT) along-track ozone profiles provided by European Space Agency (ESA) were interpolated onto isentropic levels using retrieved temperatures. As NRT data contains some spatial gaps, the ozone observations were coarsely binned in longitude (36 degree), latitude (10 degree), and time (2 days), as in Orsolini et al. (2005).

The hemispheric ozone column map from TOMS on August 10 (Fig. 1) shows low values, in the range of 250-275 DU, centred over the North Sea, and extending over Scandinavia and the British Isles. This is the region of the LOE, which will be the focus of our investigation. The TOMS time series at Oslo, Norway, (59°N, 10°E) and at Kiruna, Sweden, (67°N, 20°E) on Fig. 2a shows pronounced minima on August 10 (Julian day 222) and 11, respectively. The low values are about two standard deviations away from the June 21-to-August 30 mean, which we will refer to as the summer 2003 average. At both locations, the LOE coincided with the absolute summer minimum. Column ozone values are well below the August climatological (1978-2002) mean for Oslo (Fig. 2, circle). As seen on Fig. 1, comparably low values (250-275 DU) are also found over the Russian Arctic (120°E-180°E), the western coast of Alaska, and the North Pole.

On August 10, as the ozone column plummeted, the ozone mixing ratio at 650K, near 30 mb, also shows a pronounced minimum, indicating that the stratosphere is implicated in the column decrease. On Fig. 2b, the MIPAS ozone (60°N-70°N, 0°E-36°E) drops near 3.5 ppmv, i.e. 1.5 standard deviations below the summer mean.

An ozone map at the same level on August 9-10 (Fig. 3a, thick lines) shows a near wave-2 distortion of the pool of low-ozone polar air, away from the summer mean (Fig. 3a, dashed lines). The lowozone excursion is most pronounced over northern Europe and the northern Atlantic, and vanishes near 50°N. A low-ozone southward excursion is also present over the Russian Arctic and northern Alaska, near the dateline.

A MIPAS ozone profile in the LOE region over northern Europe (59°N, 13°E) on August 10 displays a singular, depleted layer in the pressure range of 30 to 50 mb (Fig. 4). Near 30 mb, ozone

[1]Anomalously elevated ground ozone concentrations over Europe were also reported at urban sites, as a consequence of the heat wave. The high ozone surface values do not contribute strongly to the column, and are not the subject of this article.

partial pressures are smaller than summer-mean values for the latitude band 55°N-65°N. They are closer to the summer-mean values for the 75°N-85°N latitude band, hence they are consistent with polar air being transported southward to 59°N. Low partial pressures below 100 mb are representative of lower latitude air (30°N-40°N), and consistent with northward, anticyclonic advection.

We will further demonstrate that the formation of the LOE results from the distorted stratospheric circulation aloft of tropospheric disturbances that were by themselves conducive to low-ozone column, namely conditions of high tropopause and anticyclonic circulation.

3. THE ANOMALOUS CIRCULATION IN THE TROPOSPHERE AND LOWER STRATOSPHERE IN AUGUST 2003

The tropospheric circulation over Europe in summer 2003 was characterised by anomalous high anticyclonic conditions and warm temperature (Grazzini et al., 2003). The Atlantic jet stream was displaced northward, resulting in a reduction in the passage of cyclones over central Europe. In the first half of August, an exceptionally strong and persistent anticyclone covered central Europe: Fig. 5 shows the August 1-15 mean geopotential height at 500 mb, expressed as an anomaly from a climatological August mean calculated from ERA-40[2] (1958-2002), and scaled in units of standard deviations. Hence, the high over Central Europe is four standard deviations above normal (Schär et al., 2004), a rare event. While the amplitude of the central European blocking was exceptional, the extreme surface temperatures gave the event so much impact. These resulted from local radiative budget influenced by the lasting spring-to-summer dryness, by the low background soil moisture, and the clear skies during the anticyclonic conditions (Schär et al., 2004; Black et al., 2004). There are other noteworthy features on this map: an Icelandic low displaced southwards to the central Atlantic, a positive anomaly over the eastern Canada and Labrador, and large anomalies of both signs over the central and north Pacific.

Figure 6 shows the August 10 potential temperature (theta) on the potential vorticity (PV) iso-surface 2 PV units (10^{-6} K m^2 kg^{-1} s^{-1}), an estimate of the dynamical tropopause. High theta values in a tongue stretching from low latitudes to the northeast across Western Europe indicate an elevated tropopause. Such a downstream-tilted anticyclone-forming tongue is common in cases of wintertime poleward wave breaking of the second kind (P2 breaking events) (Peters and Waugh, 1996). Such P2 events occur in the anticyclonic (equatorward) shear zone of the jet stream. Low ozone values in the lowermost stratosphere at 59N (Fig. 4) are consistent with the advected PV tongue in Fig. 6.

In order to investigate tropospheric and stratospheric disturbances in summer 2003, we calculated the amplitude of sub-monthly geopotential fluctuations. Following Niishi and Nakamura (2004, 2005), we first band-passed the geopotential field, selecting fluctuations between the synoptic and the seasonal time scales. The low-pass filter retained periods longer than 8 days, while the seasonal circulation is represented by the 31-day running mean. Sub-monthly band-passed fluctuations are departures of the low-passed filtered fields from the 31-day mean.

Figure 7 shows the band-passed filtered geopotential on August 10 at 250 mb. Close inspection reveals a zonally slanted ring of anticyclonic and cyclonic anomalies, stretching from the western Atlantic across Europe and toward Siberia. These quasi-stationary anomalies are suggestive of a global Rossby wave train propagation. Such wave trains consist of aligned centres with opposite signs over a confined longitudinal sector. In Black et al. (2004), the August-mean stream function shows the same wave train in the lower troposphere (850 mb). Note that cyclonic anomalies are present over eastern Siberia and Japan, at the eastern end of the wave train, where anomalously cold summer temperatures prevailed, but their connection to the Euro-Atlantic anomalies is unclear. Over the North Sea and Scandinavia, the prominent anticyclonic centre that contributed to the low ozone is clearly seen, flanked by two cyclonic, high ozone centres, and a low ozone centre further west over Nova Scotia (Fig. 1). The anticyclonic anomaly over the Russian Arctic and Alaska, near the date line, is also prominent on that day at 250 mb.

[2] Meteorological observations are taken from the ECMWF operational analyses or ERA-40 re-analyses. Geopotential height was de-archived on 17 pressure levels from 1000 to 5 mb. Horizontal resolution corresponds to spectral truncation T42, except for the PV isosurface, retrieved at T106.

An extensive analysis of the August 2003 blocking development over Europe and its energetics is beyond the scope of this study. Schematically, the evolution is similar to previously studied blockings that involve wave trains over Europe (Nakamura et al., 1997). To demonstrate this, we have calculated wave activity fluxes (WAFs) associated with quasi-geostrophic, quasi-stationary disturbances to a non-zonal, slowly varying basic state, according to Takaya and Nakamura (2001, hereafter TN2001). The WAF is parallel to the local three-dimensional group velocity in the WKB limit. It is a generalisation of the stationary Rossby wave flux on a zonally uniform basic state (Plumb, 1985), commonly used in several studies of stratospheric dynamics (e.g. Sabutis and Manney, 2003). In the situation considered here, the hypothesis of perturbations to a zonally symmetric basic state is not valid. The fact that the monthly-mean, basic state is asymmetric motivates an approach like the one of TN2001. The aforementioned WAF provides a snapshot of a wave-packet of stationary quasigeostrophic disturbances, allowing a qualitative determination of where the wave packet is emitted and absorbed. It has been applied by TN2001 and by Niishi and Nakamura (2004, 2005) to analyses of blockings and cyclogenesis, and is used at the Japan Meteorological Agency in routine diagnosis.

The horizontal component of the WAF is shown on Fig. 7 at 250 mb, and both the three-dimensional WAF and the band-passed geopotential at 100 mb and on August 4, 6, 8, and 10 are shown on Fig. 8. The horizontal WAF component is shown as arrows, and the vertical component is colour shaded. On August 4, a strong horizontal flux emerges from the low anomalies over the western Atlantic and points eastward, contributing to the European blocking intensification. On August 6-8, the upward flux increases noticeably, upstream of the blocking over the Atlantic. At the same time, the blocking intensifies and further extends northward. The horizontal flux convergence indicates that incipient wave packets contribute to the intensification of the blocking. On August 10, the upper-troposphere blocking shows already signs of weakening, but has further spread northward. The upward flux has also diminished. The horizontal flux is emitted from the blocking region and the accumulated wave activity is released eastward. For our purpose, the key point is the existence of an upward WAF pulse originating over the Atlantic near August 6, 2003.

How high can such disturbances penetrate into the stratosphere? The upward propagation of large-scale waves into the stratosphere is governed by the Charney-Drazin conditions (e.g. Andrews, Holton and Leovy, 1987). Zonal-mean zonal winds dictate whether waves of given wavenumbers and phase speeds can propagate vertically or are evanescent at given latitudes. Stationary Rossby waves can only propagate through westerlies, not easterlies, and the westerlies cannot be too strong. Only gravest wavenumbers can propagate high into the stratosphere. Synoptic eddies associated with wave trains can also propagate upwards in zonally confined waveguides when the local zonal wind allows propagation conditions to be met (Canziani et al., 2003). Niishi and Nakamura (2004, 2005) identified lower stratospheric wave trains emanating from quasi-stationary cyclogenesis in the southern hemisphere troposphere in winter and spring 1997, as zonally confined waveguides formed when stratospheric eastward jet overlaid the tropospheric westerlies. Aloft of the Euro-Atlantic wave train in August 2003, the winds are dominantly westward above 50 mb, hence waves are expected to be evanescent in the vertical. A longitude-pressure cross-section of the band-passed geopotential at 60°N on August 10 (Fig. 9) shows that the wave-train anomalies extend well into the mid stratosphere: they are still strong at 50 mb, but have a weak influence at 30 mb, consistent with the location of the zerowind line (dashed line). Also overlaid are the longitudinal and vertical WAF components as arrows, zonal winds and the dynamical tropopause (thick line). Note the tropopause undulations along the wave train. Hence, the fact that the August 2003 wave train can exert an influence at 50 or 30 mb, qualifies the event as a deep event.

Time series of the WAF vertical component at 100 mb (Fig. 10), averaged over latitudes 40°N-70°N and over the Atlantic sector, shows a prominent burst during the maturing phase of the blocking (e.g. August 6), indicating an enhanced upward wave propagation into the stratosphere. A similar average over the Pacific sector is also shown for comparison. While the more conventional Eliassen-Palm flux also displays coincident bursts (not shown), the use of the WAF defined by TN2001 allows us to locate the origin of the wave pulses, over the central Atlantic.

The dynamical origin of the August 2003 heat wave remains uncertain. Empirical orthogonal function analysis of geopotential height (e.g. Orsolini and Reyes, 2003 and references therein) suggests

that Euro-Atlantic patterns of low-frequency variability can be wave-train-like, characterised by a succession of positive and negative anomalies stretching across the Atlantic and Europe. Few studies have looked at summer patterns. In the month of June, Barnston and Livesey (1987) found occurrences of a high-order, low-variance pattern in the 700-mb geopotential analyses, which they called Asian Summer pattern. It comprises a weak, wave-train-like pattern extending from North America to central Asia, and at least qualitatively similar to the one that prevailed during the European heat-wave in 2003 (see Fig. 7). The pattern main center of action is however over Asia. The normalised Asian Summer pattern index is indeed anomalously high (2.5) during August 2003 in the National Center for Environmental Prediction (NCEP) analyses. The exact excitation mechanism of such a Rossby wave train has not been identified, albeit anomalies in Atlantic sea surface temperatures in spring and summer 2003 have been noted (Black et al, 2004). On the other hand, Ogi et al. (2005) invoked a highly anomalous summer northern annular mode (NAM), i.e. the leading mode of the tropospheric zonally-averaged circulation, to explain the abnormal weather over Europe, North America and Asia in the summer 2003. The mid-August heat wave studied in this paper however coincides with the decline of the anomalously high NAM (their Fig. 1), and, as we have shown, with enhancements of planetary-scale wave trains.

4. THE ANOMALOUS MID-STRATOSPHERIC CIRCULATION IN AUGUST 2003.

The lower and mid stratospheric circulations are disturbed by the anomalous forcing from the troposphere in August 2003. On August 10, at 50 mb (Fig. 11b), the low-passed filtered geopotential surprisingly reveals two high-latitude anticyclonic centres, rather than a single Arctic anticyclone. A closed high-latitude cyclonic anomaly is centred near 70°N, 90°W. At 30 mb (Fig. 11c), the Arctic anticyclonic anomaly is centred off the pole, displaced toward Asia by planetary wave-1 and 2. The troughs at 60°N and 90°W, both at 50 and 30 mb, extend upward from the Atlantic troughs seen at 250 mb (Fig. 11a), which were part of the wave train. At 50 mb, the marked elongated ridge stretching from the Arctic high southwards to the North Sea and Scandinavia.

Mid-stratospheric planetary waves, such as seen on Fig. 11c, were present earlier in the summer. A spectral analysis of the geopotential at 60°N and 30 mb (not shown for brevity), over the period July 6 to August 22, reveals westward-propagating planetary wave-1 and 2, with respective periods of 15 and 20 days. Hence, these waves cannot be forced during the mid-August blocking. It is however clear that the wave train at least disrupted the large-scale circulation over the Atlantic at 50 mb, and to a lesser extent at 30 mb.

Long-period planetary-scale disturbances have been observed in the summer polar stratosphere, but their origin remains uncertain. In the southern hemisphere, planetary waves have been identified in satellite observations of temperature, ozone or other trace constituents (Miles and Grose, 1986). Long period, westward-propagating, planetary-scale ozone disturbances near 60°N were observed in satellite solar occultation data (Hoppel et al., 1999; Akiyoshi et al., 2004) at altitudes between 20 and 30 km. At that latitude and altitude range, Park and Russell (1994) also observed intrusions of ozone-poor polar air into the mid-latitudes. Randel (1993) examined propagating global normal modes seen in the SBUV ozone data. While his study included the summer season, it did not consider polar regions. A faster, 5-day wave was identified in the stratosphere and mesosphere by Kirkwood et al. (2002), using ground-based measurements of temperature and winds at Kiruna (Sweden).

5. CONCLUSIONS

LOEs demonstrate how extreme column ozone variability can be dynamically induced. Summertime episodes have been little studied, as opposed to their winter counterparts. In mid and high latitudes, column ozone is lower in summer than in winter, as part of the ozone seasonal cycle, which is characterised by an early fall minimum. Locally, the summer absolute minimum can be reached during such LOEs, as was the case over Scandinavia in 2003. How the extreme low column ozone values and the high erythemal UV dose are reached in the summer, when human UV exposure is

greatest and health impact presumably stronger, is worth further investigations. During LOEs, the lowering of the ozone column and the cloud-free anticyclonic conditions conjure to increase UV radiation reaching the ground (Orsolini et al., 2003a).

We demonstrated that the LOE results from the conjunction of a deep tropospheric blocking over Europe, and a displaced Arctic pool of low-ozone air in the stratosphere, aloft of the anticyclone. The anticyclonic anomaly is part of a Rossby wave train, that is apparent throughout the troposphere, and whose influence is felt strongly at 50 mb, and weakly at 30 mb. While Orsolini et al. (2003a) studied two strong LOEs over Scandinavia in the summer 2000, they also pointed other LOEs over the North Pacific, near the date line, where low-ozone Arctic air also overlaid tropospheric anticyclonic disturbances. Our study of a LOE in August 2003 focused on the North Sea and Scandinavia, but a similar episode occurred at the same time over the Russian Arctic and northern Alaska. This is revealed by the total ozone map from TOMS (Fig. 1), by the mid-stratospheric ozone map from MIPAS (Fig 3), by the band-passed geopotential at 250mb (Fig. 7) or the tropopause elevation (Figs. 6, 9). Intense LOEs occur at different locations, several times during the summer depending on the formation and intensity of tropospheric anticyclonic centres, and their position with respect to migrating mid-stratospheric ozone waves. The duration of the LOE over the North Sea and Scandinavia in mid-August 2003, approximately 5 days (Fig. 2a), is governed by the blocking lifetime at its northernmost extension (Fig. 10). The mid-stratospheric ozone waves, on the other hand, are slowly migrating.

Three-dimensional wave activity fluxes associated to sub-monthly geopotential fluctuations were calculated according to the formalism of TN2001, valid for quasi-stationary disturbances embedded in a zonally asymmetric basic state. Results clearly indicate that upward wave fluxes in the lower stratosphere originate from the Atlantic sector, upstream of the blocking. The very deep blocking event in mid-August 2003 and its associated wave-train over the Atlantic and Europe (Fig. 8) perturbed the stratosphere up to 30 mb, where it at least modulated the mid-stratospheric westward-propagating planetary waves. At 50 mb, the anticyclonic stratospheric circulation broke into two anticyclonic centers. Further studies could reveal how often such a disruption occurs. Summer planetary and synoptic-scale waves deserve further study in light of their impact on recurring, severe heat waves in the troposphere, and on ozone variability both in the stratosphere and in the troposphere.

Acknowledgements

The lead author was supported by the Norwegian Science Foundation (NFR) through the joint project AEROZKLIM. We acknowledge NASA GSFC for provision of TOMS images and ECMWF for the ERA-40 re-analyses.

References

Akiyoshi, H., Sugita, T., Kanzawa, H. and Kawamoto, N. 2004 Ozone perturbations in the Arctic summer lower stratosphere as a reflection of NO_X chemistry and planetary scale wave activity, *J. Geophys. Res.*, 109 (D3), D03304.

Allen, D.R. and Nakamura, N. 2002 Dynamical reconstruction of the record low column ozone over Europe on 30 November 1999, *Geophys. Res. Lett.*, 29, 1362, doi:10.1029/2002GL014935.

Andrews, D., Holton, J.R. and Leovy, C.B. 1987 Middle Atmosphere Dynamics, Academic Press.

Barnston, A.G. and Livesey, R.E. 1987 Classification, seasonality and persistence of low-frequency atmospheric circulation patterns, *Monthly Weather Review*, 115, 1083-1126.

Black, E., Blackburn, M., Harrison, G., Hoskins, B.J. and Methven, J. 2004 Factors contributing to the summer 2003 european heatwave, *Weather*, 59, No 8, 217-22.

ESA, 2000: *Envisat, MIPAS An instrument for atmospheric chemistry and climate research*, ESA Scientific Publications Division, ESTEC, The Netherlands, SP-1229.

Canziani, P.O. and Legnani, W.E. 2003 Tropospheric-stratospheric coupling: extratropical synoptic systems in the lower stratosphere, *Q.J.R. Meteorol. Soc*., 129, 2315-2329.

Fink, A.H., Brucher, T., Kruger, A., Leckebusch, G.C., Pinto J.G. and Ulbrich, U. 2004 The 2003 European summer heatwaves and drought – synoptic diagnosis and impacts, *Weather*, 59, No 8, 209-216.

Grazzini, F., Ferranti, L., Lalaurette F. and Vitart, F. 2003 The exceptional warm anomalies of summer 2003, *ECMWF Newsletter* No 99 – Autumn/Winter 2003.

Hood, L.L., Soukharev, B.E., Fromm, M. and McCormack, J.P. 2000 Origin of extreme ozone minima at middle to high northern latitudes, *J. Geophys. Res.*, 106, 20925-20940.

Hoppel, K.W., Bowman, K.P. and Bevilacqua, R.M. 1999 Northern hemisphere summer ozonevariability observed by POAM II, *Geophys. Res. Lett.*, 26, 827-83.

James P.M., Peters D. and Waugh, D.W. 2000 Very low ozone episodes due to polar vortex displacement, *Tellus*, 52B, 1123-1137.

Kirkwood, S., Barabash, V., Brandström, B.U.E., Moström, A., Stebel, K., Mitchell N. and Hocking, W. 2002 Noctilucent clouds, PMSE and 5-day planetary waves: a case study, *Geophys. Res. Lett*. 29 (10), D1411.

Lloyd, S., Swartz, W.H., Kusterer, T., Anderson, D., McElroy, C.T., Midwinter, C., Hall, R., Nassim, K., Jaffe, D., Simpson, W., Kelley, J., Nicks, D., Griffin, D., Johnson, B., Evans, R., Quincy, D., Oltmans, S., Newman, P., McPeters, R., Labow, G., Moy, L., Seftor, C., Toon, G., Sen, B. and Blavier, J.-F. 1999 Intercomparison of total ozone observations at Fairbanks, Alaska, during POLARIS, *J. Geophys. Res.*, 104, 26767-26778.

McKenna, D., Jones, R.L., Austin, J., Browell, E.V., McCormick, M.P., Kreuger, A. and Tuck, A.F. 1989 Diagnostics studies of the Antarctic vortex during the 1987 airborne Antarctic ozone experiment :ozone miniholes, *J. Geophys. Res*., 94, 11641-11668.

Miles, T. and Grose, W.L. 1986 Transient medium-scale wave activity in the summer stratosphere, *Bull. Am. Meteor. Soc.*, 67, 674-686.

Nakamura, H., Nakamura, M. and Anderson J.L. 1997 The role of high- and low-frequency dynamics in blocking formation, *Month. Wea. Rev.*, 125, 2074-2093.

Newman, P.A., Lait, L.R. and Schoeberl, M.R. 1988 The morphology and meteorology of southern hemisphere spring total ozone miniholes, *Geophys. Res. Lett.*, 15, 923-926.

Niishi, K. and Nakamura, H. 2004 Lower-stratospheric Rossby wave trains in the southern hemisphere: A case-study for late winter of 1997, *Q.J.R. Meteorol. Soc.*, 130, 325-345.

Niishi, K. and Nakamura, H. 2005 Upward and downward injection of Rossby wave activity across the tropopause: a new aspect of the troposphere-stratosphere dynamical linkage, *Q.J.R. Meteorol. Soc.*, 131, 545-564.

Ogi M., Yamazaki, K. and Tachibana, Y. 2005 The summer northern annular mode and abnormal summer weather in 2003, *Geophys. Res. Lett.*, 32, L04706, doi:10.1029/2004GL021528.

Orsolini, Y.J., Eskes, H., Hansen, G., Hoppe, U-P., Kylling, A., Kyro, E., Notholt, J., Van der A, R. and Von der Gathen P. 2003a Summertime low ozone episodes over northern high latitudes, Quarterly Journal of the Royal Meteorological Society, 129, 3265-3276.

Orsolini, Y.J. and Doblas-Reyes, F.J. 2003b Ozone Signatures of Climate Patterns over the Euro-Atlantic Sector in the Spring, *Quart. J. Roy. Meteor. Soc.*, 129, 3251-3263.

Orsolini, Y.J., Stephenson, D.B. and Doblas-Reyes, F.J. 1998 Storm tracks signature in total ozone during northern hemisphere winter, *Geophys. Res. Lett.*, 25, 2413-241.

Orsolini, Y.J. and Limpasuvan, V. 2001 The North Atlantic Oscillation and the occurrences of ozone miniholes, Geophys. Res. Lett., 28, 4099-4102.

Orsolini, Y.J., Randall, C.E., Manney, G.L. and Allen, D.R. 2005 An observational study of the final breakdown of the southern hemisphere stratospheric vortex in 2002, J. Atm. Sci., 62, 735-747.

Park, J.H. and Russell III, J.M. 1994 Summer polar chemistry observations in the stratosphere made by HALOE, *J. Atm. Sci.*, 51, 2903-2913.

Peters, D. and Waugh, D.W. 1996 Influence of barotropic shear on the poleward advection of uppertropospheric air, *J. Atm. Sci.*, 53, 3013-3031.

Plumb, R.A. 1985 On the three-dimensional propagation of stationary waves, *J. Atmos. Sci*., 42, 217-229.

Randel, W.J. 1993 Global normal-mode Rossby waves observed in stratospheric ozone data. *J. Atm. Sci.*, 50, 406-420.

Sabutis, J.L. and Manney, G.L. 2003 Wave propagation in the 1999-2000 Arctic early winter stratosphere, *Geophys. Res. Lett.*, 27, 3205-3208.

Schär, C., Vidale, P.L., Lüthi, D., Frei, C., Häberli, C., Liniger, M.A. and Appenzeller, C. 2004 The role of increasing temperature variability in European summer heatwaves, *Nature*, 427, 332-336.

Stott, P.A., Stone, D.A. and Allen, M.R. 2004 Human contribution to the European heatwave of 2003, *Nature*, 432, 610-613.

Takaya, K. and Nakamura, H. 2001 A formulation of a phase-independent wave-activity flux for stationary and migratory quasigeostrophic eddies on a zonally varying basic flow, *J. Atm. Sci.*, 58, 608-627.

World Health Organisation (WHO) 2003 “The health impacts of 2003 summer heat waves”, http://www.euro.who.int/document/Gch/HEAT-WAVES%2ORC3.pdf

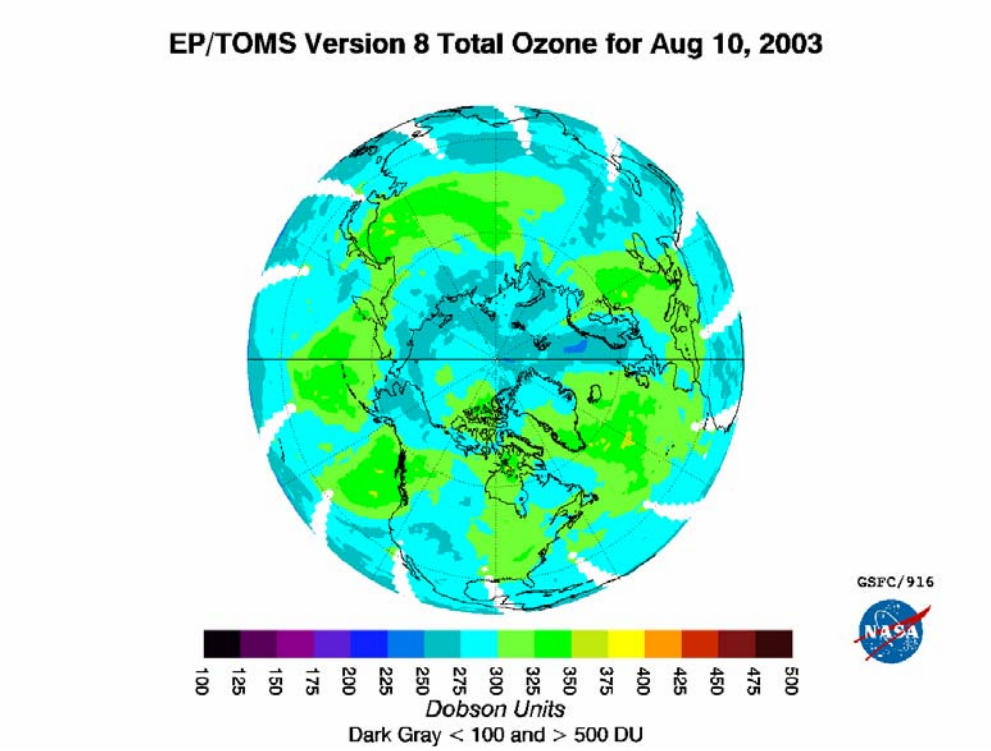

Figure 1. Column ozone map from TOMS Earth Probe on August 10, 2003. Note the local minimum over the North Sea and Scandinavia, with values in the range of 250-275 DU.

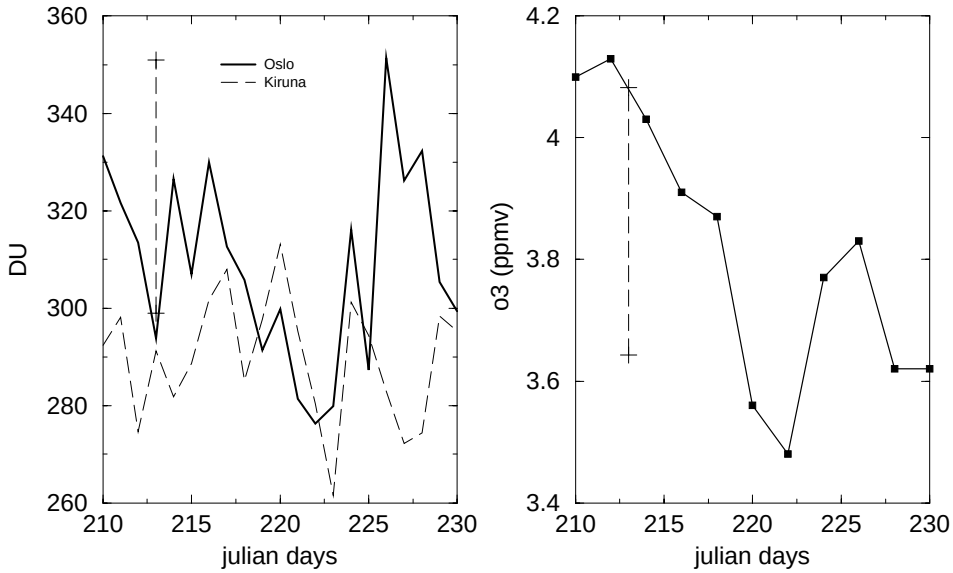

Figure 2. (a) Time series of column ozone from TOMS over Oslo (60°N, 12°E) and Kiruna (67°N, 20°E) in Scandinavia, in August 2003. Julian day 222 corresponds to August 10. (b) Ozone mixing ratio (ppmv) in the stratosphere at 650K, over the same period from the binned NRT MIPAS data (60°N-70°N, 0°E-36°E). The dashed lines in (a) and (b) indicate the extent of 1 standard deviation envelope from the 2003 summer-mean in TOMS data over Oslo, and in the binned MIPAS data (60°N-70°N, 0°E-36°E). In (a), the circle on day 222 indicates the August mean over Oslo, based on TOMS data since 1978.

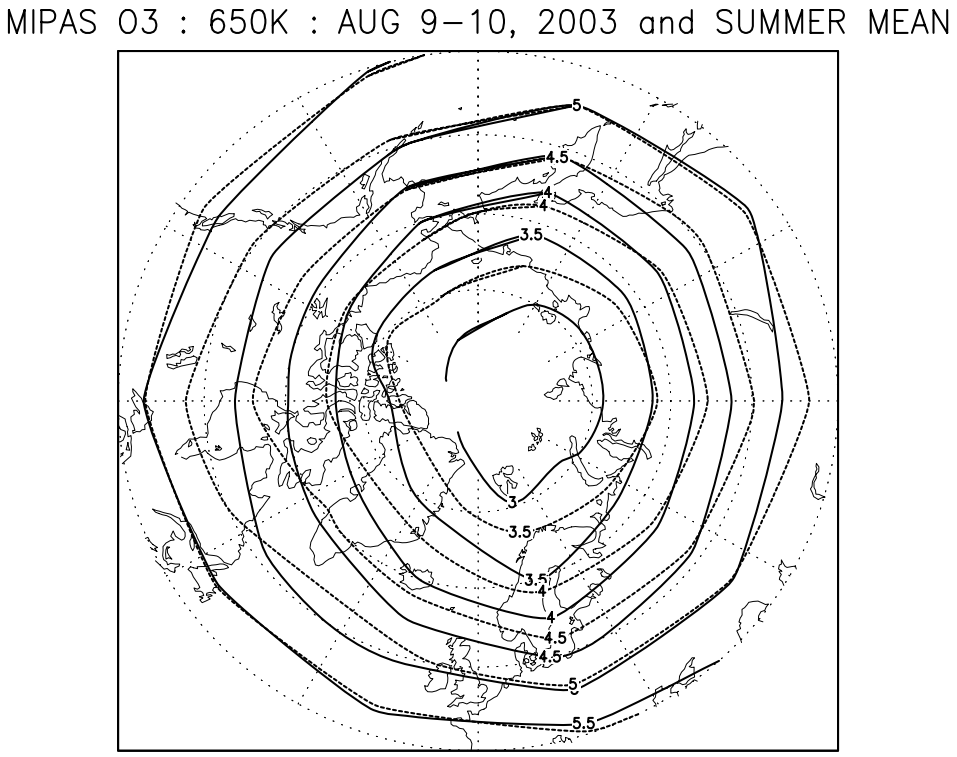

Figure 3. Isentropic map of NRT MIPAS ozone at 650K (thick line) for August 9-10, 2003, and the summer mean (dashed line).

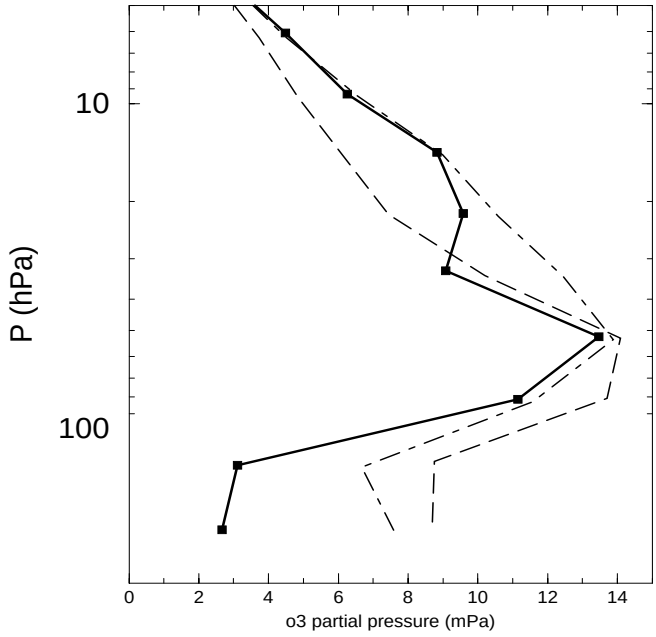

Figure 4. A NRT MIPAS ozone profile (mPa) on August 10 at (59°N, 13°E) in the LOE region. Also indicated are the NRT MIPAS summer-mean for the 30°N-40°N (dotted line), 55°N-65°N (dotdashed line), and the 75°N-85°N (long dashed line) latitude bands.

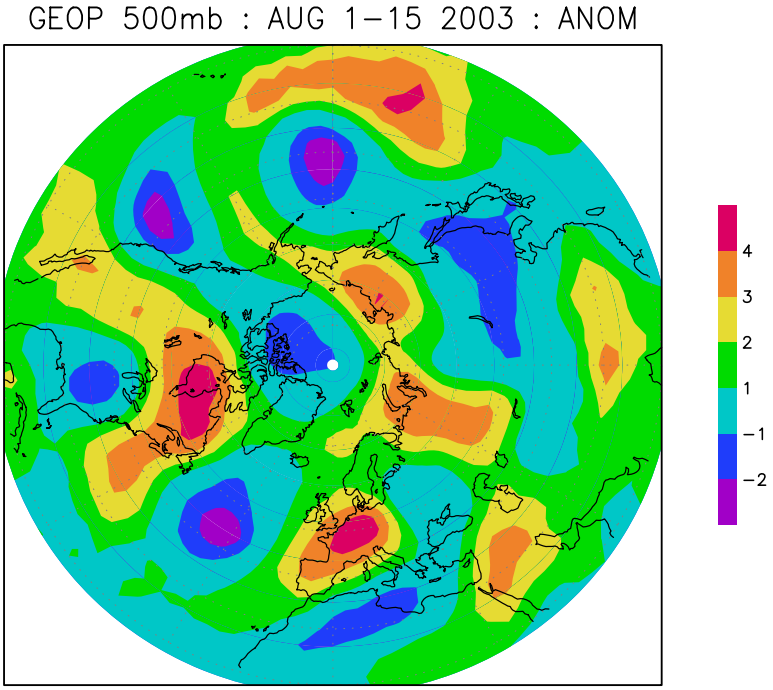

Figure 5. The August 1-15 500-mb geopotential height anomaly from the ERA-40 August climatology (1958-2000), expressed in units of standard deviation. The anticyclonic anomaly over central Europe is 4 standard deviations away from the climatology.

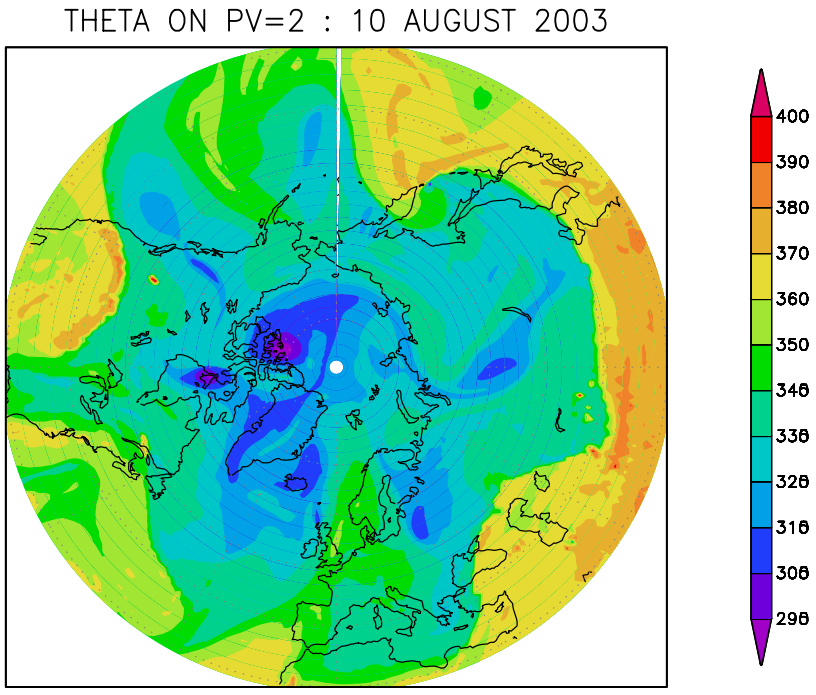

Figure 6. Potential temperature (K) on the 2 PV Unit iso-surface, an estimate of the dynamical tropopause, for August 10, 2003.

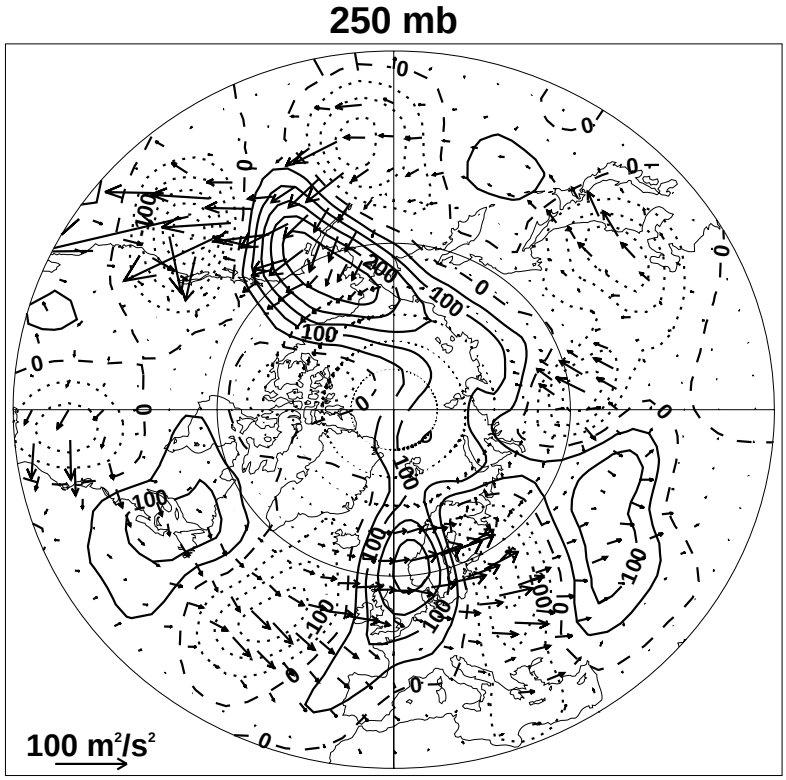

Figure 7. Band-passed 250-mb geopotential height anomaly (gpm) for August 10, 2003. Note the prominent wave train from the western Atlantic to eastern Eurasia, and the anticyclonic anomaly over the Russian Arctic. Contours for positive (negative) anomalies are solid (dotted), and the zero contour line is dashed. Contour interval is 50 gpm. Overlaid is the horizontal component of WAF, as arrows (units of $m^2 s^{-2}$).

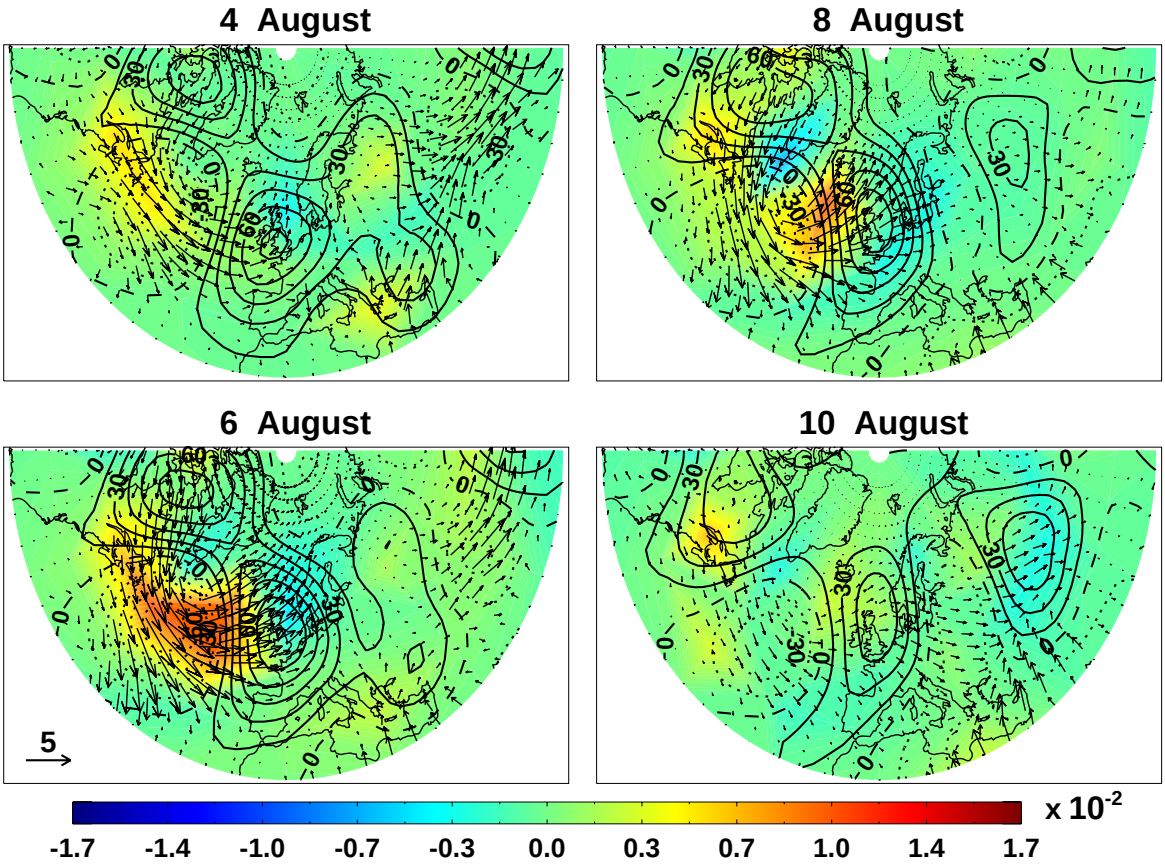

Figure 8. The 100-mb WAF, units of m^2 s^{-2}, and band-passed geopotential (gpm) on four days in August 2003 (August 4, 6, 8, 10). The horizontal WAF component is shown as arrows, and the vertical component is colour shaded. Geopotential contours are 15 gpm.

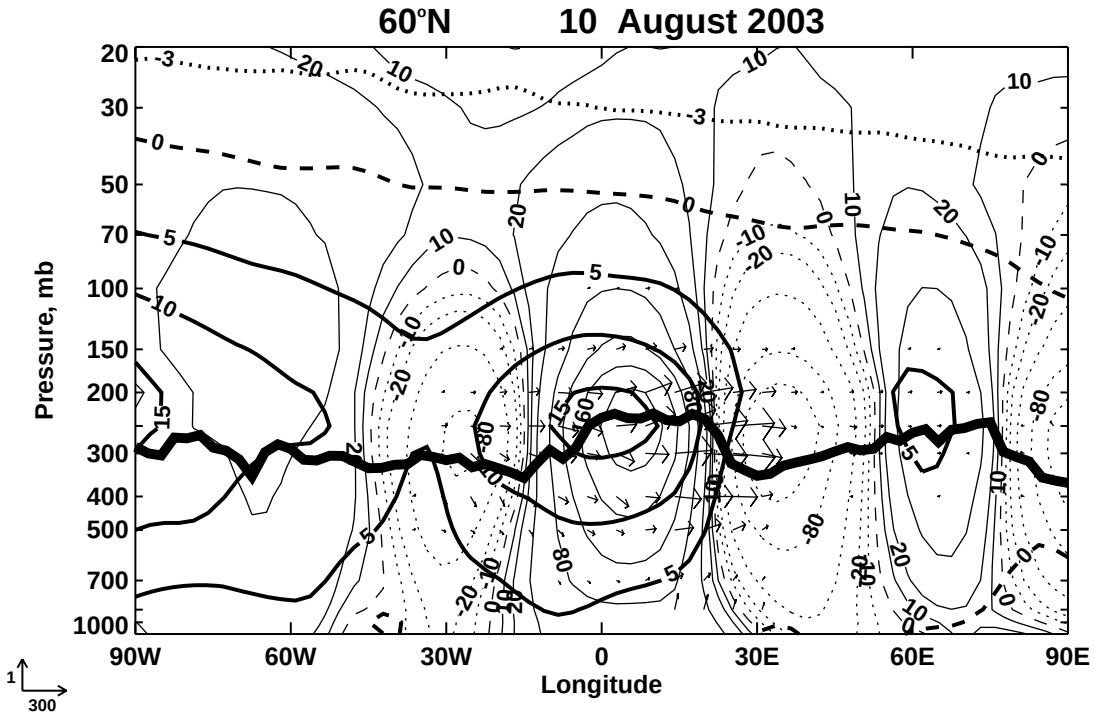

Figure 9. Longitude-height cross-section along 60°N of the band-passed geopotential (gpm, as black contours) and wave activity flux (WAF) for August 10, 2003. WAFs have been scaled by a factor (pressure/1000 mb). Scaling of arrows is indicated at left hand corner. Also shown are zonal winds (ms^{-1} as thicker contours, with zero wind line dashed) and the pressure of the dynamical tropopause (very thick line). Geopotential contours are 0, +-10, +-20, +-40 and incremented by +-40 thenafter.

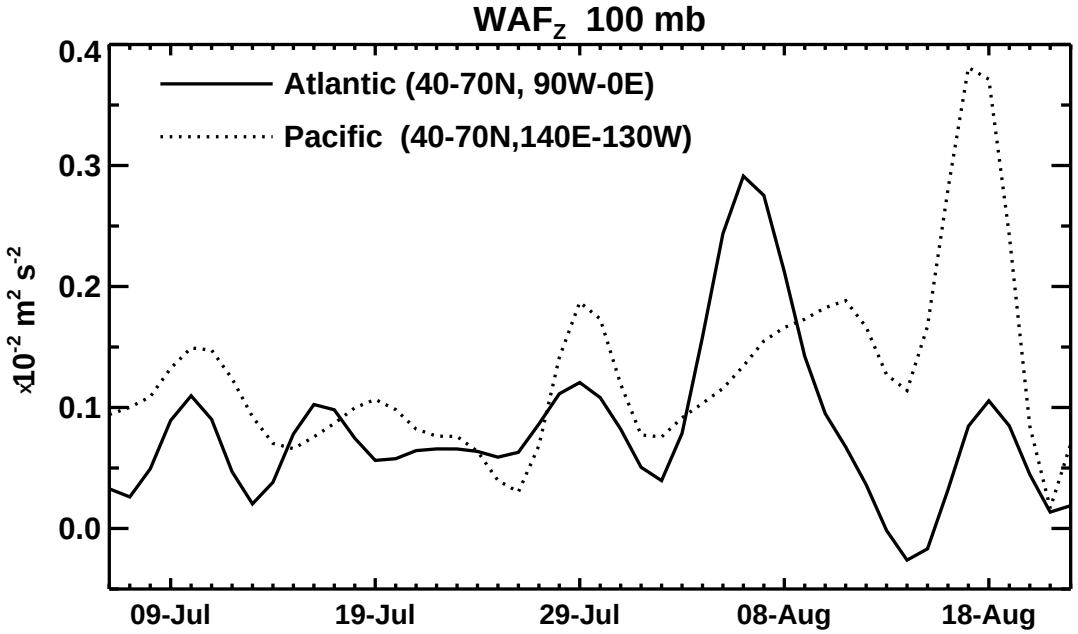

Figure 10. July-to-August 2003 time series of the WAF vertical component at 100 mb, over the Atlantic and Pacific sectors.

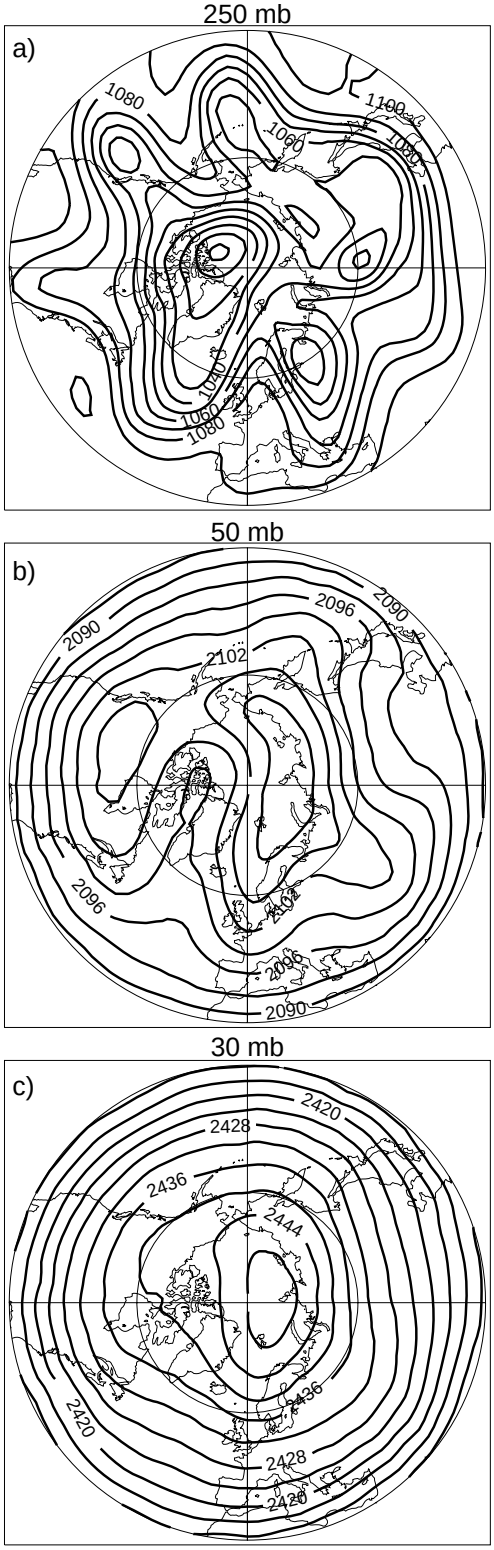

Figure 11. (a) 8-day low-passed 250-mb geopotential for August 10, 2003. (b) Same for 50 mb. Note the ridge extending south over Scandinavia and Northern Europe, and the high latitude cyclonic center on the west-northern corner of Greenland. (c) Same for 30 mb. Units are dam, and contour intervals are 10 dam (a), 3 dam (b) and 4 dam (c).

Paper V

The mean meridional circulation and midlatitude ozone buildup

G. Nikulin and A. Karpechko

Atmos. Chem. Phys. Discuss., 5, 4223-4256, 2005

Atmos. Chem. Phys. Discuss., 5, 4223–4256, 2005
www.atmos-chem-phys.org/acpd/5/4223/
SRef-ID: 1680-7375/acpd/2005-5-4223
European Geosciences Union

Atmospheric Chemistry and Physics Discussions

The mean meridional circulation and midlatitude ozone buildup

G. Nikulin[1] **and A. Karpechko**[2]

[1]Swedish Institute of Space Physics, Atmospheric Research Programme, Box 812, SE-98112 Kiruna, Sweden
[2]Finnish Meteorological Institute, Arctic Research Centre, Tähteläntie 62, FIN-99600 Sodankylä, Finland

Received: 9 May 2005 – Accepted: 26 May 2005 – Published: 30 June 2005

Correspondence to: G. Nikulin (grigory@irf.se)

Abstract

The development of wintertime ozone buildup over the Northern Hemisphere (NH) midlatitudes and its connection with the mean meridional circulation in the stratosphere are examined statistically on a monthly basis from October to March (1980–2002). The ozone buildup begins locally in October with positive ozone tendencies over the North Pacific, which spread eastward and westward in November and finally cover all midlatitudes in December. During October-January a longitudinal distribution of the ozone tendencies mirrors a structure of quasi-stationary planetary waves in the lower stratosphere and has less similarity with this structure in February–March when chemistry begins to play a more important role. From November to March, zonal mean ozone tendencies (50°–60° N) show strong correlation ($|r|=0.7$) with different parameters used as proxies of the mean meridional circulation, namely: eddy heat flux, the vertical residual velocity (diabatically-derived) and temperature tendency. The correlation patterns between ozone tendency and the vertical residual velocity or temperature tendency are more homogeneous from month to month than ones for eddy heat flux. A partial exception is December when correlation is strong only for the vertical residual velocity. In October zonal mean ozone tendencies have no coupling with the proxies. However, positive tendencies averaged over the North Pacific correlate well, with all of them suggesting that intensification of northward ozone transport starts locally over the Pacific already in October. We show that the NH midlatitude ozone buildup has stable statistical relation with the mean meridional circulation in all months from October to March and half of the interannual variability in monthly ozone tendencies can be explained by applying different proxies of the mean meridional circulation.

1 Introduction

Since the early studies of Brewer (1949) and Dobson (1955) it has been recognized that the wintertime total ozone increase in extratropics results from the diabatic

(Brewer-Dobson) circulation in the stratosphere. The zonal mean meridional circulation can be described by the Lagrangian mean approach (LM) or by the transformed Eulerian mean (TEM) approach which is more practical for estimating LM motions (Andrews et al., 1987). In the TEM formulation the residual circulation (as an approximation of Lagrangian motions projected on the meridional plane) is driven by waves, while divergence of the Eliassen-Palm (EP) flux represents a net wave forcing. The vertical component of the EP flux (F_z), which is proportional to the zonal mean eddy heat flux (HF), is widely used as a proxy of wave forcing of the residual circulation.

The connection between wave forcing and ozone variability has previously been demonstrated by several authors. Nagatani and Miller (1987) have found coherent variations between the 100 hPa F_z during September and the 30 hPa zonal mean ozone during October in the South Hemisphere (SH). The near-global structure of stratospheric ozone response to wave forcing during stratospheric warmings has been presented by Randel (1993). Fusco and Salby (1999) have shown that total ozone tendency ($\Delta O_3/\Delta t$) over the Northern Hemisphere (NH) extratropics in January strongly correlates with the 100 hPa F_z. Close correlation exists also between wintertime $\Delta O_3/\Delta t$ averaged over middle and high latitudes and wave forcing accumulated during the winter (Salby and Callaghan, 2002; Weber et al., 2003). However, Randel et al. (2002a) found only weak correlations between midlatitude $\Delta O_3/\Delta t$ and upward wave fluxes in November–December in contrast to stronger correlations in January–March. Since midlatitude ozone buildup in the NH starts between October and November (Fioletov and Shepherd, 2003) and this is thought to result from the meridional stratospheric transport, the lack of strong correlations in November–December seems somewhat surprising.

The residual circulation in the stratosphere can be estimated from the net radiative heating rates using satellite observations (e.g. Solomon et al., 1986). Despite large uncertainties in the estimations (Eluszkiewich et al., 1996, 1997), there is a broad agreement between the circulations obtained from different data sources as well as between calculations and theoretical expectations. The calculations reproduce tropical

upwelling and extratropical downwelling and also demonstrate stronger velocities in the northern winter circulation than in the southern one. That agrees well, at least qualitatively, with general concepts of the "extratropical pump" theory (see Holton et al., 1995; Plumb and Eluszkiewich, 1999). However, only a few studies have aimed to investigate direct statistical connections between the residual circulation and ozone. Geller et al. (1992) have shown positive correlations between the ozone mixing ratio and the vertical residual velocity above the ozone peak and negative correlations below the peak during December-February for 1979–1986. They have also pointed out a delay of the wintertime total ozone maximum at 60° N relative to the vertical residual velocity maximum.

The present study aims at further exploration of the dynamical influence on the total ozone variability. The velocity of the residual circulation is a more straightforward proxy for the meridional stratospheric transport than HF though the latter is easier to derive. However, uncertainties in the diabatically-derived residual velocities may hamper its application as a dynamical proxy for total ozone. Here, the attempt is made to analyse in detail the relationship of HF and the residual circulation to the NH midlatitude total ozone month by month from October to March. Of particular interest is how well the diabatically-derived residual circulation can mirror interannual variability of wave forcing and ozone buildup. The study starts with an examination of a spatial-time structure of monthly ozone tendencies and their relationship with HF. Then we demonstrate the connection between the residual velocities and wave forcing as represented by HF. Finally, we link ozone tendencies to the residual circulation.

2 Data and method

We use the version 8 of monthly TOMS/SBUV merged total ozone data (the 5° zonal mean and 10°×30° gridded sets). The 50°–60° N midlatitude region where ozone data is available in all winter months is chosen because $\Delta O_3/\Delta t$ in this region correlates more strongly with both HF and the residual circulation than in the more common

40°–60° N region. In the 1990s there are several years with missing zonal mean ozone data over 55°–60° N in December (1992–1994, 1998) and January (1993–1995). Also there is no data over 50°–60° N in December 1997. All gaps are filled by spatial extrapolation that does not appreciably influence the obtained results. Monthly $\Delta O_3/\Delta t$ is simply the difference of total ozone values between months. Monthly mean ozone values are generally associated with ozone values near the middle of the month. Hence, for example, the January $\Delta O_3/\Delta t$ here as a difference between January and December presents ozone changes from approximately 15 December to 15 January. We should emphasize that this period is not an exact rule because the period depends on total ozone distribution during the month.

For the September–March period (1979–2002) we calculate daily meridional and vertical residual mean velocities ($\bar{v}^*$,$\bar{w}^*$) and HF. The residual velocities are estimated from the quasi-geostrophic TEM thermodynamic and continuity equations:

$$\frac{\partial \bar{T}}{\partial t} + \bar{v}^* \frac{1}{a} \frac{\partial \bar{T}}{\partial \varphi} + \bar{w}^* S = \bar{Q}, \tag{1}$$

$$\frac{1}{a \cos\varphi} \frac{\partial}{\partial \varphi} (\bar{v}^* \cos\varphi) + \frac{1}{\rho_0} \frac{\partial}{\partial z} (\rho_0 \bar{w}^*) = 0. \tag{2}$$

Here $\bar{T}$ is the zonal mean temperature; $\bar{Q}$ is the zonal mean net diabatic heating; $S=HN^2/R$ is the static stability parameter; the log-pressure vertical coordinate is $z=-H\ln(p/1000\,\mathrm{hPa})$ with $H=7$ km; and a, φ, R and ρ_0 are the radius of the Earth, latitude, the gas constant and a basic state density, respectively (see for more details e.g. Dunkerton, 1978; Solomon et al., 1986; Gille et al., 1987). Temperature, wind and net diabatic heating fields for calculations are taken from the ERA-40 reanalysis. Also, for comparison, we use temperature and wind data from the NCEP/NCAR reanalysis. Estimations of the residual circulation have large uncertainties mainly due to uncertainties in the calculated net heating rates (Eluszkiewicz et al., 1997). The usual consequence of these heating rate uncertainties is that the global mean mass balance

is not maintained (the global integral of $\bar{w}^*$ on isobaric levels is not equal to zero). In order to reduce the global integral of $\bar{w}^*$ to zero, we apply a correction factor for $\bar{w}^*$ which is independent of latitude (e.g. Murgatroyd and Singelton, 1961; Shine, 1989). At an isobaric level such correction strongly influences accuracy of the estimated circulation in regions close to radiative equilibrium (small residual velocities). On average the correction is about 5–10% of uncorrected values of $\bar{w}^*$ in winter polar regions, 10–20% in the tropics and up to 30–50% in summer polar regions. Values of 10–20% in the tropics are similar to the 15% reported by Randel et al. (2002b). Large errors in the net heating rates and consequently in the estimated velocities also occur in regions closer to radiative equilibrium where the solar heating and the infrared cooling almost balance each other (Olaguer et al., 1992). The combination of initial "radiative" uncertainties and the following correction can result in a really questionable quality of the estimated velocities under conditions close to radiative equilibrium. We did not find any considerable difference in ($\bar{v}^*$,$\bar{w}^*$) calculated on a daily basis and then averaged monthly with ($\bar{v}^*$,$\bar{w}^*$) based on monthly averaged data. Weighting with the cosine of the latitude is applied for averaging in latitudinal belts.

3 Ozone tendencies

Figure 1 shows the total wintertime (November–March, Fig. 1a) and monthly (from October to March, Fig. 1b) zonal $\Delta O_3/\Delta t$ averaged over 50°–60° N. The year for the winter denotes the year as in January. The ozone merge dataset begins in November 1978 so there is no $\Delta O_3/\Delta t$ in October and November of the 1979 winter. Also there is a data gap in October of the 1996 winter. The tendencies are always negative in September (not shown) and close to zero in October which presents a transition period between summer photochemical decay and wintertime dynamical buildup. On average the tendencies increase until January when they reach a seasonal maximum and than symmetrically decrease towards spring becoming negative in April (not shown). The December and February values are of about the same magnitude. However, in some

years seasonal behaviour of $\Delta O_3/\Delta t$ differs strongly from the average, reflecting the influence of various random dynamical and chemical processes on midlatitude ozone during winter. Monthly ozone tendencies do not correlate with each other and can be regarded as independent time series. In contrast, monthly total ozone has strong autocorrelations (Fioletov and Shepherd, 2003). Only the January and February tendencies correlate significantly (r=0.52 and 0.48) with the total wintertime $\Delta O_3/\Delta t$. Indeed, low January $\Delta O_3/\Delta t$ in 1993 and 1995 (high in 1982, 1991 and 1994) result in low (high) total wintertime $\Delta O_3/\Delta t$ in those years. A combination of low $\Delta O_3/\Delta t$ in November, January and March of 2000 also leads to low wintertime $\Delta O_3/\Delta t$ even though $\Delta O_3/\Delta t$ is quite high in December and February. Thus, low $\Delta O_3/\Delta t$ at the end of winter does not necessarily mean less poleward ozone transport or more chemical loss through the whole winter.

Estimated linear trends in $\Delta O_3/\Delta t$ for the 1980–2002 period are presented in Table 1. Though no significant trends are found for any month, it is interesting to note that the sign of the trend changes from positive in November (about zero) and December to negative from January to March. Such $\Delta O_3/\Delta t$ trend distribution is similar to the HF trends in November–February shown by Randel et al. (2002a): weak insignificant positive trends in November, December and negative ones in January (at the edge of statistical significance) and February (insignificant) for 1979–2000. Newman and Nash (2000) found significant negative trends in the January–February averaged HF (1979–1999). Later Karpetchko and Nikulin (2004) confirmed significant negative trends in the January–February HF and positive trends in the November–December HF which are at the edge of statistical significance (1979–2002). Averaged in the same way $\Delta O_3/\Delta t$ shows a similar picture: an insignificant positive trend for November–December as well as a significant negative trend for January–February. The negative trend becomes stronger and more significant for January–March (see Table 1) while the total wintertime trend is still negative but insignificant because of the positive trend in November–December. Hence the decline in $\Delta O_3/\Delta t$ occurs only during January–March. We use the 1980–2002 period to be consistent in all months since there is no

data in November 1979. If, for example, we take into account 1979, the January and February trends become more negative as can be seen from Fig. 1b.

Figure 2 shows $\Delta O_3/\Delta t$ over the NH averaged for 1980–2002 in the initial (October), middle (December) and final (March) stages of the ozone buildup. Though the October zonal mean $\Delta O_3/\Delta t$ is about zero (Fig. 1b), a longitudinal distribution of tendencies in October is not uniform (Fig. 2a). A positive maximum is located over the north-eastern edge of Russia while the opposite part of the NH is covered by negative values. It is interesting to note that a subtropical minimum of $\Delta O_3/\Delta t$ is located over the Pacific just south of the positive maximum. Presence of the north-south dipole suggests intensification of northward ozone transport which is confined within the Pacific region. Also, deepening of the Aleutian low (from summer to winter) and associated decreasing of the tropopause height can result in accumulation of ozone in the lower stratosphere. In November (not shown) the positive maximum of $\Delta O_3/\Delta t$ is still centred over the north-eastern edge of Russia and positive tendencies spread eastward and westward from the maximum covering almost the whole region north of 30° N with the exception of a negative region over the Atlantic. The December $\Delta O_3/\Delta t$ (Fig. 2b) is positive over all NH midlatitudes and the second positive maximum which can be associated with the Icelandic low appears over the north-western Atlantic. The same structure with greater magnitude is seen in January (not shown). The February (not shown) and March (Fig. 2c) tendencies have less resemblance to the December-January ones especially in March when the $\Delta O_3/\Delta t$ pattern has smaller scale features and differs strongly from other months.

The longitude distribution of $\Delta O_3/\Delta t$ in October–January is similar to total ozone distribution in the same months which is related to a structure of quasi-stationary planetary waves in the lower stratosphere (Kurzeja, 1984; Hood and Zaff, 1995). These waves still exist in the lower stratosphere during the February–March period that is also mirrored in total ozone fields (not shown) but the $\Delta O_3/\Delta t$ patterns are not well tied to the wave structure as in the preceding months. The less pronounced planetary wave pattern in $\Delta O_3/\Delta t$ during February and March is most probably a result of

chemical ozone loss inside the polar vortex and following dilution of the vortex air into midlatitudes. These processes are more intensive in late winter and early spring (Hadjinicolaou and Pyle, 2004) and can introduce strong spatial deviations in the midlatitude $\Delta O_3/\Delta t$ fields, especially during the vortex breakup. Between 1980 and 2002 the vortex breakup at the 475 K level occurred 5 times in March (Karpechko et al., 2005)[1]. As a summary of the chapter we conclude that the wintertime ozone buildup begins over the north-eastern edge of Russia in October, spreads over the NH in November and finally covers all NH midlatitudes in December. In October–January total ozone is more under dynamical control and the longitude structure of $\Delta O_3/\Delta t$ mirrors the longitude structure of planetary waves in the lower stratosphere. Chemistry begins to play a more significant role in the late winter-early spring when the $\Delta O_3/\Delta t$ fields show less similarity with the planetary wave pattern.

4 Heat flux and ozone tendencies

Figure 3 shows one-point correlations of $\Delta O_3/\Delta t$ averaged over 50°–60° N with HF for (a–c) November–January and (d) March. For these plots, daily values of HF are averaged over one-month periods consistent with monthly mean $\Delta O_3/\Delta t$ (15th of previous month–15th of given month). For example the January HF means here an average from 15 December to 15 January. In November (Fig. 3a) an area of pronounced positive correlations (r_{max}=0.69) is located in the midlatitude stratosphere with a maximum stretching from 100 to 10 hPa. The positive correlations in December are weak and insignificant in most of the stratosphere north of 50° N (Fig. 3b). A small region in the lower stratosphere is on the edge of statistical significance (r_{max}=0.45). Also, there are significant negative correlations in the tropical upper troposphere. This feature is absent in other months and looks random so we do not discuss it in the paper. In

[1] Karpechko A., Kyro E., and Knudsen, B. M.: Arctic and Antarctic polar vortices 1957–2002 as seen from the ERA-40 reanalyses, in review, J. Geophys. Res., 2005.

January (Fig. 3c) positive correlations (r_{max}=0.68) cover all heights in the stratosphere with a slope from the upper subtropical to the lower midlatitude stratosphere. The February correlations north of 50° N (not shown) are qualitatively almost identical to the December ones (Fig. 3b) but the lower stratospheric maximum is clearly pronounced (r_{max}=0.69, 70 hPa, 70° N). In March (Fig. 3d) positive correlations (r_{max}=0.71) spread over all extratropical stratosphere reaching the North Pole. The correlation pattern between the wintertime $\Delta O_3/\Delta t$ and HF for the same period (not shown) is similar to the December and February ones. The maximal correlation coefficient is about 0.7, located at 70 hPa, 65° N.

There are no significant correlations between the zonal mean $\Delta O_3/\Delta t$ and HF in October when the zonal mean $\Delta O_3/\Delta t$ is about zero. However, if we average $\Delta O_3/\Delta t$ over the region with maximal positive values in Fig. 2a (60°–70° N, 105°–225° E; the North Pacific hereafter), positive correlations (r_{max}=0.7) centred at 55°–60° N appear in the stratosphere (not shown). The pattern obtained is absolutely identical to the November one for the zonal mean $\Delta O_3/\Delta t$ in Fig. 3a. Though the North Pacific $\Delta O_3/\Delta t$ is not a zonal mean quantity, the strong correlation can be explained by the fact that the considerable contribution to the October zonal mean HF also comes from the Pacific. Zonal mean HF between 50° N and 70° N (the region with maximal correlations in Fig. 3a) shows significant coherence (r =0.75÷0.85) with the Pacific HF (50°–70° N, 105°–225° E) at all levels in the stratosphere. This finding supports the idea that northward ozone transport strengthens over the Pacific already in October. We should note that the latitude belt 60°–70° N is different from other months. The October $\Delta O_3/\Delta t$ averaged over 50–60° N and the same longitudes (105°–225° E) shows only weak insignificant positive correlations with HF in the stratosphere.

Presence of positive correlations between $\Delta O_3/\Delta t$ and HF is in agreement with theoretical considerations and previous results (e.g. Randel et al., 2002a; Salby and Callaghan, 2002; Weber et al., 2003). However, the correlation patterns are not uniform during winter and maximal values of correlations are often located above 100 hPa and at different latitudes. The region 45°–75° N, 100 hPa is usually taken to define

approximately the amount of wave activity entering into the stratosphere from the troposphere. As can be seen from Fig. 3, the HF averaged over this region is not always an optimal proxy of wave forcing for the regression models describing midlatitude total ozone. $\Delta O_3/\Delta t$ has a pronounced relation with HF in the early stage of ozone buildup (October–November), although in October this relation is regional. It is not clear why correlations are weaker in the middle stage of the buildup (December) in comparison with the preceding and following months. Qualitatively the December correlation pattern is similar to the February one when correlations are strong. The November $\Delta O_3/\Delta t$ is lower than the December $\Delta O_3/\Delta t$ but shows the pronounced positive correlation with HF in the stratosphere. The extrapolation of the missing December data in 1992–1994 and 1997–1998 can have influenced the results obtained, but removing these 5 years does not change the December correlations. The correlation patterns are identical in October and November during the formation of the polar vortex but not as homogeneous as in the following months with the presence of a developed polar vortex. The position and strength of the polar vortex strongly define ozone distribution and conditions for wave propagation in the winter stratosphere. Nonuniform patterns may therefore be attributed to the behaviour of the polar vortex. Consistent results are obtained using the NCEP/NCAR Reanalysis (limited by the uppermost 10 hPa level) so both the ERA40 and NCEP/NCAR data sets are in agreement here. In general, maximal absolute values of correlation coefficients during winter are close to 0.7 (with the exception of December) thus HF explains about 50% of variance in $\Delta O_3/\Delta t$.

Randel et al. (2002) mention that one source of variability in the results is random episodic nature of wave forcing with the usual wave event duration being about 1–2 weeks. Hence the obtained correlation coefficients also depend on which part of individual wave events have fallen into an averaging period for HF from year to year. Practically, in each month (not in December) we can select an averaging period (plus-minus several days) which gives higher maximal correlation coefficients (more than 0.7). However, this "optimal" period is different from month to month so in the study we use the same period giving more or less consistent results for all winter months.

5 Heat fluxes and the residual circulation

Since HF is the simplest proxy of the wave forcing we examine relations between HF and the calculated residual velocities. An example of the January $\bar{v}^*$ and $\bar{w}^*$ averaged for 1980–2002 is shown in Fig. 4. Qualitatively the global patterns of $\bar{v}^*$ and $\bar{w}^*$ agree with previous studies (e.g. Solomon et al., 1986; Eluszkiewicz et al., 1997). Upward motions in the tropics shifting to the summer hemisphere with altitude and poleward-downward motions in the winter extratropics are the prominent features of the residual circulation. A layered circulation south of 60° S may be due both to the vertical oscillations in the ERA-40 temperature at high latitudes of the SH (SPARC 2002) and to larger uncertainties in the calculated residual velocities during the SH summer. The summer stratosphere, especially the lower, is much closer to radiative equilibrium than its winter counterpart (e.g. Shine, 1987), leading to smaller values for the calculated velocities as well to larger uncertainties. The layered circulation is not observed for example in September when the SH stratosphere is not as close to radiative equilibrium as in January. Absolute values of $\bar{w}^*$ are less than 1 mm s^{-1} in the lower stratosphere and increase up to 8 mm s^{-1} in the upper polar stratosphere. $\bar{v}^*$ has its maximum in the upper tropical stratosphere (about 2 m s^{-1}) and values less than 0.5 m s^{-1} below 5 hPa. A small region with higher $\bar{v}^*$ and $\bar{w}^*$ between 100 and 50 hPa centred at the equator is an exception that most likely represents an influence of the tropical convection. In this study we concentrate on the NH and limit the residual circulation to the region between 30° S and 90° N.

Figure 5 shows one-point correlations of HF averaged over 45°–75° N, 100 hPa with $\bar{w}^*$ for (a) November and (b) January. Daily values of the residual velocities and HF are averaged over one-month periods in the same way as in the previous section (15th of previous month–15th of given month). An area of strong negative correlations north of 60° N appears in all months from November to March. December, February and March are identical to January and not shown here. Negative correlations are confined to the lower stratosphere in November (r_{min}=–0.72) and spread up to 2–3 hPa in the

following months (r_{min}≈–0.8÷–0.9). Positive correlations with upward motions exist in the tropical stratosphere but they are nonuniform and only some patches are significant in December-March. The obtained correlations are not sensitive to a choice of level for HF in the lower stratosphere. However, if HF is taken at levels higher than 20 hPa, the polar minimum shifts upward and the tropical positive correlations become more homogeneous above 10 hPa. Newman et al. (2001) showed that correlation of HF and the polar stratospheric temperature depends on radiative damping time which is shorter in the middle and upper stratosphere and longer in the lower stratosphere (Newman and Rosenfield, 1997). One-month periods as used here can mask part of the variability in regions with shorter damping time than one month. Indeed, HF taken at 10–5 hPa and 10-day averaging for both HF and $\bar{w}^*$ bring pronounced positive correlation (r_{max}≈0.7÷0.9) between 30° S–30° N above 10 hPa. However, because of the shorter period, variability in the 10-day correlation patterns is higher than in the monthly samples. The fragmented correlation pattern in the lower tropical stratosphere for monthly samples lets us assume that interannual variability of $\bar{w}^*$ is not well captured over the region because of larger uncertainties. We can test this suggestion by using temperature tendency ($\Delta T/\Delta t$) which operates coherently with HF over the entire winter hemisphere and even over the subtropics of the summer hemisphere (Randel 1993; Salby and Callaghan, 2002). Figure 6 shows correlations of HF with $\Delta T/\Delta t$ for November and January by analogy with Fig. 5. A clear pronounced north-south dipole like in January (Fig. 6b) is observed from December to March. Negative correlations (r_{min}≈–0.7÷–0.9) cover the whole lower stratosphere in the tropics and subtropics of both hemispheres. In November (Fig. 6a) only weak negative correlations at the edge of significance exist in the NH subtropics but positive ones (r_{max}=0.74) are located in the polar lower stratosphere/upper troposphere. The $\Delta T/\Delta t$ correlation patterns also depend on radiative damping time and show similar behaviour to $\bar{w}^*$, moving upward with a 10-day averaging period and HF taken at 10–5 hPa. The strong correlation between HF and $\Delta T/\Delta t$ in the tropical lower stratosphere supports the presence of larger uncertainties in $\bar{w}^*$ over this region. In fact, the tropical lower stratosphere is close

to radiative equilibrium because the dynamical temperature response to extratropical wave forcing is much smaller (only several Kelvins) in the tropics as compared with the extratropics (Randel 1993; Salby and Callaghan, 2002). The correction applied to the velocities during calculations, as mentioned in Sect. 2, is about 10–20% of the uncorrected values of $\bar{w}^*$ in the tropics, i.e. two times greater than for the NH high latitudes. It is most likely that for the tropical lower stratosphere, the combination of small net heating rates and the correction procedure leads to large uncertainties in $\bar{w}^*$.

As expected, HF correlates positively with $\bar{v}^*$ in the extratropical stratosphere in all months from November to March. In November (Fig. 7a) an area of positive correlations (r_{max}=0.65) is narrow and elongated from the Equator to the North Pole along the 30 hPa level. During December-March the extratropical correlation patterns below 3 hPa are nearly analogous to the January pattern (Fig. 7b). Positive correlations extend upward and the maximum (r_{max}≈0.7–0.8) is located in the polar middle stratosphere north of 60° N. At the same time the positive correlations for $\bar{v}^*$ are not as uniform during winter as the negative correlations for $\bar{w}^*$.

In October when only $\Delta O_3/\Delta t$ averaged over the North Pacific is coupled with HF, no significant correlations were found between HF (45°–75° N, 100 hPa) and either $\bar{w}^*$ nor $\bar{v}^*$. However, HF taken above 30 hPa correlates well (|r|≈0.7–0.8) with both $\bar{w}^*$ and $\bar{v}^*$ in the middle stratosphere north of 60° N. Also HF shows good coherence with $\Delta T/\Delta t$ (r_{max}≈0.7) in the polar lower stratosphere that is similar with November (Fig. 6a). As for HF, the main contribution to interannual variability of zonal mean $\Delta T/\Delta t$ in October comes from the Pacific. Hence all relations between zonal mean quantities in October mainly mirror local processes over the Pacific.

Stronger HF into the stratosphere results in the stronger residual circulation and vice versa. There is a good agreement with theoretical expectations in the middle and upper tropical stratosphere as well as in the polar winter stratosphere. However, the residual circulation in the lower tropical stratosphere which is close to radiative equilibrium shows a weak relation with the wave forcing because of larger uncertainties. At the same time interannual variations of $\Delta T/\Delta t$ have much better coherence with HF

in regions close to radiative equilibrium than the estimated residual velocities. HF, $\Delta T/\Delta t$ and the residual circulation based on the NCEP/NCAR reanalysis (only heating rates from the ERA-40) give consistent results at levels presented in both datasets.

6 The residual circulation and ozone tendencies

Finally we examine how $\Delta O_3/\Delta t$ is related to the estimated residual circulation. Here we use time averaging for $\bar{w}^*$ and $\bar{v}^*$ from 20th of previous month to 20th of given month that results in approximately equal maximal absolute values of correlation coefficients in all months. Figure 8 shows one-point correlations of $\Delta O_3/\Delta t$ averaged over 50°–60° N with $\bar{w}^*$ for (a–c) November–January and (d) March. Theoretically, $\Delta O_3/\Delta t$ correlates negatively with downward velocities in the extratropics and positively with upward ones in the tropics. Midlatitude correlation patterns are similar in November-February (February not shown): an area of negative correlations is located in the lower stratosphere and centred at 50°–60° N, 50–70 hPa ($r_{min}\approx$–0.65÷–0.75). The spatial structure of extratropical correlations is more uniform from month to month in comparison with HF (Fig. 3). Noticeable correlation is observed in December (Fig. 8b) when correlation between $\Delta O_3/\Delta t$ and HF is weak (Fig. 3b). In March (Fig. 8d) negative correlations spread upward and northward covering almost the whole extratropical stratosphere. Positive correlations in the tropics are variable and more marked in January and March but weaker in other months.

The maximal response of $\bar{w}^*$ to wave forcing is observed north of 60° N (Fig. 5), but the strongest negative correlations between $\Delta O_3/\Delta t$ and $\bar{w}^*$ are found south of 60° N where the correlation between $\bar{w}^*$ and HF (45°–75° N, 100 hPa) is weak. As noted in Sect. 4, the region 45°–75° N, 100 hPa does not always coincide with a region of the strongest correlations between $\Delta O_3/\Delta t$ and HF (Fig. 3). Indeed, HF averaged over the regions with strongest correlation in separate months (Fig. 3) shows almost the same correlation patterns with $\bar{w}^*$ as $\Delta O_3/\Delta t$ in Fig. 8. Hence, HF averaged over 45°–75° N, 100 hPa describes the residual circulation in high latitudes well but not in

midlatitudes. Since the main dynamical contribution to total ozone variability comes from the lower stratosphere where ozone has a long photochemical lifetime (Brasseur and Solomon, 1986) it is not surprising that the strongest negative correlations with $\bar{w}^*$ are observed in the lower stratosphere. Maximal absolute values of correlation coefficients (≈0.7) and accordingly explained variance (≈50%) are the same as for HF. Changing the averaging period for $\bar{w}^*$ for several days can also give higher absolute correlation coefficients in separate months that is similar to the behaviour of the HF correlations.

Theoretically extratropical $\Delta O_3/\Delta t$ correlates positively with the northward mean meridional velocity in the stratosphere. Though there are expected positive correlations between $\Delta O_3/\Delta t$ and $\bar{v}^*$ in all months ($r_{max}\approx$0.6÷0.7), the correlation patterns are variable and differ from month to month contrary to the negative correlations for $\bar{w}^*$. In November (Fig. 9a) a narrow belt of positive correlations stretches from the Equator to the North Pole at 30 hPa. It is interesting to note that this feature is identical to the November correlation pattern between HF and $\bar{v}^*$ (Fig. 7a). From the following months January (Fig. 9b) with a wide area of positive correlations in the NH subtropics can be singled out. December, February and March (not shown) have two belts of significant correlations: one in the lower and another in the middle stratosphere that only is to some extent similar to November (Fig. 9a). Large uncertainties in the calculated $\bar{v}^*$ in comparison with $\bar{w}^*$ may explain why the positive correlations for $\bar{v}^*$ are nonuniform and differ from month to month while the negative correlations for $\bar{w}^*$ are almost similar. Calculation of the residual circulation is an iteration procedure when at the first step we assume that $\bar{v}^*$ is equal 0 to get the first estimate of $\bar{w}^*$ from the thermodynamic equation (1). Then we get the first estimate of $\bar{v}^*$ at a given latitude from the continuity equation (2) through integration of the vertical derivative of$\rho_0\bar{w}^*$ ($\bar{w}^*$ has already been corrected) from a pole to this latitude, assuming that $\bar{v}^*$=0 at the Poles. In this case the calculated $\bar{v}^*$ accumulates uncertainties in the vertical derivative of $\rho_0\bar{w}^*$ from a pole to the given latitude. Hence all uncertainties in $\bar{v}^*$ come non-locally from $\bar{w}^*$, and it is most likely that $\bar{v}^*$ has larger uncertainties than $\bar{w}^*$.

We showed in the previous section that temperature tendencies are strongly coupled with the wave forcing. Ozone tendencies should also be coherent with $\Delta T/\Delta t$ because interannual variability of both is controlled by the mean meridional circulation. The averaging period for $\Delta T/\Delta t$ giving the best correlation with $\Delta O_3/\Delta t$ is almost consistent with the averaging period for $\bar{w}^*$ (20th of previous month to 20th of given month) in October–January but is shifted forward by approximately 10–15 days in February–March. Figure 10 shows correlations of the (a) November and (b) January $\Delta O_3/\Delta t$ with $\Delta T/\Delta t$ averaged for 20 October–20 November and 15 December–15 January, respectively. The observed north-south dipole in the stratosphere exists in all months with the exception of December, similar to the structure of correlation between HF and $\Delta T/\Delta t$ in Fig. 6. By analogy with $\bar{w}^*$, the maximum of extratropical correlation is located south of 60° N while the strongest correlation of $\Delta T/\Delta t$ with HF (45°–75° N, 100 hPa) is found north of 60° N (Fig. 6). The explanation for the difference is the same as for $\bar{w}^*$: HF over 45°–75° N, 100 hPa does not describe the residual circulation in midlatitudes as well. HF taken over regions with maximal correlation in Fig. 3 brings almost the same correlation patterns with $\Delta T/\Delta t$ as $\Delta O_3/\Delta t$ in Fig. 10. The observed dipole is weaker in November (Fig. 10a) and becomes stronger in January (Fig. 10b) remaining similar in February and March. In December only the northward part of the dipole (r_{max}=0.45) centred at 50° N is observed. In this respect, December with weaker correlation between $\Delta O_3/\Delta t$ and both HF and $\Delta T/\Delta t$ is sharply distinguished from other months but we could not find any reasonable explanation.

In the early stage of the ozone buildup the October $\Delta O_3/\Delta t$ averaged over the North Pacific shows an small area of negative correlation with $\bar{w}^*$ in the polar lower stratosphere but no correlation with $\bar{v}^*$. Also $\Delta T/\Delta t$ averaged for 20 September–20 October correlates well (r_{max}=0.7) with the North Pacific $\Delta O_3/\Delta t$ showing a north-south dipole in the lower stratosphere. Though interannual variability in both tendencies is controled by the mean meridional circulation, $\Delta T/\Delta t$ as one more "proxy" for $\Delta O_3/\Delta t$ explains 50% of the variance in ozone tendencies thus consistent with the results for HF and $\bar{w}^*$. As in the previous section, the NCEP/NCAR Reanalysis shows similar results.

7 Summary and discussion

This study focuses on development of the wintertime ozone buildup in the NH midlatitudes (50°–60° N) during the October–March period and the statistical relationship of the buildup with the mean meridional circulation. The buildup begins locally in October when positive $\Delta O_3/\Delta t$ appears over the North Pacific. Two processes can be responsible for the local beginning of the buildup: intensification of northward ozone transport confined in the Pacific and deepening of the Aleutian low leading to accumulation of ozone in the lower stratosphere. At the same time presence of negative $\Delta O_3/\Delta t$ over the opposite part of the NH gives the October zonal mean $\Delta O_3/\Delta t$ close to zero. In November positive $\Delta O_3/\Delta t$ spreads eastward and westward from the North Pacific and finally covers all NH midlatitudes in December. In the early and middle stages of the buildup (October-January), the longitude structure of $\Delta O_3/\Delta t$ mirrors total ozone distribution (maxima and minima) which is related to quasi-stationary planetary waves in the lower stratosphere. During the final stage (February and March) $\Delta O_3/\Delta t$ shows less resemblance with the planetary wave pattern which may be explained by a dilution of ozone depleted air from the polar vortex into midlatitudes as well as the vortex breakup for March. There are no significant linear trends in monthly zonal mean $\Delta O_3/\Delta t$ for 1980–2002. However the January-February trend is negative and significant while the November–December trend is positive and insignificant. Such behaviour of $\Delta O_3/\Delta t$ trends is similar to the HF trends reported earlier (Randel et al., 2002; Karpetchko and Nikulin, 2004).

Eddy heat flux, residual velocities and temperature tendency are used to estimate the contribution from the mean meridional circulation to interannnual variability of monthly $\Delta O_3/\Delta t$. On average for all months from November to March, absolute values of correlation coefficients between zonal mean $\Delta O_3/\Delta t$ and HF, $\Delta T/\Delta t$ or $\bar{w}^*$ are close to 0.7. Two points should be noted. Firstly, the correlation patterns between $\Delta O_3/\Delta t$ and HF are not uniform during the buildup and the maxima are located at different latitudes and levels. That is the opposite to correlation patterns of $\Delta O_3/\Delta t$ with $\Delta T/\Delta t$ and $\bar{w}^*$

which are almost homogeneous from month to month. As a consequence of heterogeneity in the HF and $\Delta O_3/\Delta t$ correlation patterns, HF averaged over the usual region 45°–75° N, 100 hPa is not always an optimal proxy for total ozone variability in midlatitudes. Secondly, one partial exception is December, in the middle stage of the buildup, when both $\Delta T/\Delta t$ and $\bar{w}^*$ show a strong response to wave forcing presented by HF. However, $\Delta T/\Delta t$ and HF have weaker correlation (r_{max}=0.45) with $\Delta O_3/\Delta t$ while the $\bar{w}^*$ correlation coefficient (r_{min}=–0.7) is similar to that in other months. We have not found any explanation for this feature. Based on several parameters approximating the strength of the mean meridional circulation, an average correlation coefficient equal to 0.7 can be confidently accepted. Hence, assuming a linear relation, half of the interannual variability in the 50°–60° N zonal mean $\Delta O_3/\Delta t$ for 1980–2002 can be explained by the mean meridional circulation. The results based on the NCEP/NCAR reanalysis show very good qualitative and quantitative agreements with the results based on the ERA-40, suggesting that the obtained results are independent of which dataset is chosen.

A similar relation is found for positive $\Delta O_3/\Delta t$ over the North Pacific (60°–70° N, 105°–225° E) in October when the zonal mean $\Delta O_3/\Delta t$ is about zero but the NH ozone buildup begins locally. The October correlation patterns of the North Pacific $\Delta O_3/\Delta t$ with HF or $\Delta T/\Delta t$ are clearly pronounced and identical to the November ones for zonal mean $\Delta O_3/\Delta t$. These facts, as well as presence of the $\Delta O_3/\Delta t$ minimum in the subtropical Pacific, support the local onset of the ozone buildup over the Pacific already in October. Though the 60°–70° N belt is not exactly midlatitudes, the observed development of the NH ozone buildup emphasizes the presence of zonal asymmetries in the Brewer-Dobson circulation which are especially noticeable in October.

The worst observed correlation of $\bar{w}^*$ with HF and $\Delta O_3/\Delta t$ in the tropical lower stratosphere most likely resulted from uncertainties in the estimated residual circulation. These uncertainties come from errors in the radiative heating rates and the following latitude independent correction, reducing the global integral of $\bar{w}^*$ on isobaric levels to zero. Such latitude-independent corrections, however, have a latitude-dependent re-

sponse which introduces larger uncertainties in regions close to radiative equilibrium. During November–March $\bar{w}^*$ shows strong coherence with HF and $\Delta O_3/\Delta t$ north of 50° N where the stratosphere is far from radiative equilibrium. Of course practical implementation of the residual circulation is not as simple as HF or $\Delta T/\Delta t$ and can be used more as an additional method to check theoretically-expected relations as in the study. One useful point here is also the possibility to test the accuracy of the estimated $\bar{w}^*$, comparing the response in $\bar{w}^*$ to wave forcing with the distinct response in $\Delta T/\Delta t$.

The NH midlatitude ozone buildup has a stable relation with the mean meridional circulation in all months from October to March, though in October this relation is regional and December is somewhat questionable. The obtained half of the explained variance in $\Delta O_3/\Delta t$ is lower than in the results of Salby and Callaghan (2002) and Weber et al. (2003) where total ozone was averaged over wider latitude belts including the polar region and $\Delta O_3/\Delta t$ was calculated for the whole winter period. The explained variance in both studies is about 80%. At the same time 50% of explained variance is higher than the results of Randel et al. (2002) for 35°–60° N zonal mean $\Delta O_3/\Delta t$ where the explained variance is typically less than 50%. Hence our results correspond with the previous results according to the chosen latitude belt (50°–60° N). The absence of total ozone data at high latitudes during the polar night does not allow the same relationship for polar ozone month by month through winter to be examined.

Acknowledgements. The authors thank the TOMS science team (NASA/GSFC), ECMWF and CPC for providing data. The work of G. Nikulin is supported by the Swedish Research Council. The work of A. Karpechko is supported by the EU Commission under the project CANDIDOZ.

References

Andrews, D. G., Holton, J. R., and Leovy C. B.: Middle Atmosphere Dynamics, Academic Press, 489, 1987.

Brasseur, G. and Solomon, S.: Aeronomy of the middle atmosphere, D. Reidel Publishing Company, 441, 1986.

Brewer, A. E.: Evidence for a world circulation provided by the measurements of helium and water vapour distribution in the stratosphere, Q. J. Roy. Meteorol. Soc., 75, 351–363, 1949.
Dobson, G. M. B.: Origin of distribution of the polyatomic molecules in the atmosphere, Proc. Roy. Soc. London, 236A, 187–193, 1956.
Dunkerton, T.: On the mean meridional mass motions of the stratosphere and mesosphere, J. Atmos. Sci., 35, 2325–2333, 1978.
Eluszkiewicz, J., Crisp, D., Zurek, R., Elson, L., Fishbein, E., Froidevaux, L., Waters, J., Grainger, R. G., Lambert, A., Harwood, R., and Peckham, G.: Residual circulation in the stratosphere and lower mesosphere as diagnosed from Microwave Limb Sounder data, J. Atmos. Sci., 53, 217–240, 1996.
Eluszkiewicz, J., Crisp, D., Grainger, R. G., Lambert, A., Roche, A. E., Kumer, J. B., and Mergenthaler, J. L.: Sensitivity of the residual circulation diagnosed from the UARS data to the uncertainties in the input fields and to the inclusion of aerosols, J. Atmos. Sci., 54, 1739–1757, 1997.
Fioletov, V. E. and Shepherd, T. G.: Seasonal persistence of midlatitude total ozone anomalies, Geophys. Res. Lett., 30(7), 1417, doi:10.1029/2002GL016739, 2003.
Fusco, A. C. and Salby, M. L.: Interannual variations of total ozone and their relationship to variations of planetary wave activity, J. Climate, 12, 1619–1629, 1999.
Geller, M. A., Nash, E. R., Wu, M. F., and Rosenfield, J. E.: Residual circulations calculated from satellite data: their relations to observed temperature and ozone distributions, J. Atmos. Sci., 49, 1127–1137, 1992.
Gille, J. C., Lyjak, L. W., and Smith, A. K.: The global residual mean circulation in the middle atmosphere for the Northern winter period, J. Atmos. Sci., 44, 1437–1454, 1987.
Hadjinicolaou, P. and Pyle, J. A.: The impact of Arctic ozone depletion on northern middle latitudes: interannual variability and dynamical control, J. Atmos. Chem., 47, 25–43, 2004.
Holton, J. R., Haynes, P. H., McIntyre, M. E., Douglass, A. R., Rood, R. B., and Pfister, L.: Stratosphere-troposphere exchange, Rev. Geophys., 33, 403–439, 1995.
Hood, L. L. and Zaff, D. A.: Lower stratospheric stationary waves and the longitude dependence of ozone trends in winter, J. Geophys. Res., 100, 25 791–25 800, 1995.
Karpetchko, A. and Nikulin, G.: Influence of early winter upward wave activity flux on midwinter circulation in the stratosphere and troposphere, J. Climate, 17, 4443–4452, 2004.
Kurzeja, R. J.: Spatial variability of total ozone at high latitudes in winter, J. Atmos. Sci., 41, 695–697, 1984.

Murgatroyd, R. J. and Singleton, F.: Possible meridional circulations in the stratosphere and mesosphere, Q. J. Roy. Meteorol. Soc., 87, 125–135, 1961.
Nagatani, R. M. and Miller, A. J.: The influence of lower stratosphere forcing on the October Antarctic ozone decrease, Geophys. Res. Lett., 14, 202–205, 1987.
Newman, P. A. and Rosenfield, J. E.: Stratospheric thermal damping times, Geophys. Res. Lett., 24, 433–436, 1997.
Newman, P. A. and Nash, E. R.: Quantifying the wave driving of the stratosphere, J. Geophys. Res., 105, 12 485–12 497, 2000.
Newman, P. A., Nash, E. R., and Rosenfield, J. E.: What controls the temperature of the Arctic stratosphere during the spring?, J. Geophys. Res., 106, 19 999–20 010, 2001.
Olaguer, E. P., Yang, H., and Tung, K. K.: A reexamination of the radiative balance of the stratosphere, J. Atmos. Sci., 49, 1242–1263, 1992.
Plumb, R. A. and Eluszkiewicz, J.: The Brewer-Dobson circulation: dynamics of the tropical upwelling, J. Atmos. Sci., 56, 868–890, 1999.
Randel, W. J.: Global variation of zonal mean ozone during stratospheric warming events, J. Atmos. Sci., 50, 3308–3321, 1993.
Randel, W. J., Wu, F., and Stolarski, R.: Changes in column ozone correlated with the stratospheric EP flux, J. Meteorol. Soc. Japan, 80, 849–862, 2002a.
Randel, W. J., Garcia, R. R., and Wu, F.: Time-dependent upwelling in the tropical lower stratosphere estimated from the zonal-mean momentum budget, J. Atmos. Sci., 59, 2141–2152, 2002b.
Salby, M. L. and Callaghan, P. F.: Interannual changes of the stratospheric circulation: relationship to ozone and tropospheric structure, J. Climate, 15, 3673–3685, 2002.
Shine, K.: The middle atmosphere in the absence of dynamical heat fluxes, Q. J. Roy. Meteorol. Soc., 113, 603–633, 1987.
Shine, K.: Sources and sinks of zonal momentum in the middle atmosphere diagnosed using the diabatic circulation, Q. J. Roy. Meteorol. Soc., 115, 265–292, 1989.
Solomon, S., Kiehl, J. T., Garcia, R. R., and Grose, W.: Tracer transport by the diabatic circulation deduced from satellite observations, J. Atmos. Sci., 43, 1603–1617, 1986.
SPARC: SPARC intercomparison of middle-atmosphere climatologies, SPARC Rep.3, 96, 2002.
Weber, M., Dhomse, S., Wittrock, F., Richter, A., Sinnhuber, B.-M., and Burrows, J. P.: Dynamical control of NH and SH winter/spring total ozone from GOME observations in 1995–2002,

Geophys. Res. Lett., 30(11), 1583, doi:10.1029/2002GL016799, 2003.

Table 1. Linear trends (DU/month decade) and confidence levels (%) in zonal mean $\Delta O_3/\Delta t$ (50°–60° N) during 1980–2002.

Season	Trend	Conf. level
November	0.3	11.8
December	4.5	94.5
January	–4.9	86.1
February	–3.6	86.8
March	–3.0	69.3
Nov.–Dec.	4.8	91.0
Jan.–Feb.	-8.5	96.6
Jan.–Mar.	–11.5	99.4
Nov.–Mar.	–6.7	83.5

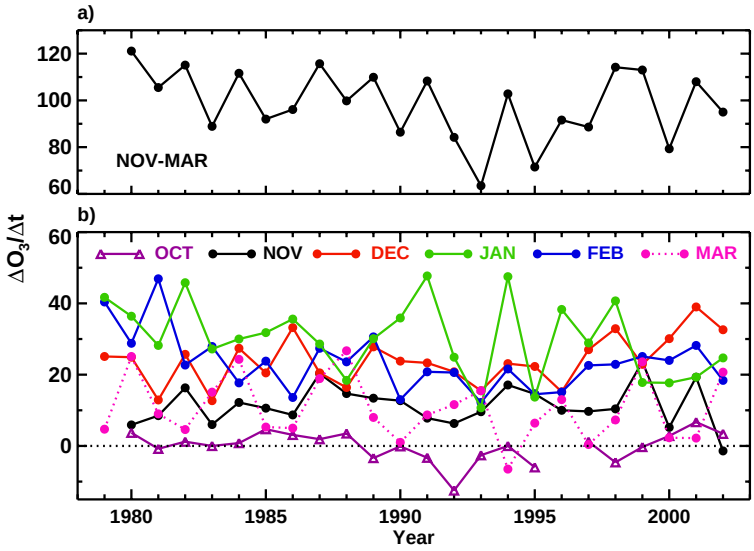

Fig. 1. Time series of zonal mean $\Delta O_3/\Delta t$ averaged over 50°–60° N **(a)** for whole winter (November–March) and **(b)** for each month from October to March (DU/month).

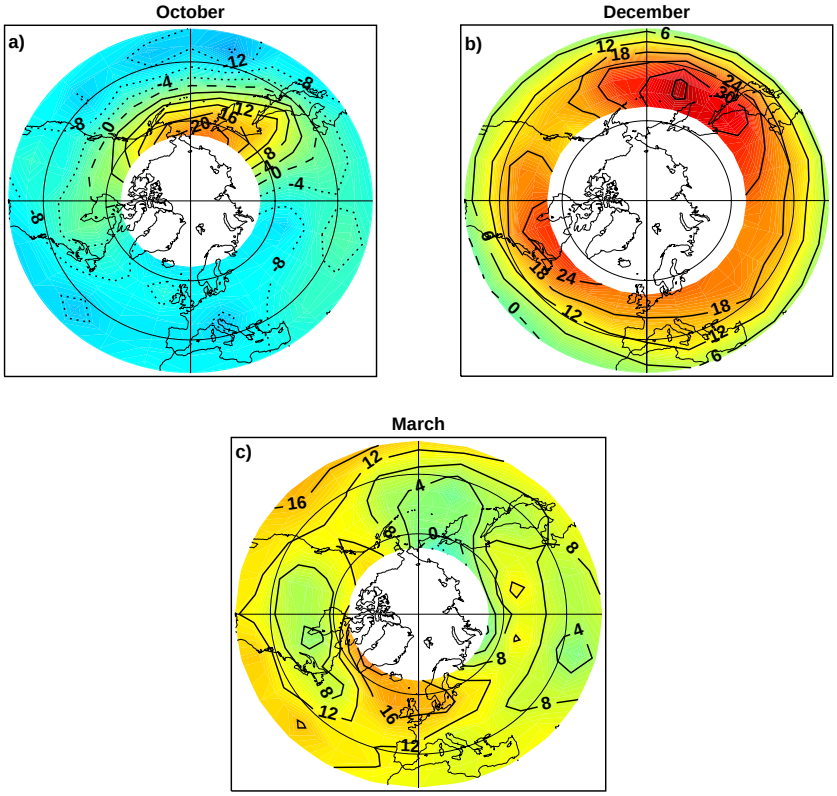

Fig. 2. $\Delta O_3/\Delta t$ (DU/month) in **(a)** October, **(b)** December and **(c)** March, averaged for 1980–2002. Contour interval is 4 DU/month for (a) and (c), and 6 DU/month for (b).

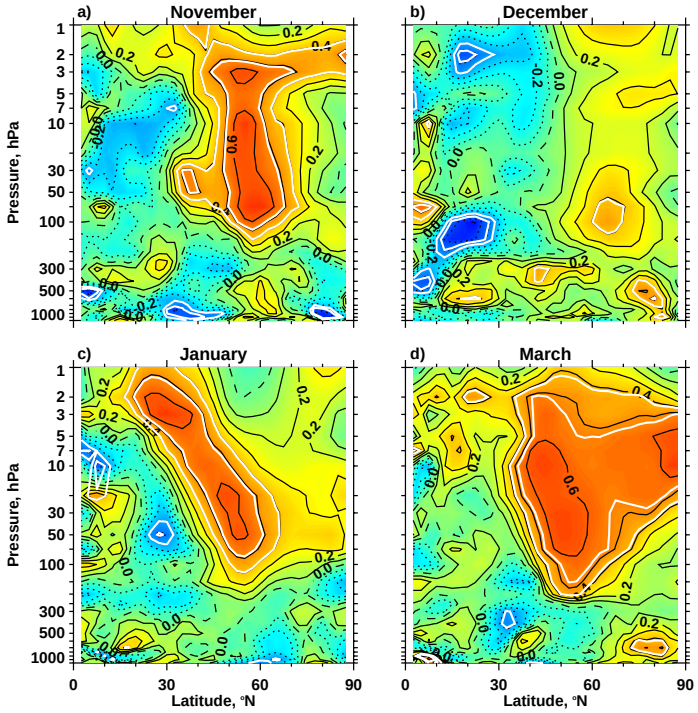

Fig. 3. Correlation between $\Delta O_3/\Delta t$ (50°–60° N) and HF in **(a)** November, **(b)** December, **(c)** January and **(d)** March. HF is averaged from 15th of previous month to 15th of given month. Positive contour values are solid, negative values are dotted and zero contours are dashed. The first and second white lines are the 95% and 99% confidence levels. Contour interval is 0.1.

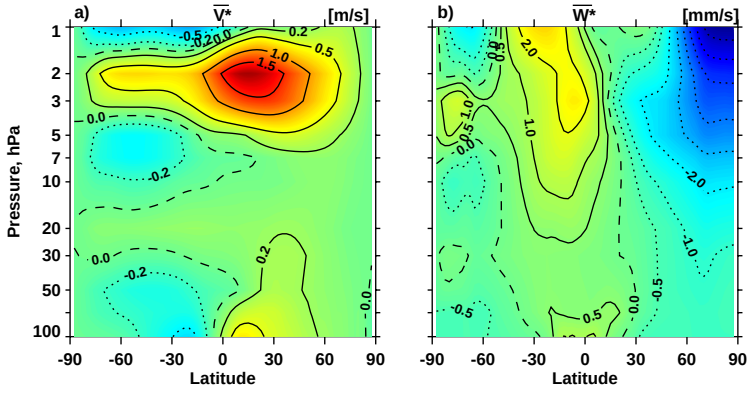

Fig. 4. The January **(a)** $\bar{v}^*$ and **(b)** $\bar{w}^*$ averaged for 1980–2002. Contours are: 0, ±0.2, ±0.5, ±1.0, ±1.5 m s^{-1} for (a), and 0, ±0.5, ±1.0, later increased by 1.0 mm s^{-1} for (b).

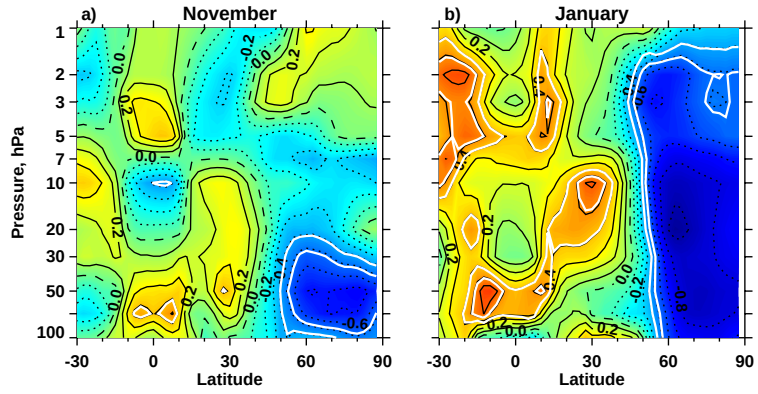

Fig. 5. Correlation between HF (45°–75° N, 100 hPa) and $\bar{w}^*$ in **(a)** November and **(b)** January. HF and $\bar{w}^*$ are averaged from 15th of previous month to 15th of given month. Contours and shading as in Fig. 3.

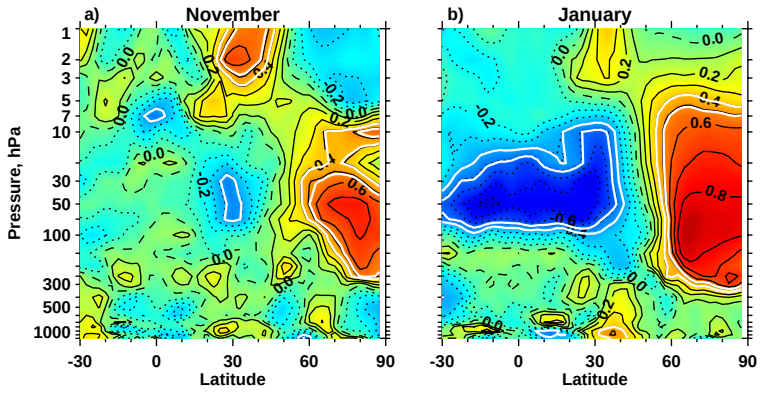

Fig. 6. Correlation between HF (45°–75° N, 100 hPa) and $\Delta T/\Delta t$ in **(a)** November and **(b)** January. HF and $\Delta T/\Delta t$ are averaged from 15th of previous month to 15th of given month. Contours and shading as in Fig. 3.

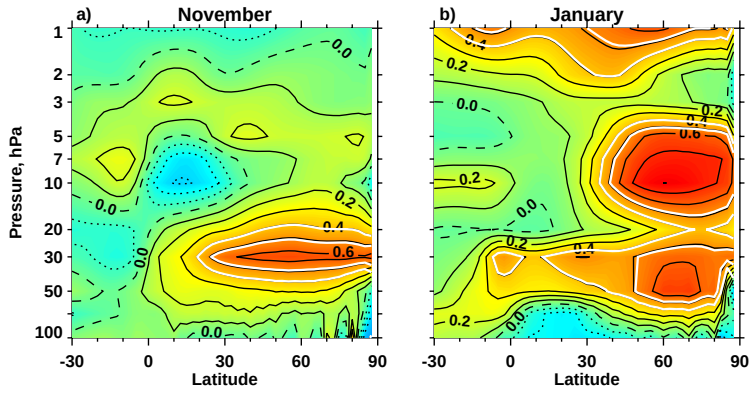

Fig. 7. As Fig. 5 but for $\bar{v}^*$.

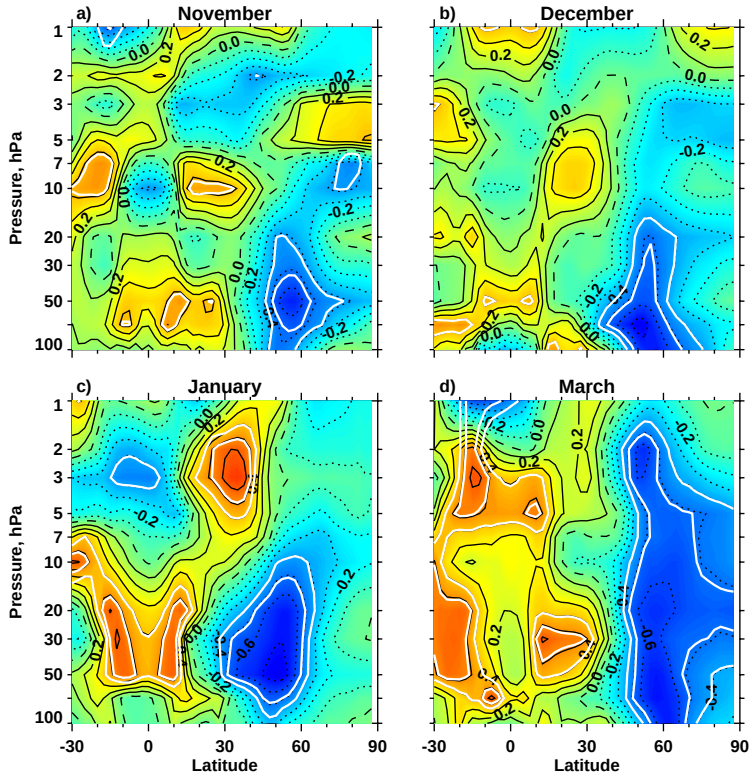

Fig. 8. Correlation between $\Delta O_3/\Delta t$ (50°–60° N) and $\bar{w}^*$ in **(a)** November, **(b)** December, **(c)** January and **(d)** March. $\bar{w}^*$ is averaged from 20th of previous month to 20th of given month. Contours and shading as in Fig. 3.

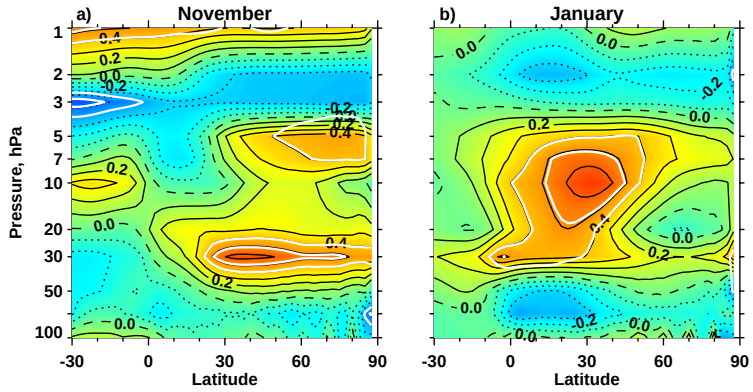

Fig. 9. Correlation between $\Delta O_3/\Delta t$ (50°–60° N) and $\bar{v}^*$ in **(a)** November and **(b)** January. $\bar{v}^*$ is averaged from 20th of previous month to 20th of given month. Contours and shading as in Fig. 3.

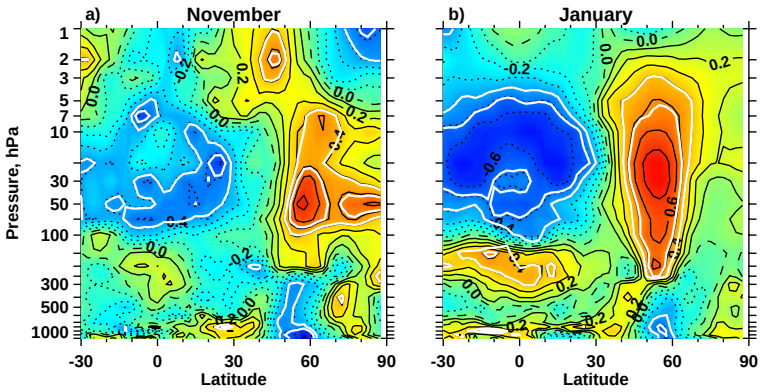

Fig. 10. Correlation between $\Delta O_3/\Delta t$ (50°–60° N) and $\Delta T/\Delta t$ in **(a)** November and **(b)** January. $\Delta T/\Delta t$ is averaged (a) for 20 October–20 November and (b) 15 December–15 January. Contours and shading as in Fig. 3.